

“Before the beginning of great brilliance, there must first be chaos. Before a brilliant person begins something great, they must look foolish in the crowd.”

- I Ching

“Hey guys. Woah! Big Gulps, eh? All right! Well...see ya later.”

- Lloyd Christmas

University of Alberta

**SEDIMENTOLOGY, ICHNOLOGY, AND RESOURCE
CHARACTERISITCS OF THE LOW-PERMEABILITY ALDERSON
MEMBER, HATTON GAS POOL, SOUTHWEST
SASKATCHEWAN, CANADA**

by

RYAN THOMAS LEMISKI

A thesis submitted to the Faculty of Graduate Studies and Research
in partial fulfillment of the requirements for the degree of

MASTER OF SCIENCE

DEPARTMENT OF EARTH AND ATMOSPHERIC SCIENCES

©Ryan Thomas Lemiski

Spring 2010
Edmonton, Alberta

Permission is hereby granted to the University of Alberta Libraries to reproduce single copies of this thesis and to lend or sell such copies for private, scholarly or scientific research purposes only. Where the thesis is converted to, or otherwise made available in digital form, the University of Alberta will advise potential users of the thesis of these terms.

The author reserves all other publication and other rights in association with the copyright in the thesis and, except as herein before provided, neither the thesis nor any substantial portion thereof may be printed or otherwise reproduced in any material form whatsoever without the author's prior written permission.

Examining Committee

Dr. Murray Gingras, Department of Earth and Atmospheric Sciences, University of Alberta

Dr. S. George Pemberton, Department of Earth and Atmospheric Sciences, University of Alberta

Dr. Doug Schmitt, Department of Physics, University of Alberta

For my parents,

There was a time when you held my hand; you gave me the strength to stand. In many respects, I still experience this sentiment. The unconditional love and support you have bestowed upon me is nothing short of remarkable. There are no words to express how grateful I am for the sacrifices you have made in your lives simply to better my own. You are the most kind, generous, and tenderhearted individuals I know. I will never forget the courage you both demonstrated during the tough challenges I once faced as a child. I am truly blessed to have such wonderful role models to look up to. You are my inspiration, and I love you both dearly.

ABSTRACT

The Upper Cretaceous Alderson Member is a prolific gas (biogenic) producer in western Canada. In the Hatton Gas Pool area (southwest Saskatchewan), Alderson Member strata from ten drill-cores have been examined and classified based on sedimentological and ichnological character. Core analysis has determined that Alderson Member deposits comprise thick intervals of pervasively bioturbated strata. Using spot-minipermeametry and high-pressure mercury injection porosimetry methods, the influence of pervasively bioturbated intervals on the overall resource potential of Alderson Member strata is evaluated. Results from permeability and porosity testing demonstrate that pervasively bioturbated rock fabrics appear to locally enhance the overall storage and vertical transmission of gas from Alderson Member reservoirs.

ACKNOWLEDGEMENTS

This thesis would not have been possible without Jesus and the mentorship of Dr. Jussi Hovikoski. Jussi, I want to thank you for your guidance, support, and hard work during the initial stages of my research. Through you, I have learned the importance of data collection, the proper ways of making detailed observations, and what scientific research truly entails. I thank you for helping me fabricate a fairly believable geological story (my committee bought it!) regarding the Alderson Member—something I did not think was possible during my first few visits to the core lab in Regina.

I would also like to acknowledge my exceptional supervisors, Dr. S. George Pemberton, and Dr. Murray Gingras. George, you are an absolute inspiration. You have taught me so much about geology, the scientific method, and life in general. You have been an amazing role model and I will always look up to you. I will never forget some of the stories you shared during your Ichnology course. One day I hope to follow in your footsteps by swimming with Great White sharks and attaching myself to a tree during a hurricane! Murray, I can't thank you enough for everything you've done for me over the past three years. Not only have you been a remarkable mentor, you have become a fantastic friend. Your passion for science is contagious. I am truly blessed to have had the opportunity to work with such a wonderful person.

Thanks to Dr. Ben Rostron for the many informative discussions regarding permeability and mercury intrusion porosimetry. I would also like to acknowledge his help in improving Chapter 3. Ben, despite your official “chair” status, I always considered you to be a co-supervisor. I am definitely going to miss our passionate CFL conversations.

I would like to acknowledge past and present members of the Ichnology Research Group (IRG) for their encouragement, support, guidance, and most

importantly, their friendship. In particular, I want to thank Dr. John-Paul Zonneveld, Curtis Lettley, Tyler Hauck, Sarah Gunn, Jon LaMothe, Lynn Dafoe, Mr. Ryan King, Jesse Schoengut, and Andrew La Croix. A special thank you to my editing guru Curtis Lettley for reviewing early versions of chapters. I am certain that Curtis endured many hours of pain and torture as he sifted through what could only be described as pure and utter gibberish. Curtis, I am truly thankful for your efforts.

Throughout the duration of my studies I have interacted with many individuals from the Department of Earth and Atmospheric Sciences. Through these people, I have gained an enormous appreciation of the bountiful resources this department has to offer. In particular, I would like to acknowledge Mark Labbe for assistance with problems related to the spot-minipermeameter (PDPK – 400), and for providing me with fabulous thin sections; Marsha Boyd, for putting up with my daily inquiries regarding the graduate degree program and potential teaching assistant positions; Michael Fisher, who never fussed during my annual, last-second poster printing crises; and Igor Jakab, for his support, and more importantly, his patience, regarding my bountiful Adobe InDesign questions.

I must also acknowledge the tremendous contributions made by team members of the 2008 University of Alberta Imperial Barrel Award Team: Andrew Mumpy, Sarah Gunn, Evan Bianco, and Jean-François Gagnon. Competing in the IBA global finals in San Antonio was by far the highlight of my graduate studies.

No graduate degree program is complete without a few bumps in the road. At this time, I would like to dis-acknowledge the exceptional procrastinating skills of IRG Members Schoengut, LaCroix, King, and Baniak. While stressed and at my weakest, these individuals took it upon themselves to take advantage of me. Through these men, I was required to take part in debates regarding sport and sport related statistics, pressured into taking prolonged coffee breaks (multiple

times a day), subjected to summaries of weekend shenanigans, daily Facebook “creeping”, Chappelle’s Show clips, and forced to spend countless hours perusing through hilarious videos on YouTube. My lengthy stint as a graduate student is a direct result of their influence. I am certain that this constitutes some type of offence and I am currently looking into legal action against the aforementioned. However, I am pressed for time and will likely get to that next week.

Finally, thank you to my family, who has always been my number one supporter, especially my amazing parents Tom and Murielle who have always been there for me. Especial thank you to the amazing and beautiful woman in my life. Christine, I cannot express in words how much you mean to me. Your love and support during the culmination of my thesis was the extra splash of fuel my tank required in order to complete this work. You are a remarkable person and I am truly blessed to have you in my life. You inspire me to achieve greatness; I owe much of my recent success to you.

TABLE OF CONTENTS

CHAPTER I – INTRODUCTION	2
REFERENCES CITED.....	7
CHAPTER II – SEDIMENTOLOGY, ICHNOLOGY, AND RESOURCE CHARACTERISTICS OF THE LOW- PERMEABILITY, GAS-CHARGED ALDERSON MEMBER, HATTON GAS POOL, SOUTHWEST SASKATCHEWAN, CANADA	10
INTRODUCTION	10
Description of the study area	13
METHODS	20
Core analysis.....	20
Spot-minipermeametry Testing.....	21
ALDERSON MEMBER FACIES – HATTON GAS POOL	24
Facies 1 (F1): Bioturbated sandy mudstone	27
Facies 1A (F1A): <i>Phycosiphon</i> -dominated sandy mudstone	27
Facies 1B (F1B): Sandy mudstone bearing a mixed-ethology trace fossil assemblage	30
Facies 1C (F1C): Burrow-mottled sandy mudstone.....	31
Facies 2 (F2): Heterolithic bedding	33
Facies 2A (F2A): Interlaminated fine-grained sands, silts, and muds	33
Facies 2B (F2B): Bioturbated heterolithic bedding	36

Facies 3 (F3): Low-angle cross-stratified sandstone	38
Facies 4 (F4): Root-bearing fine-grained sandy shale	40
Facies 5 (F5): Conglomerate / Massive medium- to coarse-grained sandstone	42
SPOT-MINIPERMEAMETRY RESULTS	43
Facies 1A (F1A): <i>Phycosiphon</i> -dominated sandy mudstone	44
Facies 2A (F2A): Interlaminated fine-grained sands, silts, and muds	48
Facies 2B (F2B): Bioturbated heterolithic bedding	48
Facies 3 (F3): Low-angle cross-stratified sandstone	49
Facies 4 (F4): Root-bearing fine-grained sandy shale	49
Facies 5 (F5): Conglomerate / Massive medium- to coarse-grained sandstone	49
DISCUSSION	50
Sedimentological and Ichnological Characteristics of Coastal Mud Accumulation Within The Alderson Member (Hatton Gas Pool)	52
Environment of Deposition – Offshore and Mud-dominated Deltaic Coast	54
“Subaqueous Deltaic” Successions	54
<i>Shore Margin and Coastal Plain Successions</i>	56
Permeability Characteristics Of Alderson Member Facies (Hatton Gas Pool): Implications On Reservoir Development	58
SUMMARY AND CONCLUSIONS	61
REFERENCES CITED	64

**CHAPTER III – THE INFLUENCE OF PERVASIVELY
BIOTURBATED INTERVALS ON THE RESOURCE
POTENTIAL OF ALDERSON MEMBER STRATA (HATTON
GAS POOL, SOUTHWEST SASKATCHEWAN, CANADA) 70**

INTRODUCTION	70
Alderson Member (Lea Park Formation)	74
METHODS	81
Alderson Member Facies	82
Spot-Minipermeametry	85
High-pressure Mercury Injection Porosimetry Testing.....	88
Spot-Minipermeametry Test Results	91
High-pressure Mercury Injection Porosimetry Test Results.....	93
DISCUSSION	97
SUMMARY AND CONCLUSIONS	105
REFERENCES CITED.....	108
CHAPTER IV – CONCLUSIONS	115
REFERENCES CITED.....	119
APPENDIX.....	120
Legend	121
16-34-13-28W3.....	122
14-29-14-29W3.....	123
13-04-15-29W3.....	124

08-25-15-27W3.....	125
10-27-15-22W3.....	126
08-15-16-28W3.....	127
06-22-17-28W3.....	128
06-32-17-27W3.....	129
11-08-18-29W3.....	130
16-24-22-26W3.....	131

LIST OF TABLES

TABLE 2.1 —Alderson Member facies descriptions (Hatton Gas Pool area, southwest Saskatchewan).....	25
TABLE 2.2 —Permeability to air (K_a) characteristics of Alderson Member facies.....	45
TABLE 3.1 —Alderson Member facies descriptions (Hatton Gas Pool area, southwest Saskatchewan).....	83

LIST OF FIGURES

FIGURE 1.1 —Basins within Canada and the United States producing gas from fine-grained, low-permeability intervals.....	5
FIGURE 2.1 —Upper Cretaceous gas fields of southeast Alberta and southwest Saskatchewan, Canada.....	14
FIGURE 2.2 —Santonian – Campanian stratigraphic architecture of Alberta, Saskatchewan, and north-central Montana.....	16
FIGURE 2.3 —Study area and locations of studied drill-core. Hatton Gas Pool, southwest Saskatchewan, Canada.....	19
FIGURE 2.4 —Core Laboratories PDPK-400 Pressure Decay Profile Permeameter.....	22
FIGURE 2.5 —Facies 1, photo plate.....	28
FIGURE 2.6 —Facies 2, photo plate.....	34
FIGURE 2.7 —Facies 2B, thin section photos.....	37
FIGURE 2.8 —Examples of Facies 3, Facies 4, and Facies 5 (photo plate).....	39
FIGURE 2.9 —Spot-minipermeametry testing of Alderson Member facies.....	46
FIGURE 3.1 —Upper Cretaceous gas fields of southeast Alberta and southwest Saskatchewan, Canada.....	75
FIGURE 3.2 —Subsurface architecture of early Campanian—late Santonian strata in southeast Alberta and southwest Saskatchewan.....	77
FIGURE 3.3 —Examples of <i>Phycosiphon</i> in drill-core, photo plate.....	79
FIGURE 3.4 —Study area and locations of examined drill-core. Hatton Gas Pool, southwest Saskatchewan, Canada.....	81
FIGURE 3.5 —Core Laboratories PDPK-400 Pressure Decay Profile Permeameter.....	86
FIGURE 3.6 —Spot-minipermeametry testing: Facies 1A and 2B.....	92
FIGURE 3.7 —High-pressure mercury injection porosimetry testing of Alderson Member facies.....	94

FIGURE 3.8 —Facies 2B: Permeability distribution and resource characteristics.....	98
FIGURE 3.9 —West-east stratigraphic transect through the Hatton Gas Pool. Facies correlations derived using gamma-ray butterfly curves..	102
FIGURE 3.10 —Sedimentological, ichnological, and stratigraphical observations used in the construction of Figure 3.9.....	104

LIST OF SYMBOLS AND ABBREVIATIONS

ICHNOFOSSILS

Ar *Arenicolites*

As *Asterosoma*

Ch *Chondrites*

Dp *Diplocraterion*

Fu fugichnia

Pa *Palaeophycus*

Ph *Phycosiphon*

Pl *Planolites*

Hm *Helminthopsis*

Sch *Schaubcylindrichnus*

Sch (fr) *Schaubcylindrichnus freyi*

Sco *Scolicia*

Sk *Skolithos*

Te *Teichichnus*

Th *Thalassinoides*

Zo *Zoophycos*

MISCELLANEOUS

BI Bioturbation Index

CT Computed Tomography

K_a Permeability to air

MRI Magnetic Resonance Imaging

SCF Standard Cubic Feet

TOC Total Organic Carbon

TCF Trillion Cubic Feet

U.S.A. United States of America

ICHNOFOSSIL OCCURRENCE

A Abundant

C Common

M Moderate

R Rare

CHAPTER 2 ABBREVIATIONS

F1	Facies 1	F3	Facies 3
F1A	Facies 1A	F4	Facies 4
F1B	Facies 1B	F5	Facies 5
F1C	Facies 1C	PC 1	Permeability Classification 1
F2	Facies 2	PC 2	Permeability Classification 2
F2A	Facies 2A	PC 3	Permeability Classification 3
F2B	Facies 2B		

CHAPTER 3 ABBREVIATIONS

F1A	Facies 1A	HPMIC	High Pressure Mercury Intrusion Curve
F2B	Facies 2B	PTS	Pore Throat Sorting
GR	Gamma-ray		

BIOTURBATION INDEX (BI)

Reineck (1963). Later modified by Droser & Bottjer (1986), and Taylor & Goldring (1993).

Grade	Percent Bioturbated	Classification
0	0	No bioturbation
1	1 – 4	Sparse bioturbation, bedding distinct, few discrete traces and/or escape structures
2	5 – 30	Low bioturbation, bedding distinct, low trace density, escape structures often common
3	31 – 60	Moderate bioturbation, bedding boundaries sharp, traces discrete, overlap rare
4	61 – 90	High bioturbation, bedding boundaries indistinct, high trace density with overlap common
5	91 – 99	Intense bioturbation, bedding completely disturbed (just visible), limited reworking, later burrows discrete
6	100	Complete bioturbation, sediment reworking due to repeated overprinting

This thesis follows a paper format. Arranging the document in this manner has resulted in the repetition of large portions of text within several chapters. To facilitate ease of reading, a short summary of each chapter is provided below.

CHAPTER 1 – Provides an introduction to the thesis and includes a general summary of fine-grained, low-permeability unconventional gas systems, their lithological characteristics, and production history.

CHAPTER 2 – Presents a facies classification scheme for Alderson Member strata in the Hatton Gas Pool area and evaluates the reservoir potential of certain facies using results from spot-minipermeametry testing.

CHAPTER 3 – The influence of pervasively bioturbated rock fabrics on the overall resource potential of the Alderson Member is evaluated using spot-minipermeametry and high-pressure mercury injection porosimetry methods.

CHAPTER 4 – Provides a detailed summary of the major findings discussed in Chapters 2 and 3.

CHAPTER I – INTRODUCTION

Over the coming decade, global growth in natural gas demand is expected to average 3.2% (Odedra et al., 2005). By the year 2025, worldwide consumption of gas will approach 162 TCF; nearly double the 1999 value of 84 TCF (DOE/EIA, 2002; Law and Curtis, 2002; EIA 2003). In conjunction with the liberalization of gas markets, demand increases shall generate immense opportunities for gas producers. In order to meet the rising energy needs of developing and industrialized nations, exploration geologists and reservoir engineers will be challenged to locate and produce higher and higher volumes of gas on an annual basis. Although conventional gas reserves appear to be sufficient for around 60 years supply at current global gas production rates (Odedra et al., 2005), the development of enormous resources contained within unconventional petroleum systems will become more important as the production from conventional gas reservoirs begins to peak.

Differentiating between conventional and unconventional gas systems varies by region. In North America, initial distinctions were based primarily on economics. In the early 1970's, most exploration geologists considered marginally economic resources such as coalbed methane, shale gas, and low-permeability sandstones unconventional (Law and Curtis, 2002). However, beginning in the late 1970's, rising commodity prices combined with federally funded research stimulated substantial development within these play types. It was

soon demonstrated that unconventional gas accumulations, like those mentioned previously, were in fact economically viable resources. Consequently, many exploration companies no longer refer to gas systems like these as unconventional (Law and Curtis, 2002).

Conventional natural gas reservoirs are well understood with recognized worldwide reserves in excess of 5.5×10^{15} SCF (EIA, 2003; Odedra et al., 2005). Together, North America and Europe have produced more than 50% of their total estimated conventional natural gas reserves (Odedra et al., 2005). In these areas, the discovery of additional reserves (conventional gas) will only occur if exploration extends deeper into sedimentary basins, into deeper waters, and into new plays (Odedra et al., 2005). In the future, unconventional gas systems will be used increasingly to supplement high volume demand in developed markets, as well as a major long-term source of energy. This trend is already evident in the United States, as more than a quarter of the nations daily gas production is currently derived from resources contained in coal beds, fractured shales, and low-permeability sandstone reservoirs (Law and Curtis, 2002). Furthermore, enormous gas reserves exist in regionally extensive, fine-grained (clays, silts, and very fine-grained sands), low-permeability intervals in various basins across Canada and the United States (*e.g.*, Cretaceous Alderson Member / Milk River Formation, Western Canada Sedimentary Basin [Canada/U.S.A.]; Devonian Antrim Shale, Michigan Basin [U.S.A.]; Devonian-Mississippian Woodford Shale, Arkoma Basin [U.S.A.]; Mississippian Barnett Shale, Forth Worth Basin

[U.S.A.]) (Figure 1.1). Moreover, in some locales, methanogenic bacteria generate immense volumes of natural gas during early burial (Odedra et al., 2005). Gas reserves of this character are located in shallow Cretaceous reservoirs in southeast Alberta, southwest Saskatchewan, and in central and eastern Montana (Shurr and Ridgley, 2002). In these areas, reservoir units are distributed as a continuous blanket over the entire northern Great Plains; however, main hydrocarbon production is limited to the margins of structural basins: the southeastern margin of the Western Canada Sedimentary Basin, the northwestern and southwestern margins of the Williston basin, and the northern margin of the Powder River basin (Figure 1.1) (Shurr and Ridgley, 2002). The Alderson Member / Milk River Formation reservoirs in southeast Alberta and southwest Saskatchewan (Western Canada Sedimentary Basin; Figure 1.1) have been estimated to contain approximately 10 – 21 TCF of gas (O’Connell, 2003; Pemberton, personal communication, 2009); however, resource volumes such as these are commonly undervalued. Unfortunately, the stigma of high risk and low recovery associated with shallow biogenic gas wells persists. In many cases, these enormous volumes are neglected as possible solutions for increased natural gas demands (Shurr and Ridgley, 2002). Compared to deep and basin-centered gas systems, shallow biogenic gas systems have received very little scientific investigation (Shurr and Ridgley, 2002). With the emergence of unconventional gas systems as viable energy resources, exploration geologists must continually modify their understanding of low-permeability, gas-charged intervals. Failure to correctly

identify the resource properties of unconventional gas systems will result in the use of inappropriate assessment methodology and the derivation of invalid reserve estimates.



FIGURE 1.1: Enormous gas reserves exist in regionally extensive, fine-grained, low-permeability intervals that blanket various basins in Canada and the United States of America. Shallow biogenic gas resources occur along the margins of the Michigan and Williston basins, and in southeast Alberta and southwest Saskatchewan, Canada. This study focuses on the Alderson Member (Lea Park Formation) of southeast Alberta and southwest Saskatchewan (Western Canada Sedimentary Basin – highlighted in orange).

Shallow, low-permeability, gas-charged formations commonly contain thick intervals of pervasively bioturbated rock fabrics. The highly prolific nature of these units has led to the suggestion that bioturbation may contribute to the

storativity and deliverability of gas. Be that as it may, bioturbation is generally considered detrimental to the permeability of reservoir rocks. This view stems from poorly sorted texture induced by the biogenic churning of laminated sediments. As a result, a reduction in overall permeability is thought to occur (Pemberton and Gingras, 2005). However, not all bioturbation is destructive and several examples of bioturbation-enhanced bulk permeability have been reported in the geological literature (*e.g.*, Dawson, 1978; Gunatilaka et al., 1987; Zenger, 1992; Gingras et al., 1999; 2004a, b; Mehrthens and Selleck, 2002; McKinley et al., 2004; Sutton et al., 2004; Pemberton and Gingras, 2005; Gingras et al., 2007; Cunningham et al., 2009). Although these positive cases are known, the understanding of permeability enhancement facilitated by biogenic processes is still quite primitive.

This study focuses on the Upper Cretaceous Alderson Member of southeast Alberta and southwest Saskatchewan (Canada), and is distinguished from earlier studies by incorporating ichnological, permeability, and porosity data. The Alderson Member is an example of a giant gas-play centered on low-permeability, gas-prone, non-associated reservoirs (Hovikoski et al., 2008). The fields contained within this play produce from continuous and laterally extensive intervals that occur at depths of less than 600 m (~ 2000 ft) (Hovikoski et al., 2008). The vast majority of Alderson Member strata are pervasively bioturbated. To assess whether or not bioturbated rock fabrics contribute to the overall resource potential of this highly prolific gas producer, core analysis

was conducted on ten drill-cores from the Hatton Gas Pool of southwest Saskatchewan. Sedimentological and ichnological characteristics were used to subdivide Alderson Member strata into five facies, and five subfacies. The results improve understanding with regard to the ichnological and sedimentological characteristic of shallow-marine mudrocks, and are potentially useful for the recognition of similar deposits elsewhere. Permeability and porosity testing of each Alderson Member facies was conducted using spot-minipermeametry and high-pressure mercury injection porosimetry methods. Analyses attempted to illustrate: 1) the storativity and deliverability potential of each facies; 2) subsurface distribution of permeability fields; and, 3) the effects pervasively bioturbated rock fabrics have on the resource potential of Alderson Member strata. The reservoir development strategies proposed herein are of particular significance, as pervasively bioturbated rock fabrics appear to be common in other low-permeability, gas-charged rock intervals.

REFERENCES CITED

- CUNNINGHAM, K.J., SUKOP, M.C., HUANG, H., ALVAREZ, P.F., CURRAN, H.A., RENKEN, R.A., AND J.F. DIXON, 2009, Prominence of ichnologically influenced macroporosity in the karst Biscayne aquifer: Stratiform “super-K” zones: Geological Society of America, Bulletin, v. 121, p. 164 – 180.
- DAWSON, W.C., 1978, Improvement of sandstone porosity during bioturbation: American Association of Petroleum Geologists, Bulletin, v. 62, p. 508 – 509.
- (DOE/EIA) U.S. DEPARTMENT OF ENERGY, ENERGY INFORMATION AGENCY, 2002, International Energy Outlook 2002, Report DOE/EIA – 0484, 21p.

- (EIA) ENERGY INFORMATION ADMINISTRATION, 2003, International Energy Outlook 2003: Natural Gas, Report DOE/EIA – 0484. World Wide Web Address: http://www.eia.doe.gov/oiaf/ieo/nat_gas.html.
- GINGRAS, M.K., PEMBERTON, S.G., MENDOZA, C.A., AND F. HENK, 1999, Assessing the anisotropic permeability of *Glossifungites* surfaces: Petroleum Geoscience, v. 5, p. 349 – 357.
- GINGRAS, M.K., MENDOZA, C.A., AND S.G. PEMBERTON, 2004a, Fossilized worm burrows influence the resource quality of porous media: American Association of Petroleum Geologists, Bulletin, v. 88, p. 875 – 883.
- GINGRAS, M.K., PEMBERTON, S.G., MUEHLENBACHS, K., AND H. MACHEL, 2004b, Conceptual models for burrow-related, selective dolomitization with textural and isotopic evidence from the Tyndall Limestone: Geobiology, v. 2, p. 21 – 30.
- GINGRAS, M.K., PEMBERTON, S.G., HENK, F., MACEachern, J.A., MENDOZA, C., ROSTRON, B., O'HARE, R., SPILA, M., AND K. KONHAUSER, 2007, Applications of ichnology to fluid and gas production in hydrocarbon reservoirs, *in* MacEachern, J.A., Bann, K.L., Gingras, M.K., and Pemberton, S.G., eds., Applied Ichnology: SEPM, Short Course Notes 52, p. 129 – 143.
- GUNATILAKA, A., AL-ZAMEL, A., SHERMAN, A.J., AND A. REDA, 1987, A spherulitic fabric in selectively dolomitized siliclastic crustacean burrows, northern Kuwait: Journal of Sedimentary Petrology, v. 57, p. 927 – 992.
- LAW, B.E., AND J.B. CURTIS, 2002, Introduction to unconventional petroleum systems: American Association of Petroleum Geologists, Bulletin, v. 86, no. 11, p. 1851 – 1852.
- McKINLEY, J.M., LLOYD, C.D., AND A.H. RUFFELL, 2004, Use of variography in permeability characterization of visually homogeneous sandstone reservoirs with examples from outcrop studies: Mathematical Geology, v. 36, p. 761 – 779.
- MEHRTHENS, C., AND B. SELLECK, 2002, Middle Ordovician section at Crown Point Peninsula, *in* J. McLelland and P. Karabinos, eds., Guidebook for fieldtrips in New York and Vermont. University of Vermont, p. B5.1 – B5.16.

- HOVIKOSKI, J., LEMISKI, R., GINGRAS, M., PEMBERTON, S.G., AND J. MACEachern, 2008, Ichnology and sedimentology of a mud-dominated deltaic coast: Upper Cretaceous Alderson Member (Lea Park Fm.), Western Canada: *Journal of Sedimentary Research*, v. 78, p. 803 – 824.
- O'CONNELL, S.C., 2003, The Second White Specks, Medicine Hat and Milk River formations – A shallow gas workshop, consult. rep.
- ODEDRA, A., BURLEY, S.D., LEWIS, A., HARDMAN, M., AND P. HAYNES, 2005, The world according to gas, *in* Dore, A.G. and Vining, B.A., eds., *Petroleum Geology: North-West Europe and Global Perspectives – Proceedings of the 6th Petroleum Geology Conference*, p. 571 – 586.
- PEMBERTON, S.G., AND M.K. GINGRAS, 2005, Classification and characterizations of biogenically enhanced permeability: *American Association of Petroleum Geologists, Bulletin*, v. 89, p. 1493 – 1517.
- SHURR, G.W., AND J.L. RIDGLEY, 2002, Unvonventional shallow biogenic gas systems: *American Association of Petroleum Geologists, Bulletin*, v. 86, no. 11, p. 1939 – 1969.
- SUTTON, S.J., ETHERIDGE, F.G., ALMON, W.R., DAWSON, W.C., AND K.K. EDWARDS, 2004, Textural and sequence-stratigraphic controls on sealing capacity of Lower and Upper Cretaceous shales, Denver basin, Colorado: *American Association of Petroleum Geologists, Bulletin*, v. 88, p. 1185 – 1206.
- ZENGER, D.H., 1992, Burrowing and dolomitization patterns in the Steamboat Point Member, Bighorn Dolomite (Upper Ordovician), northeast Wyoming: *Contributions to Geology*, v. 29, p. 133 – 142.

CHAPTER II – SEDIMENTOLOGY, ICHNOLOGY, AND RESOURCE CHARACTERISTICS OF THE LOW- PERMEABILITY, GAS-CHARGED ALDERSON MEMBER, HATTON GAS POOL, SOUTHWEST SASKATCHEWAN, CANADA

INTRODUCTION

Interdeltaic muddy shorefaces, tidal flats, and down-drift deltaic environments are typical forms of mud-dominated, open-coast shorelines. Within these environments, wave- and/or tide-agitated, hyperpycnal and hypopycnal mud plumes are common sediment dispersal mechanisms (Bhattacharya and MacEachern, 2009). Compared to their sand-dominated counterparts, mud-dominated coastlines remain understudied. Despite the growing number of modern-day examples (*e.g.*, Brazil – Guiana, Louisiana [U.S.A.], Kerala [India], Carpentaria [Australia]), documented examples of muddy coastline deposits in the geological record remain quite rare (Rhodes, 1982; Rine and Ginsburg, 1985; Mallik et al., 1988; Neill and Allison, 2005). Recently, it has been suggested that only a small portion of mud supply actually escapes to deeper-water environments in low-gradient, low-energy settings, and instead, the locale of mud accumulation is more typically the coastal zone. This idea is based on the observation that few sedimentary processes and a comparatively low sediment flux account for the transportation of fine-grained sediment to distal offshore settings (below storm-weather wave base) (Nittrouer and Wright, 1994). This shift in thought is supported by the fact that nearshore locales are prone to the formation of fluid

muds via various transport processes (*e.g.*, wave and tide agitation, estuarine flow convergence, salinity flocculation). Therefore, these environments should account for significant deposition of fine-grained sediments (*e.g.*, Nittrouer and Wright, 1994; Wright and Nittrouer, 1995; Geyer et al., 2004; Khan et al., 2005). For these reasons, the formation of thick basinal shale units has been thought to require considerable shifts of shoreline position (Dalrymple and Cummings, 2005). However, the rarity of recognized coastal mudstone units in the geological record makes the concept of mud deposition in nearshore locales quite suspicious.

The main problems regarding the recognition of ancient shallow-marine mudrocks may relate to inferring the initial water depths and the depositional energy levels of mud-dominated strata. The presence of large quantities of mud, coupled with a low-gradient, dissipative shoreline, effectively dampens incoming wave energy, even in unbarred coastal settings (Wells and Coleman, 1981; Rine and Ginsburg, 1985; Mallik et al., 1988; Huh et al., 2001; Hovikoski et al., 2008). Commonly, lithological make-up of source area material leads to suspension plumes or fluid muds rich in swelling clays (*e.g.*, Surinam Coast, northwest corner of South America). Detailed study of analogous unlithified strata is quite challenging due to logistical issues encountered in the highly turbid, fluid-bottomed settings. Additionally, shale-on-shale erosional contacts, like those produced during storms, can be subtle and potentially difficult to recognize, especially in drill-core (Schieber 1998b, 2003).

The purpose of this study is to describe the ichnological and sedimentological characteristics of a gas-charged muddy unit interpreted to represent offshore and mud-dominated, deltaic coastline deposits. This study focuses on the Upper Cretaceous Alderson Member (Lea Park Formation) of western Canada; in particular, the strata encountered within the highly prolific Hatton Gas Pool of southwest Saskatchewan. The Alderson Member comprises up to 200 metres (~ 600 ft) of bentonitic sandy mudstones that have previously been regarded as a shelfal unit deposited hundreds of kilometres seaward from the coeval shoreline (*e.g.*, Meijer Drees and Mhyr, 1981). Recently, the Alderson has been reinterpreted as deltaically influenced (O’Connell, 2003; Pedersen, 2003; Hovikoski et al., 2008). This study discusses the influence of waves and onshore tidal processes, and reports the presence of root bearing horizons within the studied successions. The results improve understanding of the ichnological and sedimentological characteristics of shallow-marine mud units, and are potentially useful for the recognition of similar deposits elsewhere. Additionally, this study presents a facies classification scheme developed for Alderson Member strata within the Hatton Gas Pool of southwest Saskatchewan. Using Core Laboratories Pressure Decay Profiler Permeameter (PDPK – 400), each facies was characterized in terms of its permeability to air (K_a). The resulting values have provided insight into possible gas storage mechanisms within this prolific gas pool—a characteristic that to date lacks a proper explanation. These data demonstrate that particular facies within the Alderson Member favor gas

deliverability; therefore, exploration on intervals of this nature should maximize production. The resulting reservoir development strategies discussed here may prove to be beneficial to those producing from similar pervasively biturbated, low-permeability gas bearing intervals.

Description of the study area

The Campanian age Alderson Member is an example of a giant gas-play revolving around low-permeability, gas-prone, non-associated reservoirs. The Alderson Member is a clastic unit comprising pervasively bioturbated marine shales, mudstones, siltstones, and fine-grained sandstones located within the subsurface of southeast Alberta and southwest Saskatchewan, Canada. The fields contained within this play produce from continuous and laterally extensive, thin bedded, fine-grained sand within muddy units that occur at depths less than 600 m (~2000 ft) (Hovikoski et al., 2008). Within these strata, methanogenic bacteria have generated immense volumes of gas during early burial (Shurr and Ridgley, 2002; Pedersen, 2003). In many cases, the productive zones are interbedded with, or are, the source rock (Hovikoski et al., 2008). The commingling of Alderson Member, Medicine Hat Member (Niobrara Formation) and Second White Specks intervals, all of which dominated by low-permeability muddy lithologies, constitutes the largest gas reservoir ever discovered in the Western Canada Sedimentary Basin (Figure 2.1) (O'Connell, 2001; O'Connell, 2003). Conservative estimates place Alderson Member / Milk River Formation gas reserves within a 10 – 21

TCF range (O’Connell, 2003; Pemberton 2009, personal communication). It is these large quantities of gas that have made the Alderson Member an extremely lucrative target for petroleum producers.

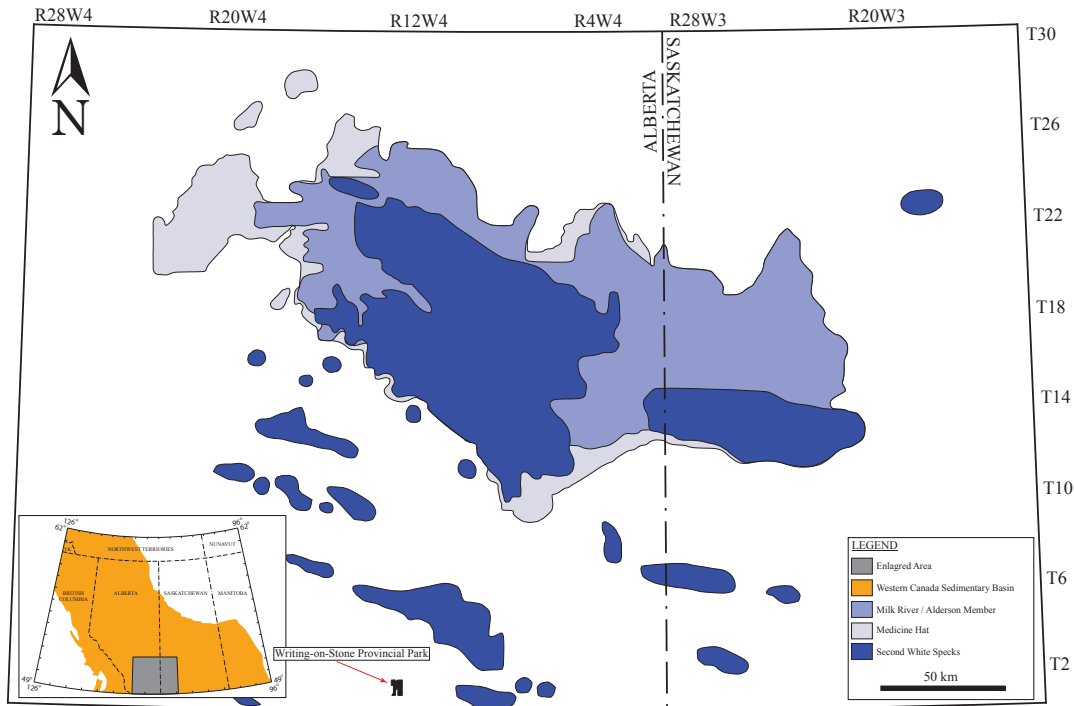


FIGURE 2.1: Upper Cretaceous gas bearing intervals of southeast Alberta and southwest Saskatchewan. The commingling of gas reserves hosted by Medicine Hat Member (Niobrara Formation), Milk River Formation / Alderson Member (Lea Park Formation), and Second White Specks strata constitutes the largest gas accumulation ever discovered in the Western Canada Sedimentary Basin. The Milk River Formation is exposed at Writing-On-Stone Provincial Park in southeast Alberta. Modified from O’Connell (2003).

In the subsurface, Alderson Member strata are present to the northeast of the depositional limit of the Virgelle sandstone (Milk River Formation) (Meijer Drees and Mhyr, 1981). The thickness of these deposits varies from approximately 110 m (~ 360 ft) in the west, to approximately 200 m (~ 660 ft) in the east (Meijer Drees and Mhyr, 1981). The northeastern limit of the Alderson is defined by the last occurrence of an extensive chert pebble horizon observed at its

top. This horizon has been dubbed the “*Milk River Shoulder*” (Meijer Drees and Mhyr, 1981; O’Connell, 2001; Payenberg, 2002a, 2002b; Pedersen, 2003), and has been interpreted as a transgressive lag, indicating a wave ravinement surface, and separates the overall regressive Milk River Formation from the transgressive Pakowki Formation (Tovell, 1956; Gill and Cobban, 1973; Meijer Drees and Mhyr, 1981). In a basinward direction (towards the northeast), this pebble bed marker disappears as it grades into a laminated shale facies (Meijer Drees and Mhyr, 1981).

In casual usage, the Alderson Member is typically referred to as a portion of the Milk River Formation, or the “*Milk River Equivalent*” (Furnival, 1946; Meijer Drees and Mhyr, 1981; Gatenby and Staniland, 2004). Although this informal terminology is commonly used, recent studies incorporating palynological, sedimentological, and radiometric data have suggested that the Alderson is, for the most part, several million years younger than the shallow marine – continental Milk River Formation deposits exposed at Writing-On-Stone Provincial Park in southern Alberta (Figure 2.1) (*e.g.*, Payenberg, 2002; Pedersen, 2003). Several studies have also established Alderson Member age equivalence with the Lea Park Formation (O’Connell, 2001; Payenberg et al., 2002; Shurr and Ridgley, 2002; O’Connell, 2003; Pedersen, 2003); however, the stratigraphic age of its lower limit has yet to be defined. For example, the base may correlate with the uppermost continental Deadhorse Coulee Member, or the top of the Milk River Formation (Shurr and Ridgley, 2002). In 2002, Payenberg

Past interpretations of the Alderson Member include deposition within a shallow, semi-restricted, epicontinental sea (Meijer Drees and Mhyr, 1981), and a shallow subtidal shelf (Goldring and Bridges, 1973). More recently, Alderson Member strata have been interpreted to represent a distal, storm-influenced shelf (Gatenby and Staniland, 2004), and a prodeltaic unit (O'Connell, 2003; Pedersen, 2003).

Despite the tremendous economic potential of the Alderson Member, surprisingly little has been published on its sedimentological, stratigraphical, and ichnological characteristics. Reasons for this deficit include:

- 1) When examining drill-core, the muddy nature of the Alderson Member makes subtle geological variations extremely difficult to observe. Repetitive work using many wells is required in order to provide significant insight (O'Connell, 2003).
- 2) Gas accumulations typically occur in broad, sheet-like sand bodies allowing for development via step-out or in-fill drilling with little requirement for detailed stratigraphical analysis. As a result, stratigraphic analyses are often disregarded as a factor in exploration success (O'Connell, 2003).
- 3) The characteristic thinly bedded reservoirs of Alderson Member strata are extremely difficult to detect on conventional wire-line logs (Meijer Drees and Mhyr, 1981).
- 4) Alderson Member strata demonstrate substantial variability in carbonate content, clay composition, TOC, and facies distribution (both laterally and

vertically). Therefore, intervals must be evaluated locally (O'Connell, 2003; Hovikoski et al., 2008).

5) Due to low rates of recovery and historically low commodity prices, gas fields of this nature have been deemed economically marginal throughout much of their history (O'Connell, 2003).

The mechanisms responsible for gas storage within the Alderson Member—like those pertaining to the highly prolific Hatton Gas Pool of southwest Saskatchewan, Canada—are poorly understood. Early facies classifications have led to the assumption that the majority of gas accumulations reside within heterolithically bedded intervals comprising thin sandstone beds and disconnected sand lenses (Meijer Drees and Mhyr, 1981; O'Connell, 2003; Pedersen, 2003). Several sequence stratigraphic and facies frameworks have been proposed for Alderson Member strata in various government reports and conference abstracts; however, to date, Hovikoski et al. (2008) have published the only extensive facies classification scheme.

This paper encompasses a comprehensive examination of Alderson Member strata using ten cores acquired from the Hatton Gas Pool area of southwest Saskatchewan, Canada. The Hatton Gas Pool covers approximately 6434 km² (~ 4000 mi²), from Townships 11 to 22, and from Ranges 22 to 30 west of the third meridian. Subsurface cores from Hatton are sparse. At the time of study, only 23 cores penetrated portions of the Alderson. The study area along with the locations of examined core is presented in Figure 2.3.

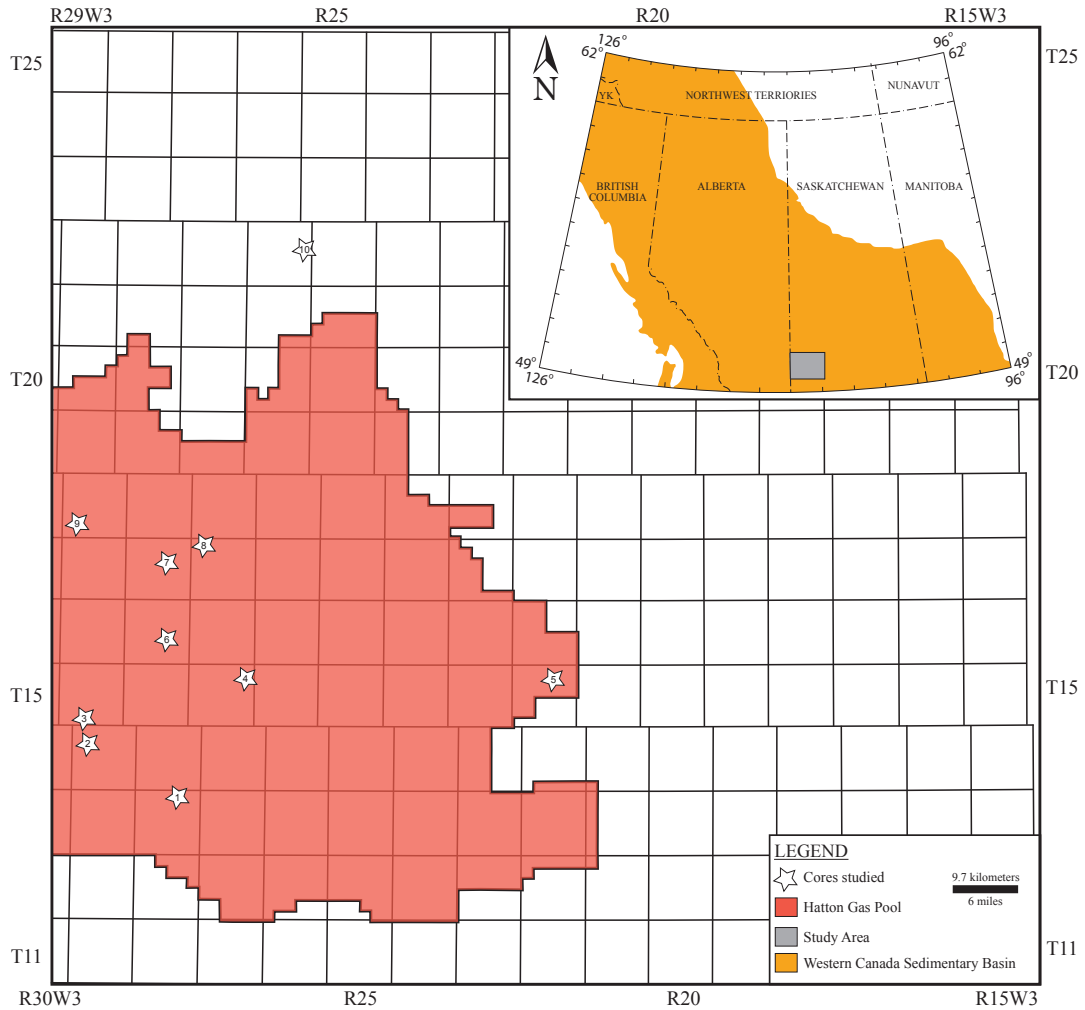


FIGURE 2.3: Study area. Top right corner shows the areal extent of the Hatton Gas Pool area in relation to the Western Canada Sedimentary Basin. The more detailed map outlines the boundaries of the Hatton Gas Pool of southwest Saskatchewan, Canada (study area). Pool boundaries are defined as of January 2003. Within the Hatton Gas Pool, nine Alderson Member drill-cores were studied. Core 10 occurs just beyond the pool limits. The locations of studied core include: 1) 16-34-13-28W3; 2) 14-29-14-29W3; 3) 13-04-15-29W3; 4) 08-25-15-27W3; 5) 10-27-15-22W3; 6) 08-15-16-28W3; 7) 06-22-17-28W3; 8) 06-32-17-27W3; 9) 11-08-18-29W3; 10) 16-24-22-26W3.

METHODS

Core analysis

This paper is based on the sedimentological and ichnological descriptions of 10 cores from the Hatton Gas Pool area of southwest Saskatchewan (Figure 2.3). Petrophysical logs along with conventional drill-core were used to collect sedimentary, stratigraphic, and ichnological data from the Alderson Member. Core analysis focused on the documentation of grain-size (visual estimation), lithology, texture, primary and secondary sedimentary structures, bedding contacts, character of bedding, soft-sediment deformation structures, the identification of important stratigraphic surfaces, and mineralogical accessories (*e.g.*, pyrite, glauconite, etc.). Ichnological data comprises description of ichnogenera and/or ichnospecies, trace fossil assemblage, and bioturbation index (BI of Reineck (1963). Later modified by Droser & Bottjer (1986), and again by Taylor & Goldring (1993)). Due to the high proportions of swelling clays present within Alderson Member facies, detailed estimations of bioturbation intensity and the ichnogenera present were not always possible. This was especially troublesome in poorly preserved facies (*e.g.*, Facies 4). Additionally, changes in grain-size are commonly subtle and not easily inferable from gamma-ray well-log data. A detailed summary of the sedimentological, ichnological, and stratigraphical observations acquired during core analysis is presented by a series of strip-logs located in the Appendix (cores 1 through 10; Figure 2.3).

Spot-minipermeametry Testing

Thirty-two core samples (10 centimetre diameter and one-third-slab) from Alderson Member drill-cores were obtained from Saskatchewan Industry and Resources Core Facility in Regina, Saskatchewan. Samples were selected in order to assess intra-facies heterogeneity. This helped to ensure a wide-ranging data set for permeability testing.

Spot-permeability analysis required a flat surface for measurements.

To facilitate this, full diameter core samples were slabbed at the University of Alberta. After each cut, compressed air was blown across the sample's test surface in order to remove sediment build up. Subsequently, spot-minipermeametry testing was conducted on Facies 1A, 2A, 2B, 3, 4, and 5 using Core Laboratories PDPK – 400 Pressure-Decay Profile Permeameter (Figure 2.4). Measurements were performed in two manners: 1) using a 5 or 10 mm spaced grid pattern, and 2) on a fabric-selective basis.

The PDPK – 400 is a pressure decay system that measures gas permeabilities from 0.001 millidarcy to greater than 30 Darcy (Core Laboratories Instruments, 1996). A schematic diagram of the PDPK – 400 is presented in Figure 2.4. Main components of this instrument include the probe assembly or travelling case (discussed below), an air tank (supplies nitrogen to the probe assembly), the core rack (holds sample), a monitor (displays measurement results), and a computer (data storage). The probe assembly comprises four accurately calibrated volumes that are initially charged with nitrogen. These

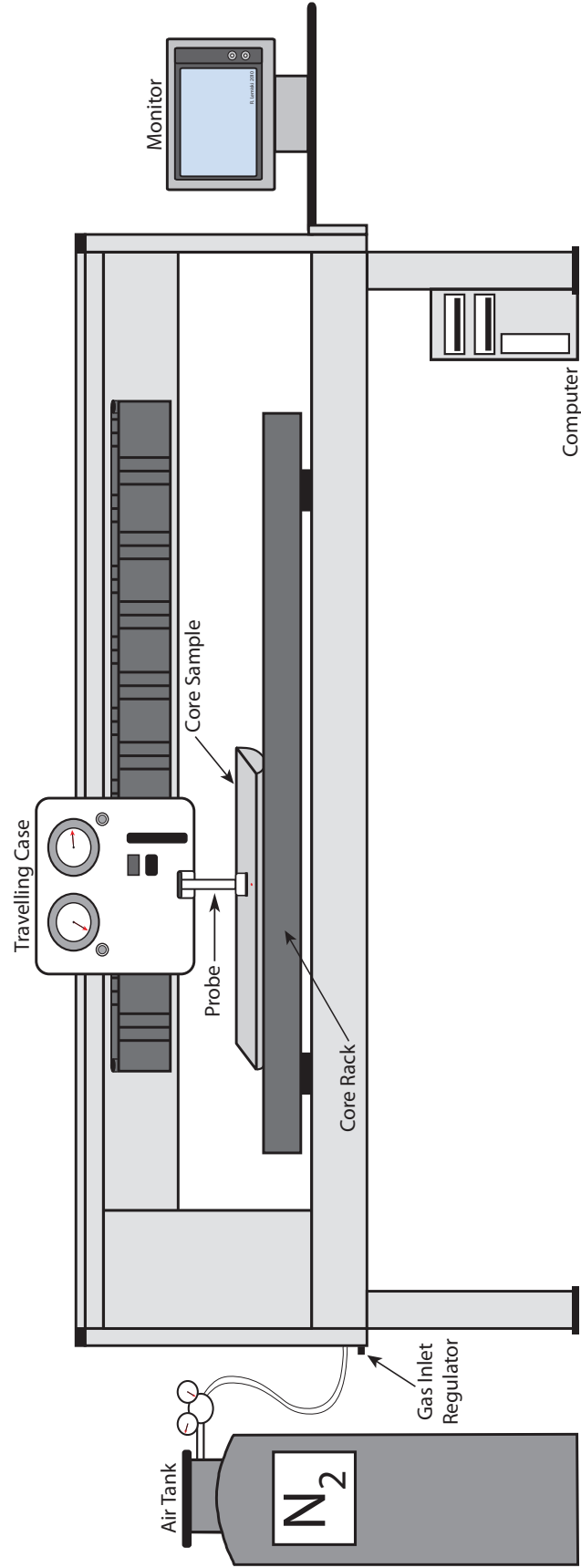


FIGURE 2.4: Core Laboratories PDPK – 400 Pressure Decay Profile Permeometer. Major components have been annotated. Modified from Core Laboratories Instruments, 1996.

volumes are referred to as the “tank supply”. Permeability measurement control devices are located on the front panel of the probe assembly. These controls consist of a probe regulator and tank supply, their respective gauges, and a firing button (initiates a permeability measurement).

Spot-minipermeametry testing was conducted by positioning the probe assembly and core rack at a desired location. To perform a permeability measurement, the probe’s rubber tip (0.46 cm diameter O-ring) was then sealed against the sample using a pneumatic cylinder. Subsequently, a computer-controlled probe valve was opened and the pressure in the tank and probe assembly was recorded as a function of time. The maximum run time of a permeability measurement is normally set at 24 seconds; however, extreme accuracy and repeatability is required for low-permeability samples (less than 0.01 md) (Core Laboratories Instruments, 1996). For that reason, a maximum run time of 30 seconds was used during spot-minipermeametry testing of Alderson Member strata.

Five measurements were obtained from each test location. Permeability values were calculated as the average of the three closest measurement values. Anomalously high measurements acquired from locations where a poor probe tip seal (*e.g.*, caused by unlevel testing surfaces, edge effects, etc.) or microfracturing was apparent were eliminated from the data set. Contour maps were then generated using the Surfer 9 gridding and contouring software package (Rockware ®, Inc., 2009).

The PDPK – 400 proved to be excellent at providing precise permeability measurements, however, due to the relatively large area tested by the probe (approximately 0.46 cm diameter), the permeability of small textural domains (*e.g.*, diminutive trace fossils) was extremely difficult to assess.

ALDERSON MEMBER FACIES – HATTON GAS POOL

In 2008, Hovikoski et al. conducted a regional subsurface study of Alderson Member strata using cores from southwest Saskatchewan and southeast Alberta. Based on sedimentological and ichnological characteristics, Alderson Member deposits were subdivided into seven recurring facies, and seven subfacies. Core analysis conducted for the purposes of this paper incorporated the facies classification developed by Hovikoski et al. (2008) as similar lithologies were encountered within the Hatton Gas Pool area.

Within the study area, five facies were identified from the suite of cores studied (F1 through F5; Table 2.1). These facies were further subdivided where distinct sedimentological or ichnological characteristics allowed. The following is a discourse on the facies classification developed for Alderson Member strata within the Hatton Gas Pool area. A summary of the facies scheme is presented in Table 2.1.

Descriptions	Occurrence / Contacts	Sedimentological Characteristics	Ichnological Characteristics	Interpretation
<p>Facies 1 (F1) F1A Phycosiphon-dominated sandy mudstone</p>	<ul style="list-style-type: none"> commonly occurs in the basal portion of upward-coarsening successions gradationally interbedded with F1B and F2 typically represents the zone of maximum flooding within a sequence 	<ul style="list-style-type: none"> light grey sandy mudstone sharp based, bioturbated sand lenses occur locally low organic matter content 	<ul style="list-style-type: none"> pervasively bioturbated (BI 4 – 6) low trace fossil diversity, including: Ph, a, Ch, m; Hm, r; Zo, r 	<ul style="list-style-type: none"> trace fossil suite represents a distal expression of the <i>Cruziana</i> ichnofacies, consistent with deposition in offshore settings lack of organic matter points to a weak deltaic influence or non-deltaic origin
<p>F1B Sandy mudstone bearing a mixed-ethology assemblage</p>	<ul style="list-style-type: none"> moderately common within middle and upper portions of the Alderson Member gradationally overlies F1A occurs below F1C, F2B, or F3 (gradational contacts) 	<ul style="list-style-type: none"> light to dark grey sandy mudstone locally high sand contents 	<ul style="list-style-type: none"> moderately to intensively burrowed (BI 2 – 6) displays a mixed-ethology assemblage moderate trace fossil diversity, including: As, r, Sch, m; Sch(fr), m; Sco, r; Ar, r; Th, m; Pl, c; Ch, c; Zo, r; Ph, a; Hm, a; fu, c typically, several size classes of each ichnogenera are present 	<ul style="list-style-type: none"> upper offshore – offshore transition environments
<p>F1C Burrow-mottled sandy mudstone</p>	<ul style="list-style-type: none"> common near the top of the Alderson Member gradationally overlies F1B, F2, or F3 grades upward into F4 or is erosionally overlain by F5 	<ul style="list-style-type: none"> light to dark grey sandy mudstone rhizolites present crosscutting the ichnofossil assemblage 	<ul style="list-style-type: none"> pervasively bioturbated (BI 5 – 6) low diversity trace fossil suite consisting of indistinct burrow mottling recognized trace fossils include: small Pl, c; Pa, r; Te, r; Dp, r; Th, r 	<ul style="list-style-type: none"> stressed (low-salinity?) setting gradation from F1C to F4 represents a change from subaqueous deposition to a subaerially exposed setting low-energy or episodic sediment accumulation in a sheltered locale
<p>Facies 2 (F2) F2A Interlaminated fine-grained sands, silts, and muds</p>	<ul style="list-style-type: none"> common in the middle portion of upward-coarsening successions within the lower Alderson Member gradationally overlies F1 grades vertically into F1C, F2B, or F3 	<ul style="list-style-type: none"> mud-dominated heterolithic bedding characterized by interlaminated sands and shales, and lenticular bedding soft-sedimentary deformation forms metre-scale successions undulating, massive dark grey shale laminae commonly 1 to 10 mm thick sandstone intervals occur as muddy and planar-parallel laminations and as mud-draped ripples high amounts of terrestrially derived organic matter 	<p>Mud rich examples:</p> <ul style="list-style-type: none"> low-diversity suite of sand filled Pl, c bioturbation intensity variable, typically low (BI 2 – 3) locally, diminutive Ch, r; Te, r; Ph/Hm, r; are present <p>Sandier examples:</p> <ul style="list-style-type: none"> contain a moderate- to low-diversity ichnofossil assemblage, including: diminutive Ph, c; Sch(fr), m; Zo, r; Th, r; Ar, r; Hm, c Th burrows sand-filled, occasionally display a muddy mantle 	<ul style="list-style-type: none"> periods of rapid episodic deposition, high sediment water contents, low and/or fluctuating salinities and high turbidity stresses, likely the result of deltaic sediment-gravity flows and wave-reworking tidal influence
<p>F2B Bioturbated heterolithic bedding</p>	<ul style="list-style-type: none"> common near the top of upward-coarsening successions gradationally overlies F2A in places, burrowed shale-on-shale erosional contacts occur 	<ul style="list-style-type: none"> bioturbated heterolithic bedding sand lithosome consists of 1 to 5 cm thick, normally graded lenses or beds sand intervals comprise scour-and-fill structures, symmetric ripples, and locally thin intervals of low-angle cross-stratification or heterolithic planar lamination interbedded mud lithosome typically consist of alternating micro-laminated, unburrowed, massive sandy shale and bioturbated shale (F1A) 	<ul style="list-style-type: none"> sand lithosome bioturbated with robust Hm, c; “lam-scrum” fabric bioturbated intervals consist of either F1A or F1B (BI 2 – 6) 	<ul style="list-style-type: none"> tempestivities active deposition under wave and/or current influence

TABLE 2.1

<p>Facies 3 (F3) Low-angle cross-stratified sandstone</p>	<ul style="list-style-type: none"> found in distinct levels near the tops of major upward-coarsening successions basal contact sharp or gradational with F2B grades vertically into F4 or F1 (rare) 	<ul style="list-style-type: none"> low-angle cross-stratified, fine- to medium-grained sandstone typically observed in 10 to 20 cm thick successions locally cemented by calcite or siderite 		<ul style="list-style-type: none"> records intervals of increased exposure to wave activity and shallower water depths siderite consistent with a paucity of ocean-derived sulphate which can be attributed to the presence of freshwater or groundwater influx inshore localities associated with LST
<p>Facies 4 (F4) Root-bearing fine-grained sandy shale</p>	<ul style="list-style-type: none"> present in the middle and upper portions of the Alderson Member gradationally overlies F1C or F2A gradationally overlain by F1 Locally, upper contact is erosional with F5 	<ul style="list-style-type: none"> grey, root bearing, massive appearing, bioturbated or heterolithically laminated to bedded, rubbly shale thin sandy interlaminae, shell-hash, and abundant terrestrial organic matter observed (coal) 10 cm to several metre thick successions pedogenic slickensides occur locally in thin intervals 	<ul style="list-style-type: none"> bioturbation typically consists of indistinct burrow mottling bioturbated, heterolithically bedded intervals display high bioturbation intensities (BI 5 – 6) lower bioturbation intensities are associated with heterolithically laminated to bedded, rubbly, fine-grained sandy shale intervals (BI 1 – 3) 	<ul style="list-style-type: none"> muddy costal plain subaerial exposure and incipient pedogenic alteration
<p>Facies 5 (F5) Conglomerate / massive coarse- to medium-grained sandstone</p>	<ul style="list-style-type: none"> discrete, sharp-based surfaces in the lower and upper portions of the Alderson Member erosionally overlies F3, F4, and to a lesser extent, F1C upper contact gradational with F1 	<ul style="list-style-type: none"> cm-thick, clast- or matrix-supported conglomeratic beds framework clasts subrounded to sub-angular, and are up to 10 mm in diameter glauconite observed locally within sandy matrix locally cemented by siderite 		<ul style="list-style-type: none"> denotes a transgressive surface of erosion (flooding surface) co-planar surface of erosion

TABLE 2.1 (continued): Facies descriptions derived from the sedimentological and ichnological logging of Alderson Member strata (Hatton Gas Pool, southwest Saskatchewan). Interpretations are expanded upon in the main body of the text. Terminology and abbreviations used in this table are summarized in a terminology and abbreviations section prior to Chapter 1.

Facies 1 (F1): Bioturbated sandy mudstone

Facies 1 is common throughout the studied intervals and comprises light to dark grey, bioturbated sandy mudstone. Bentonite and organic detritus are present in the matrix in varying amounts. The stratigraphic occurrence of this facies depends on the sub-facies (see below).

Facies 1 can be subdivided into three subfacies based on ichnological criteria: Facies 1A (F1A) is *Phycosiphon*-dominated; Facies 1B (F1B) comprises a mixed-ethology trace fossil assemblage; and Facies 1C (F1C) is characterized by small-scale burrow mottling (Figure 2.5). Subfacies 1B and 1C typically display higher interstitial sand content when compared to F1A.

Facies 1A (F1A): Phycosiphon-dominated sandy mudstone

Description

Facies 1A is common throughout the Alderson Member and generally occurs in the basal portions of extremely subtle, upward-coarsening successions. Facies 1A comprises *Phycosiphon*-burrowed, light grey, sandy mudstone (Figure 2.5A – 2.5C), and forms decimetre- to metre-scale successions. Facies 1A is gradationally interbedded with Facies 1B and 2, and locally contains sporadically distributed, sharp-based, very fine- to fine-grained sand lenses that are commonly bioturbated (Figure 2.5A). This subfacies typically contains low proportions of organic matter and interstitial sand. Other ichnogenera present include *Helminthopsis*, rare and diminutive *Schaubcylindrichnus freyi*, *Zoophycos*,

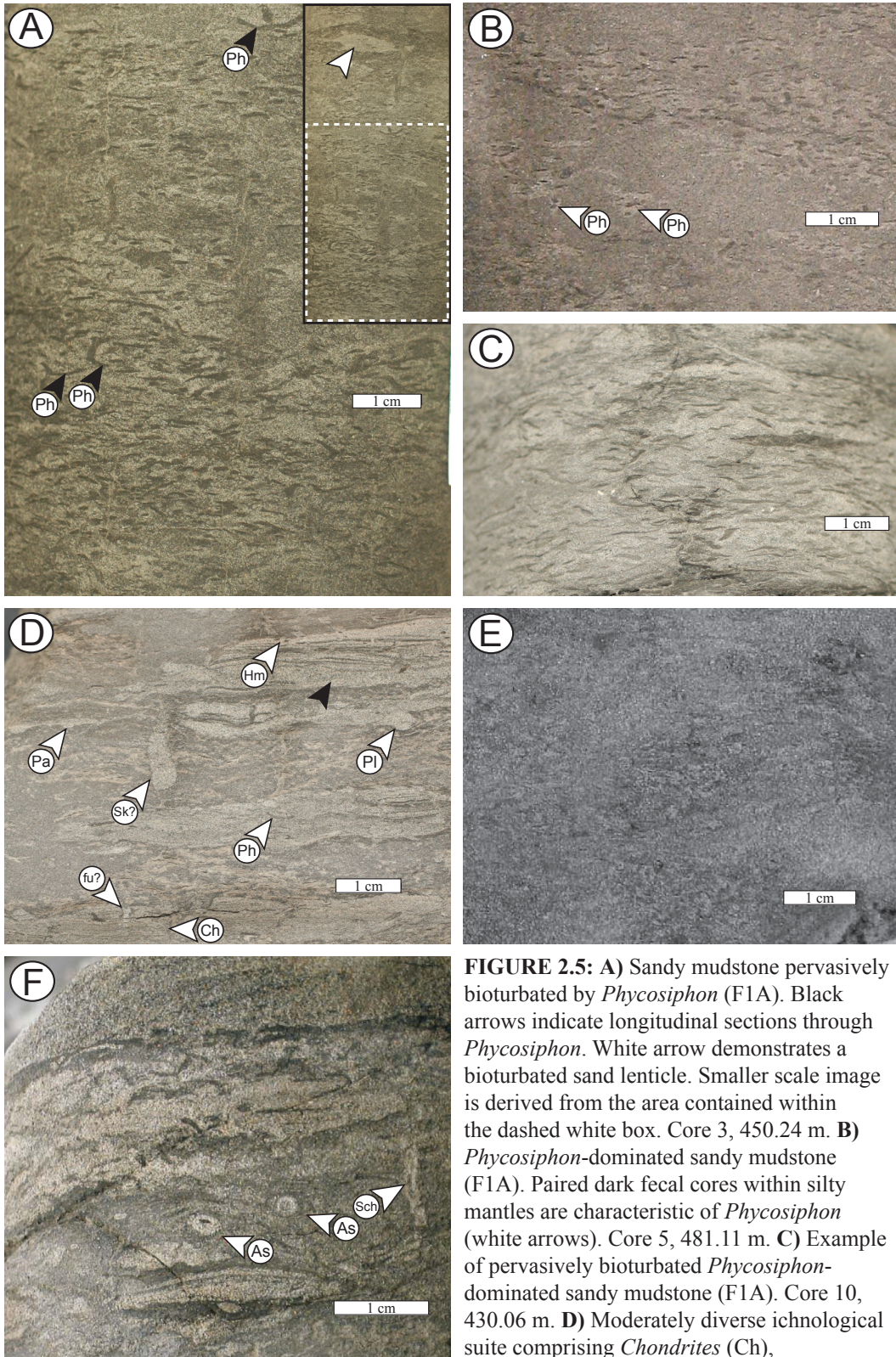


FIGURE 2.5: **A)** Sandy mudstone pervasively bioturbated by *Phycosiphon* (F1A). Black arrows indicate longitudinal sections through *Phycosiphon*. White arrow demonstrates a bioturbated sand lenticle. Smaller scale image is derived from the area contained within the dashed white box. Core 3, 450.24 m. **B)** *Phycosiphon*-dominated sandy mudstone (F1A). Paired dark fecal cores within silty mantles are characteristic of *Phycosiphon* (white arrows). Core 5, 481.11 m. **C)** Example of pervasively bioturbated *Phycosiphon*-dominated sandy mudstone (F1A). Core 10, 430.06 m. **D)** Moderately diverse ichnological suite comprising *Chondrites* (Ch),

FIGURE 2.5 (continued): *Palaeophycus* (Pa), *Planolites* (Pl), *Phycosiphon* (Ph), possibly *Skolithos* (Sk) and escape structures (fu), within a sandy mudstone lithology (F1B). Black arrow highlights a sharp-based, planar laminated sandstone interbed/lenticle. Core 9, 457.02 m. **E)** Burrow-mottled sandy mudstone (F1C). Core 8, 471.39 m. **F)** Moderately diverse trace fossil assemblage within sandy mudstone (F1B). White arrows highlight *Asterosoma* (As) and *Schaubcylindrichnus* (Sch). Less distinct ichnofossils include *Planolites*, *Schaubcylindrichnus freyi*, and *Phycosiphon*. Core 1, 445.30 m.

Chondrites, and *Planolites*. The bioturbation index ranges from localized and limited, to pervasive and intense (BI 2 – 6); however, the vast majority of F1A occurrences display extremely high bioturbation levels (BI 4 – 6).

Interpretation

Facies 1A is dominated by a grazing behavior trace-fossil suite, and represents a distal expression of the *Cruziana* Ichnofacies (MacEachern et al. 2007a, MacEachern et al. 2007b). The range in bioturbation index (BI 2 – 6) is consistent with fluctuating temperatures, salinities, and food resources in a moderate- to low-energy environment (Pemberton, 2001). As a result, burrows are predominantly constructed horizontally (*e.g.*, *Helminthopsis*, *Planolites*, *Phycosiphon*) (Pemberton et al., 2001). The extremely fine-grained nature of this facies along with the local presence of sharp-based, very fine- to fine-grained sand lenses indicates deposition near storm-weather wave base, likely within a proximal offshore to lower shoreface (above storm-weather wave base) setting.

Facies 1B (F1B): Sandy mudstone bearing a mixed-ethology trace fossil assemblage

Description

Facies 1B is moderately common within the Alderson Member. Stratigraphically, Facies 1B gradationally overlies Facies 1A and commonly occurs below Facies 1C, 2B (gradational contacts), or 3 (sharp or gradational contact). This facies consists of bioturbated, light to dark grey, very fine- to fine-grained sandy mudstone. Commonly, Facies 1B contains thin, sharp-based, planar laminated or cross-laminated, fine-grained sandstone interbeds and/or lenses (Figure 2.5D and 2.5F). Facies 1B is moderately to intensively burrowed (BI 2 – 6), has a high interstitial sand content, and exhibits a moderately diverse trace fossil assemblage comprising medium-sized *Asterosoma*, *Schaubcylichnus freyi*, *Scolicia (Laminites)*, *Arenicolites*, *Thalassinoides*, *Planolites*, *Chondrites*, *Zoophycos*, *Phycosiphon*, *Helminthopsis* and fugichnia. Typically, several size-classes of each ichnogenera are present.

Interpretation

The highest diversity examples of Facies 1B bear similarities with the archetypal *Cruziana* Ichnofacies (Pemberton et al., 2001; MacEachern et al. 2007a, MacEachern et al. 2007b). These occurrences display a mixed-ethology assemblage that consists of several suites (event, post-event, fair-weather), dominated by deposit feeding and grazing behaviors, with subordinate escape and

suspension feeding behaviors. Suites such as these tend to occur within proximal offshore to distal lower-shoreface environments (Pemberton et al., 2001).

However, Facies 1B commonly displays lower trace-fossil diversity and contains higher mud proportions. As a result, the ichnological suite appears more stressed than that characteristic of the archetypal *Cruziana* Ichnofacies.

Facies 1B forms part of a progradational offshore-coastline succession. In a landward direction, F1B grades through a burrow-mottled sandy mudstone facies (F1C) into a root-bearing shale facies (F4). Unlike that of a normal wave-dominated offshore-foreshore succession, this suggests that wave energy becomes less prominent towards the foreshore environment. This implies that occurrences of Facies 1B likely extend to shallow-water environments in the Alderson Member such as muddy lower shorefaces and/or muddy shorefaces.

Facies 1C (F1C): Burrow-mottled sandy mudstone

Description

Facies 1C comprises decimetre-scale successions of light to dark grey, fine-grained sandy mudstone that are typically rich in organic matter. Stratigraphically, Facies 1C gradationally overlies Facies 1B, 2, or 3. Upward, it grades into Facies 4 (F4; root-bearing shale), or is erosionally overlain by Facies 5 (F5; conglomerates).

Facies 1C exhibits a low diversity trace fossil suite consisting mainly of indistinct burrow mottling (Figure 2.5E). The recognized trace fossils include

pervasively distributed, diminutive *Planolites*. Subordinate traces include *Palaeophycus*, *Teichichnus*, subvertical *Diplocraterion*, and muddy mantle-bearing *Thalassinoides*. Grazing structures are locally present. Bioturbation intensities within Facies 1C are extremely high (BI 5 – 6); as a result, no primary sedimentary structures are preserved within this facies.

Interpretation

The very low diversity trace fossil suite, diminutive nature of the ichnofossils, predominance of morphologically simple deposit feeding structures such as *Planolites*, and the lack of more specialized feeding traces are all typical features of a stressed environmental setting (*e.g.*, Pemberton and Wightman, 1992; MacEachern et al., 2007a).

Stratigraphically, Facies 1C occurs below a root-bearing horizon (Facies 4). The transition from Facies 1C to Facies 4 represents a change from subaqueous deposition to a subaerially exposed setting. The high-bioturbation intensities along with the lack of typical wave-generated sedimentary structures are consistent with low-energy sediment accumulation in a sheltered locale. The presence of *Diplocraterion* and equilibrium structures such as *Teichichnus* indicates that events of high-energy sediment accumulation have also occurred (organisms attempting to keep pace with sedimentation) (Pemberton et al., 2001). Additionally, the presence of muddy-mantle bearing burrows indicates low substrate consistency. The sedimentary features and stratigraphic occurrence of

Facies 1C allows for the interpretation of episodic mud and very fine-grained sand accumulation on a low-gradient, dissipative shoreline.

Facies 2 (F2): Heterolithic bedding

Facies 2 is a volumetrically dominant facies type and is typically present in 4 to 8 metre thick successions. In the subsurface, packages comprising Facies 2 are laterally extensive and can be followed for up to tens of kilometres. Lithological and ichnological characteristics allow Facies 2 to be divided into two subfacies: Facies 2A (F2A) is mud-dominated and bears unburrowed, massive mudstone laminae; while Facies 2B (F2B) is sandy, and typically bioturbated.

Facies 2A (F2A): Interlaminated fine-grained sands, silts, and muds

Description

Facies 2A consists of mud-dominated heterolithic bedding that is principally characterized as interlaminated fine-grained sands and muds (Figure 2.6D and 2.6F). Facies 2A commonly displays penecontemporaneous soft-sedimentary deformation (Figure 2.6D and 2.6G), forms successions of metre-scale thickness that occur in the core of upward coarsening successions, and contains high proportions of continentally derived organic matter.

Stratigraphically, Facies 2A gradationally overlies Facies 1. Upward, it grades into Facies 1C, 2B, or 3. In rare instances, the top Facies 2A is gradational with Facies 4. The undulating, massive, dark grey mud laminae are commonly 1 to 10 mm

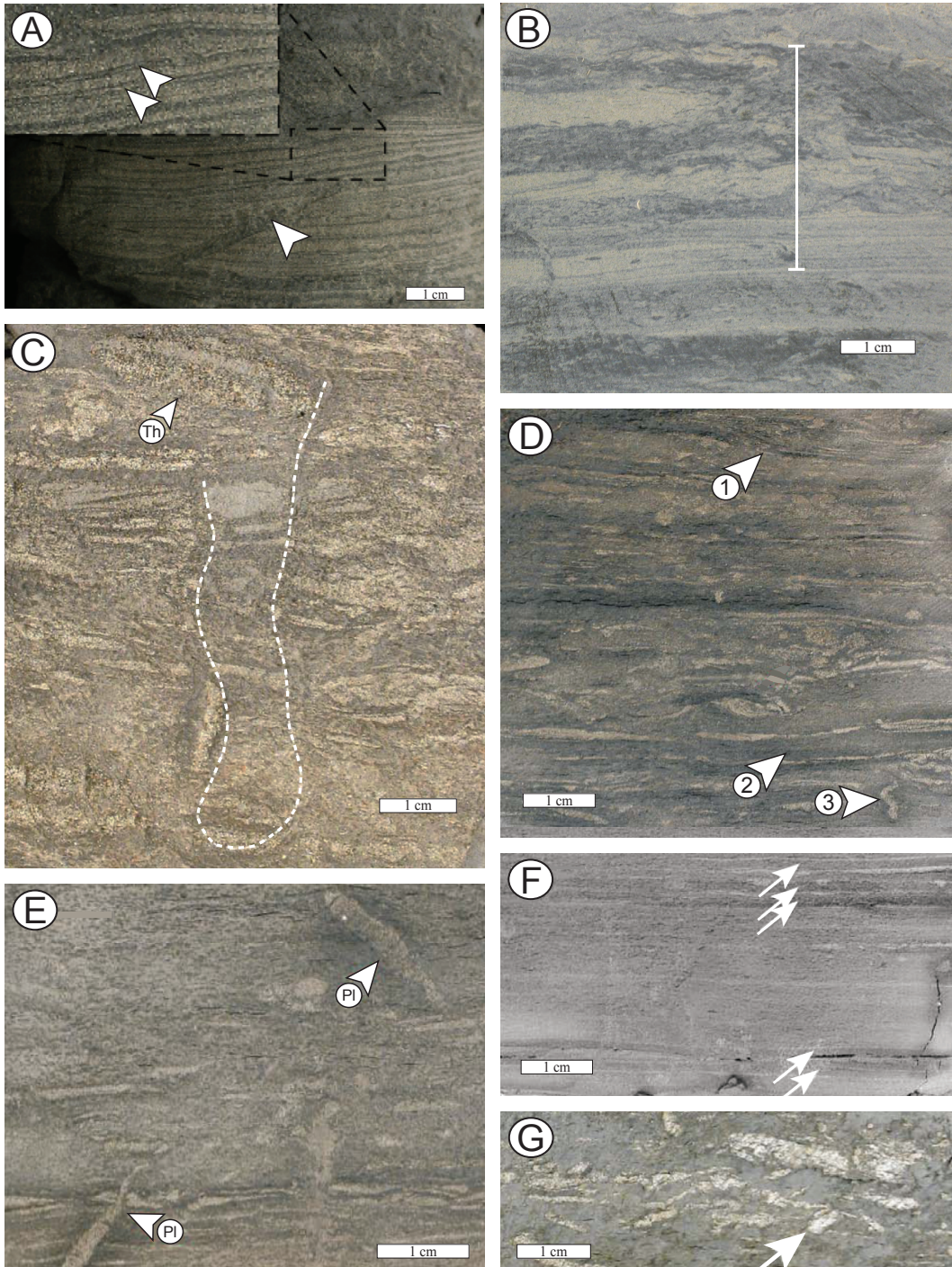


FIGURE 2.6: **A)** Heterolithic planar lamination (F2A). White arrows denote the presence of paired mud drapes. Core 7, 419.36 m. **B)** F2B – White bar highlights a laminated-to-burrowed (“lamsram”) interval. Core 2, 442.49 m. **C)** Bioturbated heterolithic bedding (F2B). Dashed white line outlines a deeply penetrating, muddy mantle-bearing *Arenicolites*. White arrow points to a sand filled *Thalassinoides* (Th). Core 4, 438.78 m. **D)** Interlaminated sand and mud fabric of F2A. Arrow 1 points to a deformed interlamination; arrow 2 demonstrates massive-appearing mud laminae/bed; arrow 3 highlights an unidentifiable deformed burrow. Core 5, 473.34 m. **E)** Deformed *Planolites* (F2A). Core 8, 462.08 m. **F)** Close-up of the interlaminated mud and sand fabric of F2A. White arrows highlight unburrowed mud laminae. Core 8, 468.97 m. **G)** Loading structure present within F2A (white arrow). Core 8, 470.87 m.

thick. Fine-grained sandy intervals occur as muddy planar-parallel laminations, and as mud-draped combined flow ripples (Figure 2.6A). Unlike Facies 2B, the tops of these particular units are normally unburrowed.

Mud-rich examples of Facies 2A commonly display deformed burrows and exhibit a very low-diversity suite of sand-filled *Planolites* (Figure 2.6D and 2.6E). Locally, diminutive *Chondrites*, *Teichichnus*, and *Phycosiphon/Helminthopsis* are present. Bioturbation intensity is variable but typically low (BI 2 – 3). Sandier examples of Facies 2A contain a low- to moderate-diversity ichnofossil assemblage, including diminutive *Phycosiphon*, *Schaubcylindrichnus freyi*, *Zoophycos*, *Thalassinoides*, *Arenicolites*, and *Helminthopsis*. *Thalassinoides* are sand-filled (fine-grained sand) and occasionally display a muddy mantle.

Interpretation

The unbioturbated, massive mud-laminae that are associated with soft-sediment deformation are best explained as the result of periods of rapid deposition. The abundance of *Planolites*-dominated suites combined with the lack of more specialized feeding traces (*e.g.*, structures attributed to suspension-feeding organisms) may point to low and/or fluctuating salinities and high turbidity stresses (MacEachern *et al.*, 2005; MacEachern *et al.*, 2007a). The deformed, mantled burrows and loading structures point to high water content within the sediment, further suggesting rapid deposition (*e.g.*, Lobza and Schieber, 1999). Rapid episodic deposition, salinity fluctuations, high turbidity,

and high water content in muddy sediments are consistent with deltaic sediment-gravity flows (Bhattacharya and MacEachern, 2009). This interpretation is further supported by high contents of terrestrially derived organic matter, which was likely delivered to the sedimentary system from a point source (untraceable in the study area).

Fluid mud deposits are typical in river-dominated and tidally influenced deltaic settings (Bhattacharya and MacEachern, 2009). In environments such as these, the intermingling of fluvial-derived clay with marine waters and/or mixing of the river effluent through tidal action (tidal influence is evidenced by mud draped combined-flow ripples) causes increased turbidity due to flocculation. As a result, concentration of fine-grained sediment occurs.

The sedimentological and ichnological characteristics of Facies 2A allow for an interpretation of deposition within a distal prodeltaic environment.

Facies 2B (F2B): Bioturbated heterolithic bedding

Description

Facies 2B is common within the Alderson Member and comprises bioturbated heterolithic bedding that occurs near the top of upward-coarsening successions in the Hatton Gas Pool area (Figure 2.6B and 2.6C). Stratigraphically, Facies 2B gradationally overlies Facies 2A. Typically, the sand-rich fraction of F2B consists of 1 to 5 cm thick, normally graded fine-grained lenses or beds. The lower contact of the sand lithosome is sharp, whereas the upper margin is

gradational and populated with robust *Helminthopsis*, leading to a laminated-to-burrowed fabric commonly referred to as “lamsclam” (Figure 2.6B). Sandstone intervals exhibit scour-and-fill structures, symmetric ripples, and locally occurring thin intervals of low-angle cross-stratification or heterolithic planar laminations. The interbedded mud lithosome typically consists of alternating micro-laminated to unburrowed massive sandy mudstone (Figure 2.7B) and bioturbated mud. In places, burrowed, shale-on-shale erosional contacts occur (Figure 2.7A). Bioturbated intervals resemble Facies 1A or 1B (BI 2 – 6). Due to the abundance of swelling clays present within the examined cores, an arbitrary limit was chosen to distinguish Facies 1A and 1B from 2B. Where the vertical distance between two sand lenses was less than 20 cm, the facies was designated Facies 2B.

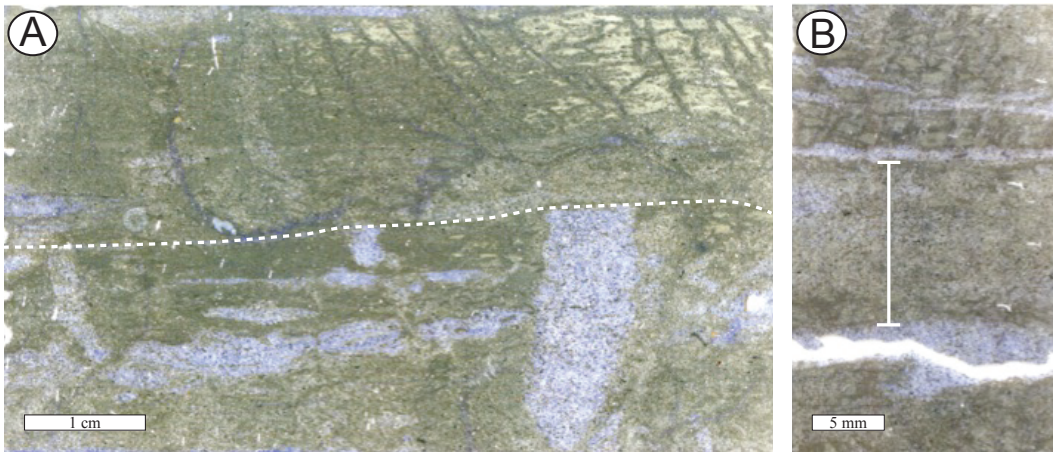


FIGURE 2.7: A) Thin section image of facies F2B. Dashed white line denotes a shale-on-shale erosional contact. This undulatory surface truncates several sub-vertical burrow structures. Core 10, 434.27 m. **B)** F2B – Thin section photo highlighting a massive sandy mudstone interval (indicated by white bar). Core 10, 434.32 m.

Interpretation

Isolated, erosionally based, low-angle cross-stratified fine-grained sand lenses are best interpreted to record periods of increased wave activity. Normal grading in these sandstone intervals, along with periodic occurrence of a “lam-scam” texture is consistent with this interpretation. Within the depositional system, a limited availability of sand is demonstrated by the presence of massive and micro-laminated muds (laminae or bed scale). Micro-laminae, intervals of unburrowed massive sandy mud, and shale-on-shale erosional contacts demonstrate active deposition under variable processes. Therefore, Facies 2B is best interpreted as a result of deposition during increased periods of wave energy (possibly tempestite deposits).

Facies 3 (F3): Low-angle cross-stratified sandstone

Description

Facies 3 occurs at the tops of major upward-coarsening successions in the Hatton Gas Pool area. Facies 3 consists of low-angle, cross-stratified, fine- to medium-grained sandstone (Figure 2.8A and 2.8B). Vertically, Facies 3 grades into Facies 4, and in rare instances Facies 1. The basal contact of Facies 3 was observed to be sharp or gradational with Facies 2B. Typically, Facies 3 is observed in 10 to 20 cm thick successions that are locally cemented by siderite. Intervals consisting of Facies 3 are unburrowed (BI 0 – 1).

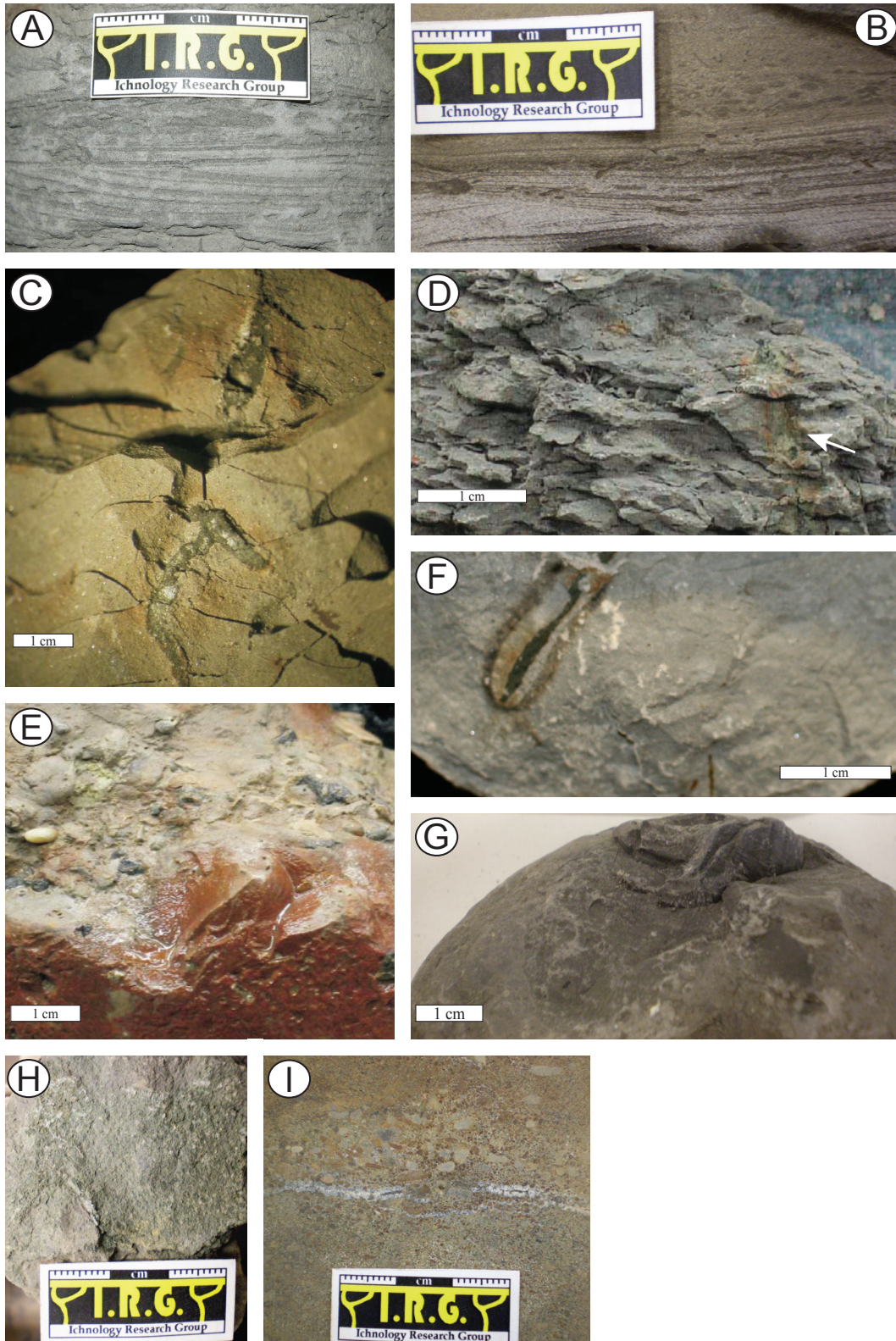


FIGURE 2.8: A, B) F3 – Examples of low-angle cross-stratified sandstone. Core 1 (444.57 m) and core 7 (427.75 m) respectively. C) F4 – Close-up of a pyritized bifurcating subvertical rhizolith. Core 5, 453.65 m. D) White arrow highlights a vertical root preserved within rubbly, organic rich shale (F4). Note the oxidized halo around the root. Core 5, 458.12 m. E) F5 – Conglomerate. Core

FIGURE 2.8 (continued): 7, 462.28 m. **F)** F4 – Bedding plane orientated organic detritus. Core 3, 449.12 m. **G)** F4 – Example of pedogenic slickensides. Core 7, 436.50 m. **H)** F5 – Massive coarse-grained sandstone bearing a glauconitic matrix (bedding plane view). Core 4, 437.53 m. **I)** F5 – Coarse-grained sandstone containing a matrix consisting of glauconite (cemented by siderite). Core 1, 474.03 m.

Interpretation

As with Facies 2B, the presence of low-angle cross-stratified sandstone is interpreted to represent exposure to increased wave activity. Siderite cement is consistent with a paucity of ocean-derived sulphate, and can be associated with the post-depositional influx of groundwater (fresh water). Stratigraphically, Facies 3 occurs at the top of very subtle upward-coarsening successions; therefore, this facies is likely associated with the late phase of progradation. The sedimentological characteristics and stratigraphic occurrence of Facies 3 allows for an interpretation of deposition within a nearshore locale under moderate to high energy levels.

Facies 4 (F4): Root-bearing fine-grained sandy shale

Description

Facies 4 consists of decimetre- to metre-thick successions of grey, root bearing, massive appearing, bioturbated (BI 5 – 6) or heterolithically laminated to bedded (BI 1 – 3), rubbly, fine-grained sandy-shale (Figures 2.8C, 2.8D, and 2.8G). Typically, Facies 4 gradationally overlies Facies 1C or 2A, while its top is marked by a gradation to Facies 1. Locally, the upper contact of Facies 4

is erosional with Facies 5 (sharp contact). In general, bioturbation consists of indistinct burrow mottling. In the Hatton Gas Pool area, root-bearing intervals occur sporadically and are interbedded with bioturbated mud or heterolithic bedding. Fine-grained sandy interlaminae, partially dissolved shell-hash, abundant terrestrial organic matter (Figure 2.8F) and coal fragments are also present in this facies. Pedogenic slickensides occur locally in thin intervals (Figure 2.8G). Facies 4 is commonly poorly preserved. As a result, detailed ichnological and sedimentological observations are extremely difficult to acquire.

Interpretation

Roots and sporadic slickensides are indicative of subaerial exposure and local pedogenic alteration. Pedogenic features are interbedded with bioturbated mud and heterolithic intervals, suggesting alternating periods of subaerial exposure and subaqueous deposition. Stratigraphically, Facies 4 occurs near the top of interpreted progradational coastal successions and commonly occurs within bioturbated mudstones (F1) and heterolithically bedded intervals (F2). The sedimentological, ichnological, and stratigraphic occurrence of Facies 4 demonstrates that the shoreline was likely mud-dominated. Facies 4 is interpreted to have been deposited downdrift from a shoreline sediment input within a coastal plain environment.

Facies 5 (F5): Conglomerate / Massive medium- to coarse-grained sandstone

Description

Facies 5 occurs as discrete, sharp-based conglomerate or coarse-grained sand layers within the Alderson Member. Facies 5 is present as centimetre-thick, clast- or matrix-supported conglomeratic layers of undefined composition (Figures 2.8E). Framework clasts are moderately rounded to subangular, and are up to 10 mm in diameter. The fine- to medium-grained, sandy matrix of Facies 5 is commonly sideritic, with medium-grained glauconite present locally (Figures 2.8H and 2.8I). Facies 5 erosionally overlies Facies 2, 3, or 4, while its upper contact is gradational with Facies 1. No biogenic structures were observed in this facies (BI 0).

Interpretation

Facies 5 punctuates or terminates progradational successions by recording erosional truncation of root-bearing shale or deltaic deposits. The presence of glauconitic sand coupled with the apparent deepening across the surface is indicative of transgressive reworking. Siderite cement is consistent with a paucity of ocean-derived sulphate, and can be associated with the post-depositional influx of groundwater (fresh water). Occurrences of Facies 5 are interpreted to overlie a transgressive surface of erosion (TSE), likely generated by wave or tidal-scour ravinement.

SPOT-MINIPERMEAMETRY RESULTS

Spot-minipermeametry test results demonstrate that facies within the Alderson Member can be characterized by one of three permeability classification types, these include:

Permeability Classification 1 (PC 1): Extremely low permeability measurements generally ranging from 1×10^{-3} to 1×10^{-1} md. These values are typically associated with Facies 3, 4, and 5.

Permeability Classification 2 (PC 2): Slightly contrasting permeability fields, where matrix permeability is within two orders of magnitude relative to burrow-associated permeability. Permeability fields of this character are typically observed in Facies 1A. Within Facies 1A, matrix permeability ranges from 2×10^{-2} to 2×10^{-1} md, while burrow-associated permeabilities range from 2×10^{-1} to greater than 1 md.

Permeability Classification 3 (PC 3): Well defined, highly contrasting permeability fields, where matrix permeability differs by more than two orders of magnitude from that of higher permeability domains. Permeability fields of this character are typically associated with Facies 2A and 2B (*e.g.*, Facies 2A – matrix permeability ranging from 2×10^{-2} to 4×10^{-1} md, while the permeability of interbedded sand laminae ranges from 1×10^1 to 8×10^1 md).

The results of spot-minipermeametry testing are presented in Table 2.2. This table contains details regarding the testing method used (either a 5 or 10 mm spaced grid arrangement, or a fabric selected test format), permeability characteristics, and a remarks column, which provides a summary of reservoir properties (if any), and the corresponding permeability classification of each Alderson Member facies. Figure 2.9 presents photos of tested core samples. The photos are annotated with spot-minipermeametry test locations and the corresponding permeability measurements in millidarcy (left). Core photos of facies comprising higher permeability measurements have been contoured to illustrate permeability field distribution within their respective fabrics. Facies exhibiting extremely low permeability measurements are not contoured due to the absence of contrasting permeability fields.

The results of spot-minipermeametry testing of Alderson Member facies and a description of the permeability fields contained within each facies, if present, are discussed below.

Facies 1A (F1A): Phycosiphon-dominated sandy mudstone (PC 2)

Although the diminutive nature of *Phycosiphon* does not permit the assessment of individual burrow permeabilities, unburrowed matrix can be compared to adjacent burrowed media. Muddy matrix fabrics exhibit permeabilities ranging from 2×10^{-2} to 2×10^{-1} md, whereas the *Phycosiphon*-dominated fabric generally display permeability measurements of approximately 2×10^{-1} to greater than 1 md (Figure 2.9A and 2.9B).

The resulting distribution of permeability fields varies from irregular, decimetre scale units, to crudely planiform, laterally discontinuous, centimetre scale “beds”.

Facies	Testing Method	Permeability Characteristics	Remarks
Facies 1A <i>Phycosiphon</i> -dominated sandy mudstone	<ul style="list-style-type: none"> • 5 mm and 1 cm grid spacing • fabric selective 	<ul style="list-style-type: none"> • diminutive biogenic sedimentary structures do not allow permeability assessment for individual burrows • muddy matrix: $2 \times 10^{-2} - 2 \times 10^{-1}$ md • <i>Phycosiphon</i>-dominated fabric: $2 \times 10^{-1} - > 1$ md • burrow permeability slightly elevated when compared to background muddy matrix 	<ul style="list-style-type: none"> • may connect discontinuous sand lenticles of F2B • possible gas reservoir / flow conduit • K classification: 2
Facies 2A Interlaminated fine-grained sands, silts, and muds	<ul style="list-style-type: none"> • 5 mm grid spacing • fabric selective 	<ul style="list-style-type: none"> • unburrowed mud laminae: $2 \times 10^{-2} - 3 \times 10^{-1}$ md • interbedded sand laminae: $1 \times 10^1 - 8 \times 10^1$ md • in general, the distribution of permeability fields follows a 1 to 20 mm thick horizontal planiform arrangement 	<ul style="list-style-type: none"> • sand lithosome is an example of a permeability streak (flow conduit) • K classification: 3
Facies 2B Bioturbated heterolithic bedding	<ul style="list-style-type: none"> • 5 mm grid spacing • fabric selective 	<ul style="list-style-type: none"> • permeabilities are variable, largely depending on the degree of bioturbation • bioturbated sand lenses: $2 - > 5$ md, whereas less bioturbated sand lenses can reach K-values approaching 7×10^1 md • interbedded muddy intervals: $6 \times 10^{-1} - 8 \times 10^{-1}$ md • permeability fields occur as planiform, vertically stacked, decimeter-scale zones 	<ul style="list-style-type: none"> • gas reservoir / flow conduit • K classification: 3
Facies 3 Low-angle cross-stratified sandstone	<ul style="list-style-type: none"> • fabric selective 	<ul style="list-style-type: none"> • cemented (siderite) intervals: $6 \times 10^{-3} - 5 \times 10^{-1}$ md • uncemented intervals: $> 1 \times 10^2$ md 	<ul style="list-style-type: none"> • K classification: 1 • K classification: 3
Facies 4 Root-bearing fine-grained sandy shale	<ul style="list-style-type: none"> • fabric selective 	<ul style="list-style-type: none"> • low permeability values ranging from $2 \times 10^{-2} - 5 \times 10^{-1}$. Values greater than 1 md do occur; however, these are rare. 	<ul style="list-style-type: none"> • K classification: 1
Facies 5 Conglomerate / massive medium- to coarse-grained sandstone	<ul style="list-style-type: none"> • fabric selective 	<ul style="list-style-type: none"> • low permeability values ranging from $5 \times 10^{-3} - 1 \times 10^1$ md. Values greater than 1 md do occur; however, these are rare. 	<ul style="list-style-type: none"> • K classification: 1

TABLE 2.2: Permeability to air (K_a) characteristics derived from spot-minipermeability testing of Alderson Member facies (Hatton Gas Pool, southwest Saskatchewan). Spot-minipermeametry was conducted using a 5 mm or 1 cm spaced grid pattern, or on a fabric selective basis. Permeability properties are characterized in three different manners. K-classification 1: extremely low permeabilities; K-classification 2: slightly contrasting permeability fields where matrix permeability is within two orders of magnitude relative to burrow-associated permeability; and, K-Classification 3: well defined, highly contrasting permeability fields where matrix permeability differs by more than two orders of magnitude relative to that of higher permeability domains.

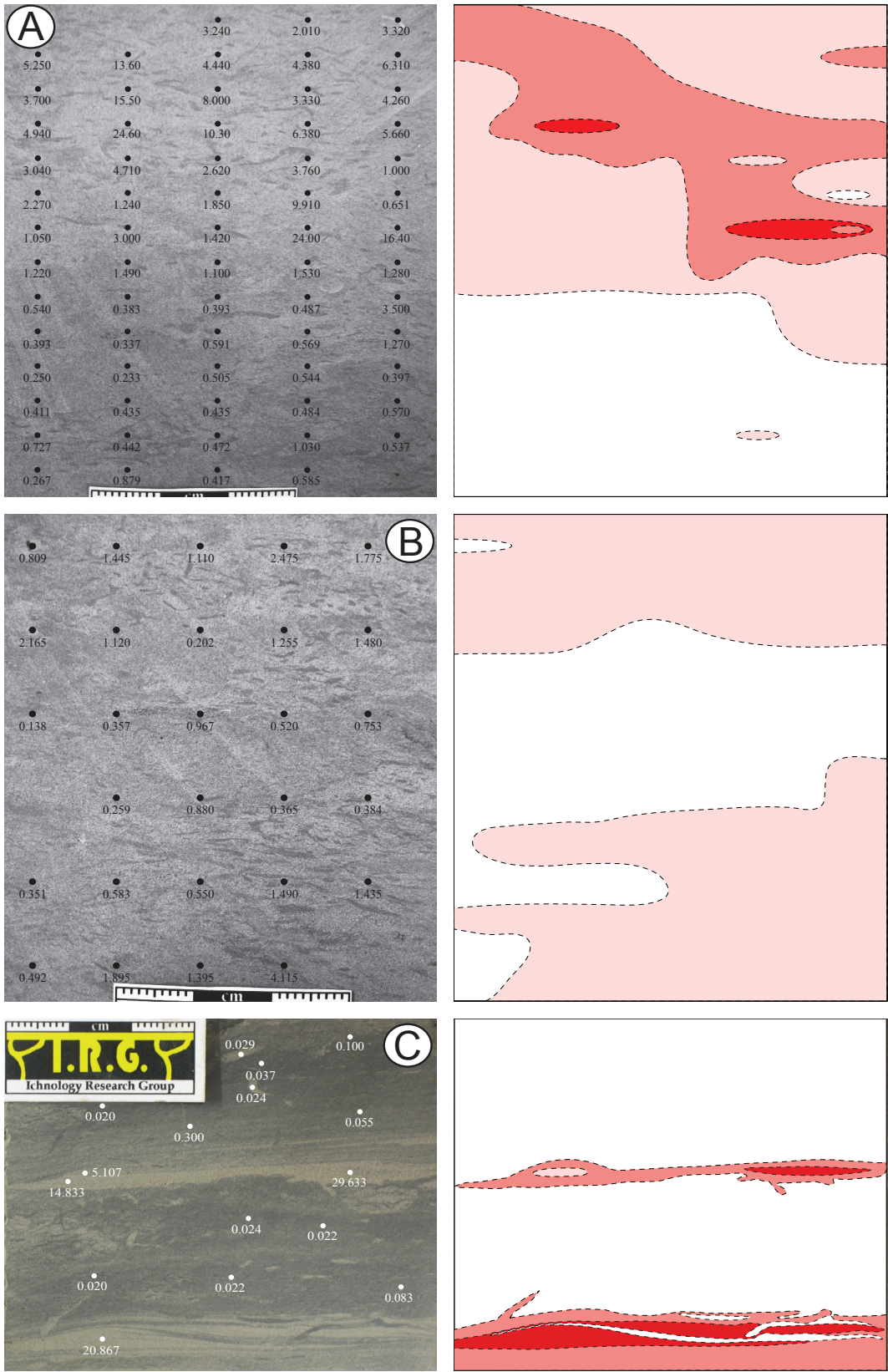


FIGURE 2.9 (figure caption located on page 48)

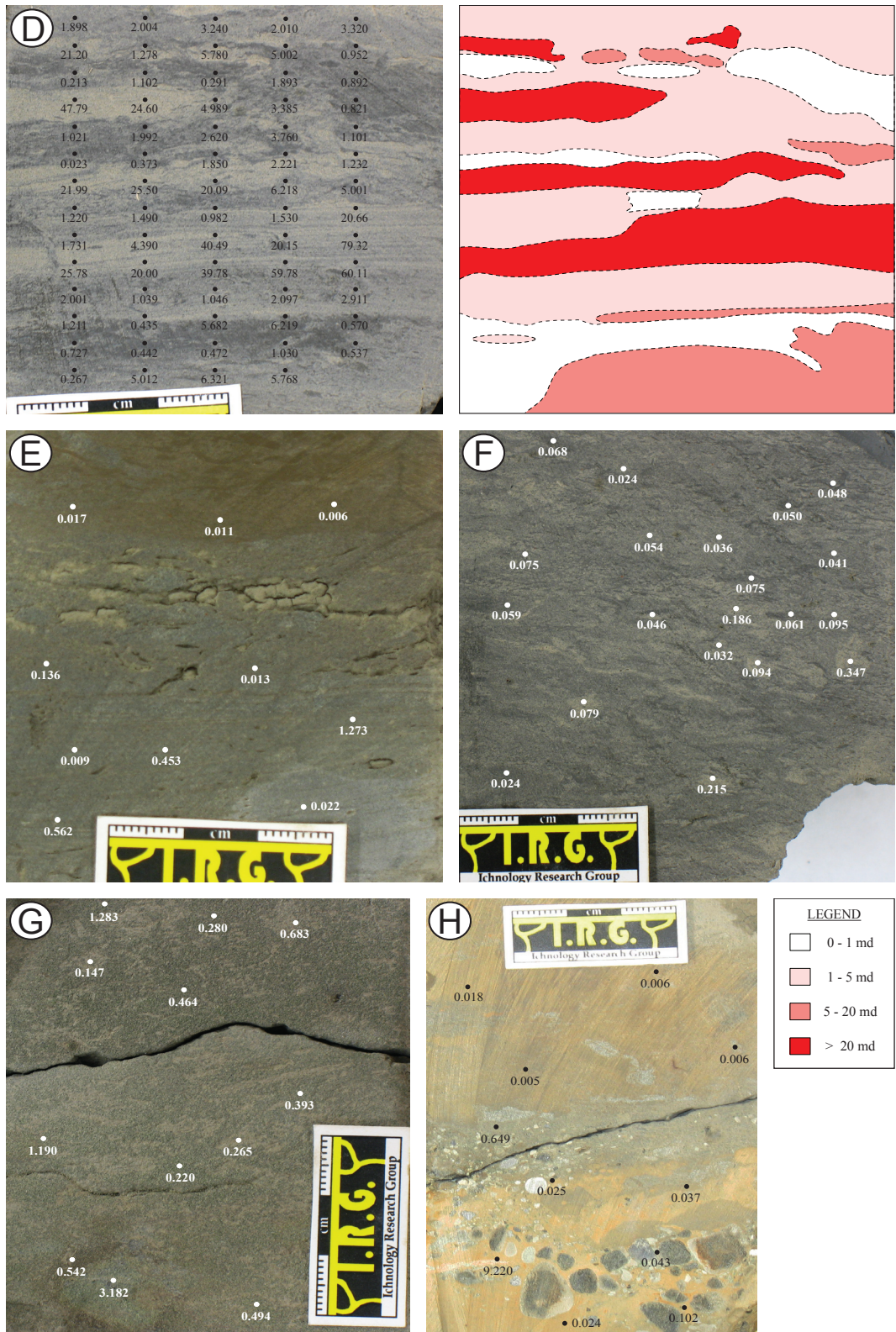


FIGURE 2.9 (figure caption located on page 48)

FIGURE 2.9: Permeability to air (K_a) characteristics of Alderson Member facies. Core photos have been annotated with spot-minipermeametry test locations and the corresponding permeability values in millidarcy. Core photos of facies comprising higher permeability values have been contoured using a combination of computer generated contours and manual contour editing. Higher permeability fields are indicated by dark pink to red colors, while light pink to white colors indicate extremely low permeability fields. **A, B)** *Phycosiphon*-dominated sandy mudstone (F1A). Slight permeability enhancement is associated with the pervasively bioturbated lithosome. Core 4, 451.45 and 452.24 m respectively. **C)** F2A - High permeability measurements are associated with unbioturbated sandy lithosomes (potential flow conduits). Massive mud lithosomes display negligible permeability. Core 5, 474.0 m. **D)** The highest K_a measurements recorded from spot-minipermeameter testing of Alderson Member facies are associated with bioturbated heterolithically bedded intervals (F2B). Core 2, 442.49 m. **E)** Low-angle cross-stratified sandstone (F3) displaying extremely low permeability measurements. Core 4, 428.98 m. **F)** Extremely low permeabilities are associated with root-bearing sandy shales (F4). Core 4, 431.00 m. **G)** F5 – Massive medium-grained sandstone exhibiting extremely low K_a measurements. Core 5, 447.82 m. **H)** Conglomerate exhibiting extremely low K_a measurements (cemented by siderite). Core 4, 437.20 m.

Facies 2A (F2A): Interlaminated fine-grained sands, silts, and muds (PC 3)

Within Facies 2A, unburrowed mud laminae exhibit permeabilities ranging from 2×10^{-2} to 3×10^{-1} md, while interbedded sand laminae display permeabilities that range from 1×10^1 to 8×10^1 md (e.g., Figure 2.9C). Locally, vertical to subvertical orientated sand-filled burrows are present and commonly exhibit permeability measurements of approximately 3×10^1 md.

In general, the distribution of permeability fields follows a 1 to 15 mm thick horizontal planiform arrangement. Additionally, local soft-sediment deformation and vertical biogenic structures serve to connect zones of higher permeability.

Facies 2B (F2B): Bioturbated heterolithic bedding (PC 3)

Due to varying degrees of bioturbation, permeabilities within Facies 2B are variable. For example, bioturbated sand lenses exhibit permeabilities ranging from 2 to greater than 5 md, whereas less bioturbated examples display permeabilities

that approach 7×10^1 md (e.g., Figure 2.9D). Interbedded bioturbated mud intervals exhibit permeabilities ranging from 6×10^{-1} to 8×10^{-1} md.

Permeability fields generally occur as planiform, vertically stacked, decimetre-scale zones. Higher permeability zones are laterally compartmentalized owing to the lensoidal shape of the sandy bedforms.

Facies 3 (F3): Low-angle cross-stratified sandstone (PC 1)

Cemented examples of Facies 3 exhibit extremely low permeability measurements ranging from 6×10^{-3} to 5×10^{-1} md (e.g., Figure 2.9E). In rare instances, thin, non-cemented, low-angle cross-stratified sandstone intervals occur. These fabrics generally exhibit permeabilities on the order of 1×10^2 md.

Facies 4 (F4): Root-bearing fine-grained sandy shale (PC 1)

In general, root-bearing fine-grained sandy shales exhibit low permeability measurements ranging from 2×10^{-2} to 5×10^{-1} md (Figures 2.9F). Locally, permeabilities greater than 1 md occur; however, these are rare.

Facies 5 (F5): Conglomerate / Massive medium- to coarse-grained sandstone (PC 1)

As with Facies 4, Facies 5 exhibits low permeability measurements ranging from 5×10^{-3} to 1×10^{-1} md (Figures 2.9G and 2.9H). Locally, permeabilities greater than 1 md occur; however, these are likely the result of a poor probe tip seal during spot-permeametry testing.

DISCUSSION

Current depositional models suggest that prograding open-coastal, distal (sea) – proximal (shore/land) successions lead to upward-coarsening grain size trends, and that facies associated with shoreline environments are commonly represented by prominent sand bodies. However, significant deviations from this model can arise, especially in locales where the availability of sand-sized sediment is limited (*e.g.*, riverine environments where sediment load is primarily dominated by suspended silt and clay particles). As a result of grain-size segregation, and dissipative, low-gradient shoreline processes, mud-dominated open-coast coastlines can result. Modern examples include the Louisiana and Brazil – Guiana coasts (*e.g.*, Wells and Coleman, 1981; Rine and Ginsburg, 1985; Neill and Allison, 2005). Furthermore, mud-dominated shallow marine depositional systems commonly develop in coastal embayments and shallow epicontinental seas, like that of the Gulf of Carpentaria (Australia) and the Adriatic Sea (Europe) (Rhodes, 1982; Cattaneo et al., 2003).

Discriminating between shallow-water and deeper-water mud deposits can be quite troublesome. This stems from difficulties in interpreting depositional energy levels within sand-deprived sedimentary systems (Schieber 1998a; Schieber et al., 2007). Underestimating the impact limited grain-size variability has on a depositional system can result in shallow marine mud deposits becoming misinterpreted as quiescent deeper-marine sediments. Recently it has been demonstrated that many fine-grained intervals contain significant volumes of

natural gas (*e.g.*, Alderson Member, southwest Saskatchewan, Canada; Barnett Shale, Fort Worth Basin, Texas, U.S.A.). Paleoenvironmental misidentification in these economically important strata is particularly hazardous, as it can lead to flawed facies interpretations, incorrect facies correlations, poor estimations on facies geometry and architecture, mapping errors, and inaccurate hydrocarbon reserve calculations. This can ultimately result in mismanaged reservoir development.

Modern mud-dominated coastal sedimentary systems commonly feature inland riverine environments that transport fine-grained sediment towards the coast. As sediment enters the marine realm, along-coast dispersal ensues. A requirement for long-distance, along-shore transportation of sediment is the presence of turbulent coastal waters. Energy of this type prevents seabed consolidation while maintaining clay and silt-size particulates in a resuspended state. This can be facilitated by wave and tide agitation, and can be further enhanced by coastal winds or storms (Geyer et al., 2004).

The aforementioned sedimentary processes result in ichnological and sedimentological properties that are characteristic to mud-dominated coastlines. These include:

- 1) High contents of continentally derived organic matter.
- 2) Low and/or fluctuating bioturbation intensities resulting from high and/or variable depositional rates (*e.g.*, Rine and Ginsburg, 1985; Neill and Allison, 2005).

3) Soft-sediment deformation and fluid mud intervals due to high interstitial water contents and soft substrate consistencies.

4) Reduced or variable trace-fossil diversity owing to turbid sedimentation. Event and post-event trace-fossil suites are impoverished as a result of heightened water turbidities and the development of soupy substrates. This causes a reduction in the proportions of trace fossils attributed to suspension-feeding and/or filter feeding-habits (Moslow and Pemberton, 1988; MacEachern et al., 2005).

5) Sedimentary structures restricted to various types of heterolithic bedding. The combination of limited grain-size variation and active wave and/or tide agitation results in shale-on-shale erosional contacts, micro-laminated and weakly nonparallel-laminated shale/mud intervals that are unbioturbated (Rine and Ginsburg, 1985; Neill and Allison, 2005; Schieber et al., 2007).

6) Intervals enriched with shelly material (*e.g.*, shell hash).

Therefore, sediment accumulation in deeper-water environments can be distinguished from coastal fluid muds due to their: 1) lack of onshore tidal signatures; 2) more episodic nature of sedimentation; and, 3) lack of wave-generated structures due to deposition below storm-weather wave base.

*Sedimentological and Ichnological Characteristics of Coastal Mud
Accumulation Within The Alderson Member (Hatton Gas Pool)*

Within Alderson Member strata, unburrowed massive muds (laminae or bed scale) displaying low substrate consistencies and high depositional rates (*e.g.*,

loading and fluid-escape structures [Figure 2.6G]) are commonly observed. These sedimentary characteristics are consistent with hyperpycnal fluid mud accumulation (Bhattacharya and MacEachern, 2009). Characteristic ichnologic properties within these depositional affinities include reduced and/or fluctuating bioturbation intensities, and reductions in trace-fossil sizes. Another very distinctive feature within intervals such as these is the common occurrence of deformed mantled burrows (Figure 2.6E). The preservation of structures such as these reflects high interstitial water contents at the time of deposition.

In addition to hyperpycnal mud accumulation, buoyant hypopycnal sedimentation appears to have been prevalent during Alderson Member deposition. During hypopycnal fluid mud accumulation, substantial portions of the depositional system are subjected to an abundance of terrestrially derived organic matter and fine-grained particulates as the system becomes more prone to turbidity-induced stresses. These stresses produce a characteristic ichnofaunal assemblage comprising predominantly deposit feeding and grazing structures such as *Phycosiphon*, *Helminthopsis*, and *Chondrites* (Bhattacharya and MacEachern, 2009). Moreover, complex feeding structures such as *Zoophycos* are locally observed in facies characteristic of shallower water depths. This is likely a result of the bountiful food resources available in these settings. Consequently, ichnofossil assemblages attributable to distal expressions of the *Cruziana* Ichnofacies may occur in shallower water than normally be expected.

The presence of wave and onshore tidal indicators suggests a coastal affinity for portions of the Alderson Member. Wave influence is indicated by the presence of parallel-laminated scour-and-fill structures, combined flow ripples, and thin intervals of low-angle cross-stratification (Figure 2.8A and 2.8B). Furthermore, thin-section analysis reveals that mud-dominated intervals comprise micro-laminae exhibiting shale-on-shale erosional contacts, suggesting active mud deposition under wave and current influence (Figure 2.7) (Hovikoski et al., 2008). The distribution of wave-generated structures indicates that Alderson Member strata were deposited above storm-weather wave base. This data also suggests limited availability of sand within the depositional system. Finally, tidal influence in these strata is indicated by the presence of mud-draped ripple foresets and paired mud-drapes (Figure 2.6A).

Environment of Deposition – Offshore and Mud-dominated Deltaic Coast

Within the Hatton Gas Pool area, Alderson Member facies are interpreted to represent deposition within: 1) “subaqueous deltas”; and 2) successions comprising offshore, muddy shoreface or tidal flat, and muddy coastal plain deposits. These interpretations are expanded upon below.

“Subaqueous Deltaic” Successions

The term “subaqueous delta” is applied here to laterally extensive, upward coarsening, prodelta like successions in which a fluvial point source cannot be

traced. Within the Hatton Gas Pool area, successions such as these are widespread and can be traced for several kilometres (see Chapter 3, Figure 3.8, this volume). These successions also contain ample evidence of wave and tide reworking (*e.g.*, parallel-laminated scour-and-fill structures, combined flow ripples, intervals of low-angle cross-stratified sandstones, mud-draped ripple foresets and double mud-drapes) and locally pass upward into root-bearing muds. This data suggests that Alderson Member deposits likely represent alongshore redistributed mud wedges rather than direct, seaward prograding river deltas (Hovikoski et al., 2008). The lateral extent of the mud belt suggests that across-shelf oriented sediment transport also occurred, likely resulting from sediment remobilization during storms (Hovikoski et al., 2008).

An example of a typical “subaqueous deltaic” succession occurs within well 08-25-15-27W3 (Figure 2.3), from approximately 469.00 – 441.00 m (see strip log of Core 4 in the Appendix). Succession of this type commonly consist of the following components:

- 1) The basal portion of “subaqueous deltaic” successions consists of lithologies dominated by grazing-behavior trace-fossil suites (*e.g.*, *Phycosiphon*-dominated sandy mudstones [F1A]). Moving vertically, the early stages of progradation are marked by an increase in organic matter content and depositional rates.
- 2) Moving up-succession, bioturbation intensity progressively fluctuates as grazing-behavior dominated trace-fossil suites grade into unburrowed interlaminated muds and sands (Facies 2A). The transition into Facies 2A is

reflected by elevated concentrations of fine-grained sand and the presence of muddy parallel-laminae (attributed to wave- and tide-agitated fluid-mud flows).

3) Thin intervals of low-angle, cross-stratified fine-grained sandstones, and the presence of scour-and-fill structures become more common moving up the succession (*e.g.*, Facies 3 and 2B respectively). The presence of sedimentary structures such as these reflect the influence of wave activity (wave activity becoming more apparent in a vertical direction). These strata exhibit a subdued ichnological signal and high mud contents in the fair-weather deposits. Within these intervals, tide influence is also apparent as demonstrated by local double mud-drape bearing combined flow-ripples. The upper limit of subaqueous deltaic successions is defined by the last occurrence of bioturbated heterolithically bedded intervals of Facies 2B.

The bioturbated mud – interlaminated sand and mud – interbedded sand and mud succession is remarkably similar to deltaic successions on the Louisiana coast (Neill and Allison, 2005).

Shore Margin and Coastal Plain Successions

Within the Alderson Member, shore margin deposits comprise successions that, in ascending order, consist of organic-rich, bioturbated mud intervals (F1A – muddy offshore to offshore transition), heterolithic bedding (F2 and F3 – muddy shoreface), and root-bearing sandy mudstone (F4 – muddy coastal plain). An example of a typical shore margin succession occurs in well 10-27-15-22W3

(Figure 2.3), from approximately 484.00 – 448.00 m (see strip log of core 5 in the Appendix). In general, shoreface successions demonstrate considerable variability with regard to ichnological signature and bioturbation intensity, the degree of wave influence, and sand to mud ratios. Successions dominated by mud exhibit decreasing wave energy toward the top, suggesting a low-gradient, dissipative shoreline. On the other hand, sandier examples form upward coarsening offshore to foreshore successions. The highest trace-fossil diversities, and the largest variability in ethology are associated with these sandier successions. Trace fossils such as *Schaubcylindrichnus*, *Scolicia (Laminites)*, and *Asterosoma* are typically only present in these sand-rich successions. This data seems to agree well with observations made in modern mud-dominated coastlines, where wave dissipation is strongly influenced by the presence of fluid mud (*e.g.*, Augustinus, 1980; Wells and Coleman, 1981; Rine and Ginsburg, 1985; Huh et al., 2001). In coastal locals where fluid muds are not present, coarser-grained shoreline facies develop as a result of increased wave energy reaching the shore (*e.g.*, Dolique and Anthony, 2005).

Muddy coastal plain successions approximately 7 – 10 metres in thickness also occur within the Alderson Member (*e.g.*, ~ 436.00 – 429.50 m, Core 4, Appendix). These successions comprise heterolithically bedded intervals (F2) that grade upward into root-bearing shales (F4). Within these successions, local intervals of thin shell beds displaying partially dissolved shell-hash or shell-hash-bearing sandy mudstone are also present. In some locales coal fragments occur.

These intervals are also characteristically rich in bedding-plane-orientated organic detritus and locally contain pedogenic slickensides.

*Permeability Characteristics Of Alderson Member Facies (Hatton Gas Pool):
Implications On Reservoir Development*

As the petroleum industry struggles to deliver energy to a planet with an ever-growing demand, declining conventional hydrocarbon reserves has presented a notable challenge. Reserves once considered unconventional (*e.g.*, gas shales), have recently become economically viable options to petroleum producers (Law and Curtis, 2002). Research conducted on fine-grained, low-permeability intervals has demonstrated that strata of this nature may contain significant volumes of hydrocarbons (*e.g.*, O'Connell, 2001; Law and Curtis, 2002; Shurr and Ridgley, 2002; O'Connell, 2003; Pedersen, 2003; Odedra et al., 2005; Hovikoski et al., 2008). For example, it has been estimated that gas reserves held within Alderson Member / Milk River Formation reservoirs in southeast Alberta and southwest Saskatchewan range from 10 – 21 TCF (O'Connell, 2003; Pemberton 2009, personal communication). It is reserve volumes such as these that have prompted petroleum producers to direct some of their attention toward fine-grained, low-permeability units. Be that as it may, the reservoir characteristics of intervals such as these remain poorly understood and present a multitude of challenges with respect to reservoir development.

Spot-minipermeametry testing of Alderson Member strata has provided insight on potential gas storage and transmission mechanisms. The results

demonstrate that non-reservoir rock fabrics consist of Facies 3, 4, and 5, as each of these facies exhibits extremely low permeabilities. The highest permeability values measured are associated with Facies 2, while slight permeability enhancement was observed in Facies 1A (see Table 2.2). This data indicates that interlaminated sand, silt, and mud, and bioturbated heterolithically bedded intervals are capable of significant contributions to the storativity and deliverability of gas. This confirms hypotheses proposed by several authors who have considered these heterolithic bedded intervals as the main gas reservoirs within the Alderson Member (Shurr and Ridgley, 2002; O'Connell, 2003; Pedersen, 2003; Payenberg, 2003; Gatenby, 2004). However, significantly more gas reserves may be present within the Alderson Member, especially if the volumes present within pervasively bioturbated rock fabrics are considered.

In general, bioturbation is considered to be detrimental to the permeability of reservoir rocks. This view stems from poorly sorted texture induced by the biogenic churning of laminated sediments, resulting in the reduction of overall permeability (Pemberton and Gingras, 2005). However, not all bioturbation is detrimental. Several examples of bioturbation-enhanced bulk permeability have been reported in the geological literature (*e.g.*, Dawson, 1978; Gunatilaka et al., 1987; Zenger, 1992; Gingras et al., 1999; 2004a, b; Mehrthens and Selleck, 2002; McKinley et al., 2004; Sutton et al., 2004; Pemberton and Gingras, 2005; Gingras et al., 2007). Although these positive cases are known, the understanding of permeability enhancement facilitated by biogenic processes is still quite primitive.

Spot-minipermeability testing of pervasively bioturbated *Phycosiphon*-dominated sandy mudstones (F1A) has demonstrated that fabrics of this nature exhibit slightly elevated permeability when compared to the surrounding muddy matrix. In effect, bioturbated media appear to enhance the vertical transmissivity of an otherwise extremely low permeability Alderson Member matrix. Consequently, pervasively bioturbated rock fabrics can be considered secondary fluid flow conduits. This has significant implications with respect to reservoir management strategies. Neglecting heavily bioturbated intervals will result in lower than actual reserve estimations, which may lead to potential economic targets being overlooked. In order to maximize hydrocarbon production from the Alderson Member, its bioturbated rock fabrics must be considered. Commingled production of main reservoir (Facies 2) and heavily bioturbated facies is suggested, as this shall allow for more efficient reservoir development. This reservoir development strategy is suggested when attempting production from pervasively bioturbated, low-permeability, gas-charged formations such as the Alderson Member.

For a more detailed discussion on *Phycosiphon*-dominated sandy mudstones (F1A), and their implications on the resource potential of Alderson Member gas wells, see chapter 3 (this volume).

SUMMARY AND CONCLUSIONS

The Alderson Member is a 110 to 200 metre-thick clastic unit located in the subsurface of southeast Alberta and southwest Saskatchewan, Canada. Alderson Member lithologies include pervasively bioturbated marine shales, mudstones, siltstones, and fine-grained sandstones. Enormous volumes of biogenic gas reside within Alderson Member deposits. Conservative estimates place Alderson Member / Milk River Formation gas reserves within a 10 – 21 TCF range (O’Connell, 2003; Pemberton 2009, personal communication); however, explanations for these substantial gas accumulations, like those residing within the highly prolific Hatton Gas Pool of southwest Saskatchewan, remain poorly understood.

In order to gain a better understanding of the mechanisms responsible for gas storage and transmission within Alderson Member strata, ten cores were analyzed from the Hatton Gas Pool area (Figure 2.3). Based on sedimentological and ichnological characteristics, Alderson Member strata were subdivided into five recurring facies, and five subfacies (Facies 1 – 5; Table 2.1).

Wave and onshore tidal indicators suggests a coastal affinity for Alderson Member strata in the Hatton Gas Pool area. Within Alderson Member facies, wave influence is indicated by the presence of parallel-laminated scour-and-fill structures, thin intervals of low-angle cross-stratification, and combined flow ripples. Additionally, shale-on-shale erosional contacts present in mud-dominated intervals further suggest active mud deposition under wave and current influence.

Overall, the distribution of wave-generated structures within Alderson Member facies indicates deposition above storm-weather wave base and a limited availability of sand within the depositional system. Finally, tidal influence is indicated by the presence of mud-draped ripple foresets.

Alderson Member strata are interpreted to represent deposition within “subaqueous deltas”, and offshore, muddy shoreface or tidal flat, and muddy coastal plain environments (shore margin successions). “Subaqueous deltaic” successions are aerially extensive, contain ample evidence of wave and tide reworking, and grade locally into root bearing mud intervals. This suggests that successions of this type likely represent alongshore-redistributed mud-wedges rather than direct seaward progradation. Shore margin deposits consist of organic-rich, bioturbated mud intervals (F1A – muddy offshore to offshore transition), heterolithic bedding (F2 and F3 – muddy shoreface or mud flat), and root-bearing sandy shale (F4 – muddy coastal plain). Within these successions, mud lithosomes demonstrate decreasing wave energy toward the foreshore, suggesting a low-gradient, dissipative shoreline. This data appears to agree well with observations from modern mud-dominated coastlines, where wave dissipation is strongly controlled by the presence of fluid mud (*e.g.*, Augustinus, 1980). On the other hand, sandier shore margin intervals form upward coarsening, offshore to foreshore successions that contain high trace-fossil diversities and the largest variability in ethological activities. These observations demonstrate that several ichnological and sedimentological properties are characteristic of mud-

dominated coastlines, these include: 1) high contents of continentally derived organic matter; 2) low and/or fluctuating bioturbation intensities; 3) soft-sediment deformation and the presence of fluid mud intervals; 4) reduced or variable trace-fossil diversities displaying impoverished event and post-event suites; 5) sedimentary structures restricted to various types of heterolithic bedding; and, 6) intervals enriched with shelly material. These results improve understanding of the ichnological and sedimentological characteristics of shallow-marine mud-dominated intervals. Their use is far reaching as they may aid in the recognition of similar deposits elsewhere.

Spot-minipermeametry was conducted on Facies 1A, 2A, 2B, 3, 4, and 5 using Core Laboratories PDPK-400 Pressure-Decay Profile Permeameter. Permeability testing indicates that non-reservoir rock fabrics consist of Facies 3, 4, and 5, while reservoir quality intervals comprise Facies 2, and to a lesser degree, Facies 1A (Table 2.2). Of the reservoir rock fabrics, bioturbated heterolithically bedded intervals (Facies 2B) appear to make the most significant contribution to the overall storativity and deliverability of gas from the Alderson Member. Within these intervals, matrix permeability differs by more than two orders of magnitude when compared to the higher permeability field (Table 2.2). Slight permeability enhancement was observed within *Phycosiphon*-dominated sandy mudstones (Facies 1A). In these intervals, matrix permeability is within two orders of magnitude relative to the burrow permeability (Table 2.2). Effectively, bioturbated media appear to enhance the vertical transmissivity

of an otherwise impermeable Alderson Member matrix. In order to maximize hydrocarbon production from the Alderson Member commingled production of main reservoir and heavily bioturbated facies is suggested. This strategy should result in substantial increases in the cumulative amount of derived hydrocarbons when producing from pervasively bioturbated, low-permeability, gas-charged formations.

REFERENCES CITED

- AUGUSTINUS, P., 1980, Actual development of the chenier coast of Suriname (South America): *Sedimentary Geology*, v. 26, p. 91 – 113.
- BHATTACHARYA, J.P., AND J.A. MACEachern, 2009, Hyperpynal rivers and prodeltaic shelves in the Cretaceous seaway of North America: *Journal of Sedimentary Research*, v. 79, p. 184 – 209.
- CATTANEO, A., CORREGGIARI, A., LANGONE, L., AND F., TRINCARDI, 2003, The late Holocene Gargano subaqueous delta, Adriatic shelf: sediment pathways and supply fluctuations: *Marine Geology*, v. 193, p. 61 – 91.
- CORE LABORATORIES INSTRUMENTS, 1996, Profile Permeameter PDPK – 400 Operations Manual, 40p.
- DALRYMPLE, R., AND D. CUMMINGS, 2005, The offshore transport of mud: why it doesn't happen and the stratigraphic implications (abstract): *Geological Society of America, Abstracts with Programs*, v. 37, 403 p.
- DAWSON, W.C., 1978, Improvement of sandstone porosity during bioturbation: *American Association of Petroleum Geologists, Bulletin*, v. 62, p. 508 – 509.
- DOLIQUE, F., AND E. ANTHONY, 2005, Short-term profile changes of sandy pocket beaches Affected by Amazon-derived mud, Cayenne, French Guiana: *Journal of Coastal Research*, v. 21, p. 1195 – 1202.
- DROSER, M.L., AND D.J., BOTTJER, 1986, A semiquantitative field classification of Ichnofabrics: *Journal of Sedimentary Petrology*, v. 56, p. 558 – 559.

- FURNIVAL, G.M., 1946, Cypress Lake map-area, Saskatchewan: Geological Survey of Canada, Memoir 242, 161p.
- GATENBY, W., AND M. STANILAND, 2004, Preliminary sedimentology of Milk River equivalent in the New Abby/Lacadena gas fields, Saskatchewan (abstract): Canadian Society of Petroleum Geologists, Core Conference Abstract Book, p. 55 – 68.
- GEYER, W., HILL, P., AND G. KINEKE, 2004, The transport, transformation and dispersal of sediment by buoyant coastal flows: Continental Shelf Research, v. 24, p. 927 – 949.
- GILL, J.R., AND W.A. COBBAN, 1973, Stratigraphy and geologic history of the Montana Group and equivalent rocks, Montana, Wyoming and North and South Dakota: United States Geological Survey, Professional Paper 776, 37p.
- GINGRAS, M.K., PEMBERTON, S.G., MENDOZA, C.A., AND F. HENK, 1999, Assessing the anisotropic permeability of *Glossifungites* surfaces: Petroleum Geoscience, v. 5, p. 349 – 357.
- GINGRAS, M.K., MENDOZA, C.A., AND S.G. PEMBERTON, 2004a, Fossilized worm burrows influence the resource quality of porous media: American Association of Petroleum Geologists, Bulletin, v. 88, p. 875 – 883.
- GINGRAS, M.K., PEMBERTON, S.G., MUEHLENBACHS, K., AND H. MACHEL, 2004b, Conceptual models for burrow-related, selective dolomitization with textural and isotopic evidence from the Tyndall Limestone: Geobiology, v. 2, p. 21 – 30.
- GINGRAS, M.K., PEMBERTON, S.G., HENK, F., MACEachern, J.A., MENDOZA, C., ROSTRON, B., O'HARE, R., SPILA, M., AND K. KONHAUSER, 2007, Applications of ichnology to fluid and gas production in hydrocarbon reservoirs, *in* MacEachern, J.A., Bann, K.L., Gingras, M.K., and Pemberton, S.G., eds., Applied Ichnology: SEPM, Short Course Notes 52, p. 129 – 143.
- GOLDRING, R., AND P. BRIDGES, 1973, Sublittoral sheet sandstones: Journal of Sedimentary Petrology, vol. 43, p. 736 – 747.
- GUNATILAKA, A., AL-ZAMEL, A., SHERMAN, A.J, AND A. REDA, 1987, A spherulitic fabric in selectively dolomitized siliclastic crustacean burrows, northern Kuwait: Journal of Seimentary Petrology, v. 57, p. 927 – 992.

- HOVIKOSKI, J., LEMISKI, R., GINGRAS, M., PEMBERTON, S.G., AND J. MACEachern, 2008, Ichnology and sedimentology of a mud-dominated deltaic coast: Upper Cretaceous Alderson Member (Lea Park Fm.), Western Canada: *Journal of Sedimentary Research*, v. 78, p. 803 – 824.
- HUH, O., WALKER, N.D., AND C. MOELLER, 2001, Sedimentation along the eastern chenier plain coast: down drift impact of a delta complex shift: *Journal of Coastal Research*, v. 17, p. 72 – 81.
- KHAN, S., IMRAN, J., BRADFORD, S., AND J. SYVITSKI, 2005, Numerical modeling of hyperpycnal plumes: *Marine Geology*, v. 222 – 223, p. 193 – 211.
- LAW, B.E., AND J.B. CURTIS, 2002, Introduction to unconventional petroleum systems, American Association of Petroleum Geologists: *Bulletin*, v. 86, no. 11, p. 1851 – 1852.
- LOBZA, V., AND J. SCHIEBER, 1999, Biogenic sedimentary structures produced by worms in soupy, soft muds: observations from the Chattanooga Shale (Upper Devonian) and experiments: *Journal of Sedimentary Research*, v. 69, p. 1041 – 1049.
- MACEachern, J.A., BANN, K.L., BHATTACHARYA, J.P., AND C.D. HOWELL, 2005, Ichnology of deltas: organism responses to the dynamic interplay of rivers, waves, storms and tides, *in* Bhattacharya, B.P., and Giosan, L., eds., *River Deltas: Concepts, Models and Examples: SEPM, Special Publication 83*, p. 49 – 85.
- MACEachern, J.A., PEMBERTON, S.G., BANN, K.L., AND M.K. GINGRAS, 2007a, Departures from the archetypal ichnofacies: effective recognition of environmental stress in the rock record, *in* MacEachern, J.A., Bann, K.L., GINGRAS, M.K., and Pemberton, S.G., eds., *Applied Ichnology: SEPM, Short Course Notes 52*, p. 65 – 94.
- MACEachern, J.A., PEMBERTON, S.G., GINGRAS, M.K., AND K.L. BANN, 2007b, The Ichnofacies concept: a fifty-year retrospective, *in* Miller, W., III, ed., *Trace Fossils: Concepts, Problems, Prospects: Amsterdam, Elsevier*, p. 50 – 75.
- MALLIK, T., MUKHERJI, K., AND K. RAMACHANDRAN, 1988, Sedimentology of the Kerala mud banks (fluid muds?): *Marine Geology*, v. 80, p. 99 – 118.
- McKINLEY, J.M., LLOYD, C.D., AND A.H. RUFFELL, 2004, Use of variography in permeability characterization of visually homogeneous sandstone reservoirs with examples from outcrop studies: *Mathematical Geology*, v. 36, p. 761 – 779.

- MEHRTENS, C., AND B. SELLECK, 2002, Middle Ordovician section at Crown Point Peninsula, *in* J. McLelland and P. Karabinos, eds., Guidebook for fieldtrips in New York and Vermont. University of Vermont, p. B5.1 – B5.16.
- MEIJER DREES, N.C., AND D.W. MYHR, 1981, The Upper Cretaceous Milk River and Lea Park Formations in southeastern Alberta: *Bulletin of Canadian Petroleum Geology*, v. 29, p. 42 – 74.
- MOSSLOW, T.F., AND S.G. PEMBERTON, 1988, An integrated approach to the sedimentological analysis of some Lower Cretaceous shoreface and delta front sandstone sequences, *in* James, D.J., and Leckie, D.A., eds., *Sequences, Stratigraphy, Sedimentology: Surface and Subsurface*: Canadian Society of Petroleum Geologists, Memoir 15, p. 373 – 386.
- NEILL, C.F., AND M.A. ALLISON, 2005, Subaqueous deltaic formation on the Atchafalaya Shelf, Louisiana: *Marine Geology*, v. 214, p. 411 – 430.
- NITTROUER, C.A., AND L.D. WRIGHT, 1994, Transport of particles across continental shelves: *Reviews of Geophysics*, v. 32, p. 85 – 113.
- O'CONNELL, S.C., 2001, The Second White Specks, Medicine Hat and Milk River formations – A shallow gas workshop, consult. rep.
- O'CONNELL, S., 2003, The unknown giants – low permeability shallow gas reservoirs of southern Alberta and Saskatchewan, Canada: Canadian Society of Exploration Geophysicists, Conference Abstracts.
- ODEDRA, A., BURLEY, S.D., LEWIS, A., HARDMAN, M., AND P. HAYNES, 2005, The world according to gas, *in* Dore, A.G. and Vining, B.A., eds., *Petroleum Geology: North-West Europe and Global Perspectives – Proceedings of the 6th Petroleum Geology Conference*, p. 571 – 586.
- PAYENBERG, T.H.D., BRAMAN, D., DAVIS, D., AND A. MIAL, 2002, Litho- and chronostratigraphic relationships of the Santonian-Campanian Milk River Formation in southern Alberta and Eagle Formation in Montana utilizing stratigraphy, U-Pb geochronology, and palynology: *Canadian Journal of Earth Sciences*, v. 39, p. 1553 – 1577.
- PAYENBERG, T.H.D., 2002a, Integration of the Alderson Member in southwestern Saskatchewan into a litho- and chronostratigraphic framework for the Milk River/Eagle shoreline in southern Alberta and north-central Montana, *in* Summary of Investigations 2002, Volume 1, Saskatchewan Geological Survey, Sask. Industry Resources, Misc. Rep. 2002-4.1, CD – ROM, p. 134 – 142.

- PAYENBERG, T.H.D., 2002b, Litho-, chrono- and allostratigraphy of the Santonian to Campanian Milk River and Eagle formations in southern Alberta and north-central Montana: Implications for differential subsidence in the Western Interior Foreland Basin. University of Toronto, PhD Thesis, 221p.
- PEDERSEN, P., 2003, Stratigraphic relationships of Alderson (Milk River) strata between the Hatton and Abbey-Lacadena Pools, southwestern Saskatchewan—preliminary observations, *in* Saskatchewan Geological Survey, Summary of Investigations 2003, Volume 1, p. 1 – 11.
- PEMBERTON, S.G., AND D.M. WIGHTMAN, 1992, Ichnological characteristics of brackish water deposits, *in* Pemberton, S.G., ed., Applications of Ichnology to Petroleum Exploration: SEPM, Core Workshop 17, p. 141 – 167.
- PEMBERTON, S.G., SPILA, M., PULHAM., A.J., SAUNDERS, T., MACEACHERN, J.A., ROBBINS, D., AND I.K. SINCLAIR, 2001, Ichnology and sedimentology of shallow to marginal marine systems: Ben Nevis and Avalon reservoirs, Jeanne d’Arc Basin: Geological Association of Canada, Short Course Notes Volume 15
- PEMBERTON, S.G., AND M.K. GINGRAS, 2005, Classification and characterizations of biogenically enhanced permeability: American Association of Petroleum Geologists: Bulletin, v. 89, p. 1493 – 1517.
- REINECK, H.E., 1963, Sedimentgefüge im Bereich der südlichen Nordsee. *Abhandlungen der senckenbergische naturforschende Gesellschaft*, v. 505, p. 1 – 138.
- RHODES, E., 1982, Depositional model for a chenier plain, Gulf of Carpentaria, Australia: *Sedimentology*, v. 29, p. 201 – 221.
- RINE, J., AND R. GINSBURG, 1985, Depositional facies of a mud shoreface in Surinam, South America – a mud analogue to sandy shallow-marine deposits: *Journal of Sedimentary Petrology*, v. 55, p. 633 – 652.
- ROCKWARE ®, INC., 2009, Surfer 9.0 Gridding and Contouring Software.
- SCHIEBER, J., 1998a, Deposition of mudstone and shales: Overview, problems and challenges, *in* Schieber, J., Zimmerle, W., and Sethi, P.S., eds., *Mudstones and Shales: Recent Progress in Shale Research*: Stuttgart, Schweizerbart Publishers, p. 131 – 146.

- SCHIEBER, J., 1998b, Sedimentary features indicating erosion, condensation, and hiatuses in the Chattanooga Shale of Central Tennessee: relevance for sedimentary and stratigraphic evolution, in Schieber, J., Zimmerle, W., and Sethi, P.S., eds., *Mudstones and Shales: Recent Progress in Shale Research*: Stuttgart, Schweizerbart Publishers, p. 187 – 215.
- SCHIEBER, J., 2003, Simple gifts and buried treasures – implications of finding bioturbation and erosion surfaces in black shales: *The Sedimentary Record*, v. 1, p. 4 – 9.
- SCHIEBER, J., SOUTHARD, J., AND K. THAISEN, 2007, Accretion of mudstone beds from migrating floccule ripples: *Science*, v. 318, p. 1760 – 1763.
- SHURR, G., AND J. RIDGLEY, 2002, Unconventional shallow biogenic gas systems: *American Association of Petroleum Geologists, Bulletin*, v. 86, p. 1939 – 1969.
- SUTTON, S.J., ETHERIDGE, F.G., ALMON, W.R., DAWSON, W.C., AND K.K. EDWARDS, 2004, Textural and sequence-stratigraphic controls on sealing capacity of Lower and Upper Cretaceous shales, Denver basin, Colorado: *American Association of Petroleum Geologists, Bulletin*, v. 88, p. 1185 – 1206.
- TAYLOR, A.M., AND R. GOLDRING, 1993, Description and analysis of bioturbation and ichnofabric: *Journal of the Geological Survey, London*, vol. 150, p. 141 – 148.
- TOVELL, W.M., 1956, Some aspects of the geology of the Milk River and Pakowki Formations (southern Alberta). University of Toronto, Thesis, v. 2, 114p.
- WELLS, J., AND J. COLEMAN, 1981, Physical processes and fine-grained sediment dynamics, coast of Surinam, South America: *Journal of Sedimentary Petrology*, v. 51, p. 1053 – 1068.
- WRIGHT, L.D., AND C.A. NITTRouer, 1995, Dispersal of river sediments in coastal seas: six contrasting cases: *Estuaries*, v. 18, p. 494 – 508.
- ZENGER, D.H., 1992, Burrowing and dolomitization patterns in the Steamboat Point Member, Bighorn Dolomite (Upper Ordovician), northeast Wyoming: *Contributions to Geology*, v. 29, p. 133 – 142.

CHAPTER III – THE INFLUENCE OF PERVASIVELY BIOTURBATED INTERVALS ON THE RESOURCE POTENTIAL OF ALDERSON MEMBER STRATA (HATTON GAS POOL, SOUTHWEST SASKATCHEWAN, CANADA)

INTRODUCTION

Low-permeability gas-charged intervals commonly contain thick pervasively bioturbated rock packages. The highly prolific nature of these strata has led to the suggestion that pervasively bioturbated rock fabrics may contribute to the overall storativity and deliverability of hydrocarbons. In the past, heavily bioturbated intervals have been regarded as troublesome and enigmatic with respect to reservoir development; however, recent advances in permeability testing and burrow modeling have begun to shed light on the ways in which bioturbated rock fabrics may impact the resource potential of low-permeability gas-charged strata (*e.g.*, Gingras et al., 2002; Gingras et al., 2004a, b; Pemberton and Gingras 2005).

Bioturbation is generally considered to be detrimental to the permeability of reservoir rocks. This view stems from the development of poorly sorted texture due to biogenic churning of laminated sediments, which results in the reduction of overall permeability (Pemberton and Gingras, 2005). However, not all bioturbation destroys permeability, and several examples of bioturbation-enhanced bulk permeability have been reported in the geological literature (*e.g.*, Dawson, 1978; Gunatilaka et al., 1987; Zenger, 1992; Gingras et al., 1999; 2004a, b; Mehrthens and Selleck, 2002; McKinley et al., 2004; Sutton et al., 2004;

Pemberton and Gingras, 2005; Gingras et al., 2007; Cunningham et al., 2009).

These range from biogenic modifications of the primary depositional fabric (burrow-mediated) to diagenetic alterations (typically recrystallization) of the sedimentary matrix (Pemberton and Gingras, 2005). Although positive cases are known, the understanding of permeability enhancement facilitated by biogenic processes is still poorly explored.

The benefit of trace fossils is not limited to palaeoenvironmental interpretation. Recent research has shown that ichnology has significant application to production geology. For example, in modern sediments, the creation of macropores by bioturbators such as earthworms, decapod crustaceans, amphipods, and polychaetes, has long been known to enhance permeability and porosity characteristics (*e.g.*, Meadows and Tait, 1989; Lavoie et al., 2000; Schmidt et al., 2002; Bastardie et al., 2003; Katrak and Bird, 2003). In the past, trace fossil research within petroliferous strata was usually limited to the exploration phase. However, the development of improved techniques using ichnology to aid with reservoir evaluation and production has been the focus of many contemporary academic studies. Recent studies have demonstrated that biogenic aspects of rock character can influence the bulk permeability of sedimentary rocks and thus their reservoir quality (Gingras et al., 1999; Gingras et al., 2004a, b; Pemberton and Gingras, 2005; Gingras et al., 2007). As a result, the incorporation of ichnological description during reservoir evaluation has quickly

become a widely recognized and valuable aspect when assessing the resource potential of pervasively bioturbated hydrocarbon-bearing strata.

Overlooking the effects of ichnology in heavily bioturbated reservoirs can potentially lead to erroneous reserve calculations. Pemberton and Gingras (2005) defined, classified, and characterized biogenically enhanced permeability. Biogenic flow networks in which matrix permeability is within two orders of magnitude relative to burrow-associated permeability are classified as *dual-porosity* systems. Dual-porosity systems occur where matrix- and burrow-permeabilities are similar. On the other hand, well defined, highly contrasting permeability fields, where matrix- and burrow-associated permeabilities differ by more than two orders of magnitude are defined as *dual-permeability* flow networks. The presence of a dual-porosity versus a dual-permeability network, along with the stratigraphic configuration of biogenically enhanced permeability are the primary considerations when classifying the type of biogenic flow media encountered. According to Pemberton and Gingras (2005), there are five flow-media types: 1) surface-constrained discrete textural heterogeneities; 2) non-surface-constrained discrete textural heterogeneities; 3) weakly defined textural heterogeneities; 4) diagenetic textural heterogeneities, and, 5) cryptic biogenic heterogeneities.

Several methods were used to demonstrate the dual nature of porosity and permeability networks within bioturbated media samples, these methods included the use of: 1) a profile permeameter, which assessed spot-permeabilities; 2) bulk-

flow tests and Darcy experiments, which aided in determining bulk permeabilities; 3) flow-through tracer tests, which assessed relative dispersivities and tortuosities of flow conduits; and, 4) MRI imaging, CT scans, and X-radiography, which characterized heterogeneities related to porosity. Pemberton and Gingras (2005) also demonstrated that substrate-controlled ichnofossil assemblages could enhance the permeability and vertical transmission of an otherwise relatively impermeable matrix. This permeability enhancement can originate when burrows excavated into a low-permeability firmground substrate are subsequently filled with texturally contrasting permeable sediment subtending from the overlying strata. In this case, an anisotropic porosity and permeability network exists and can dramatically impact reserve calculations. If the resulting burrow fills have reduced permeability, reserve calculations may be too high. Correspondingly, if the burrow fills have enhanced permeability, reserve calculations will be too low (Pemberton and Gingras, 2005).

The Upper Cretaceous Alderson Member of southwest Saskatchewan, Canada, is an example of a giant gas-play centered on low-permeability, gas-prone, non-associated reservoirs (Payenberg, 2002b; O'Connell, 2003; Pedersen, 2003; Hovikoski et al., 2008). The fields contained within this play produce from laterally extensive, thinly bedded, fine-grained sand interbedded with mud-dominated units that occur at depths of less than 600 m (~ 2000 ft) (Hovikoski et al., 2008). In many cases the productive zones are interbedded with, or are, the source rock (Hovikoski et al., 2008).

Within Alderson Member strata, characteristic silty halos associated with three-dimensionally interconnected *Phycosiphon* (a trace fossil) have been hypothesized as a storage mechanism for gas. The segregation of clean silt-sized sediment into an otherwise low-permeability muddy matrix has led to the assertion that rock fabrics of this type could enhance the vertical transmission of fluids from the subsurface. Thus, discounting the effects this facies may have on production potential could result in erroneous hydrocarbon reserve estimates.

This paper presents an ichnological study that highlights the effects of trace fossils on the production potential of Alderson Member strata from the Hatton Gas Pool area (southwest Saskatchewan, Canada). This analysis is relevant to calculated reserve volumes, deliverability of gas, and reservoir management strategy. Results from this work can be used to improve gas-exploration techniques applied to the Alderson Member as well as pervasively bioturbated intervals occurring within other prolific low-permeability gas producing provinces.

Alderson Member (Lea Park Formation)

The Alderson Member (Lea Park Formation) of southwest Saskatchewan and southeast Alberta, Canada, is a clastic unit that comprises pervasively bioturbated marine shales, mudstones, siltstones, and fine-grained sandstones of Campanian age (Meijer Drees and Mhyr, 1981; O'Connell et al., 1999; Ridgley, 2000; Payenberg, 2002a, b; O'Connell, 2003; Pedersen, 2003; Gatenby and Staniland,

2004; Hovikoski et al., 2007; Hovikoski et al., 2008). The Alderson Member hosts large quantities of biogenic gas (Fuex, 1977) within shallow sandstone reservoirs situated within predominantly fine-grained media (Payenberg, 2002; Shurr and Ridgley, 2002; Pedersen, 2003; Gatenby, 2004). Conservative gas-in-place estimates place Milk River Formation / Alderson Member reserves within a 10 – 21 TCF (28-60 Mm³) range (O’Connell, 2003; Pemberton 2009, personal communication). Together with the commingling of Medicine Hat Member (Niobrara Formation) and Second White Specks strata, these rock bodies host the largest gas reservoir in the Western Canada Sedimentary Basin (Figure 3.1) (O’Connell, 2003). It is these large quantities of gas that have made the Alderson Member a lucrative target for petroleum producers.

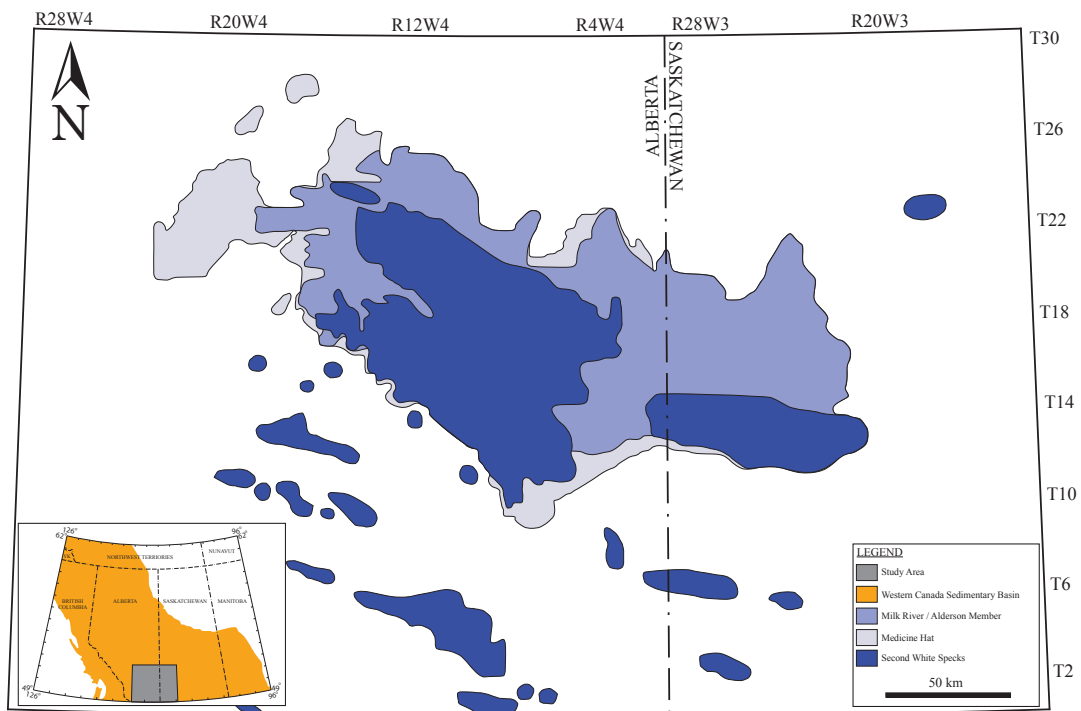


FIGURE 3.1: Areal extent of major gas fields in southeast Alberta and southwest Saskatchewan, Canada. The commingling of gas reserves hosted within the Medicine Hat Member (Niobrara Formation), Milk River Formation / Alderson Member (Lea Park Formation), and Second White Specks intervals constitutes the largest gas reservoir ever discovered in the Western Canada Sedimentary Basin. Modified from O’Connell (2003).

In casual usage, the Alderson Member is regarded as a portion of the Milk River Formation, or the “*Milk River Equivalent*” (Furnival, 1946). Although this informal terminology is commonly used, it should be noted that the Milk River Formation is not equivalent to the Alderson Member, and is in fact separated from it by a significant time gap (Figure 3.2) (Ridgley, 2000; O’Connell, 2001; Shurr and Ridgley, 2002; Payenberg, 2002a, 2002b; Pedersen, 2003). The Alderson Member is present beyond the northeast depositional limit of the Virgelle sandstone of the Milk River Formation, and its thickness varies from approximately 110 m (~ 360 ft) in Alberta, to approximately 200 m (~ 660 ft) in Saskatchewan (Meijer-Drees and Mhyr, 1981). The northeastern limit of the Alderson Member is defined by the last occurrence of an extensive chert pebble horizon observed at its top (Meijer Drees and Mhyr, 1981). This pebble bed has been interpreted as a transgressive wave ravinement surface, and separates the overall regressive Milk River Formation from the transgressive Pakowki Formation (Tovell, 1956; Gill and Cobban, 1973; Meijer-Drees and Mhyr, 1981). This horizon is referred to as the “*Milk River Shoulder*” (Meijer-Drees and Mhyr, 1981; O’Connell, 2001; Payenberg, 2002a, 2002b; Pedersen, 2003).

Despite the enormous economic significance of the Alderson Member, surprisingly little has been published on its sedimentological, stratigraphical, and ichnological characteristics. Of those publically available, few studies have considered bioturbate textures and their effects on resource potential. Several reasons for the deficit of Alderson Member studies in scientific literature include:

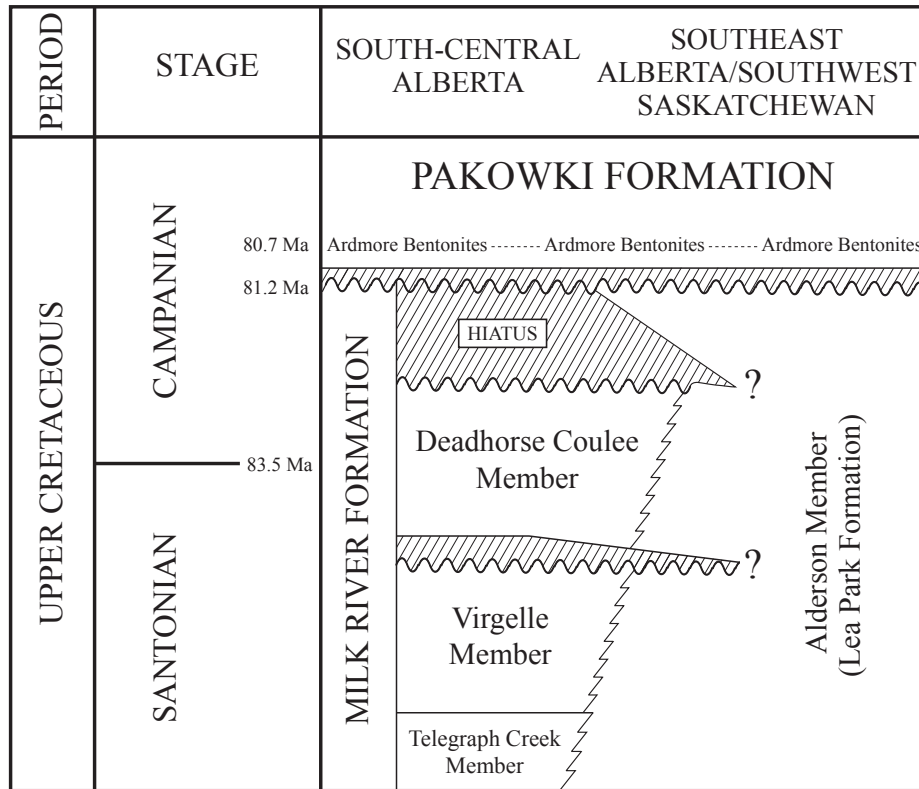


FIGURE 3.2: Subsurface architecture of early Campanian – late Santonian strata in southeast Alberta and southwest Saskatchewan. The Alderson Member represents approximately 2 million years of deposition (Payenberg, 2002); however, the exact age of its lower contact has yet to be defined (Payenberg et al., 2002; Shurr and Ridgley, 2002; Hovikoski et al., 2008). Modified from Payenberg et al. (2002).

1) the muddy nature of the Alderson Member makes subtle geological variations extremely difficult to observe, requiring repetitive work using many wells to provide significant insight; 2) in the Alderson Member, gas accumulations typically occur in broad, sheet-like sand bodies. This geometry allows for development via step-out or in-fill drilling with little requirement for detailed stratigraphical analysis. As a result, stratigraphic analysis has been deemed unimportant to exploration success; and, 3) low rates of recovery have made these fields economically marginal throughout much of their history, thus attracting little past attention (O’Connell, 2001; Law and Curtis, 2002; O’Connell, 2003).

The mechanisms responsible for gas storage within the Alderson Member are poorly understood. Early facies classifications have led to the assumption that the majority of gas accumulation resides within heterolithically bedded intervals comprising thin sandstone beds and disconnected sand lenses (Meijer-Drees and Mhyr, 1981; O'Connell et al., 1999; O'Connell, 2003; Pedersen, 2003). In a more recent regional subsurface study, seven Alderson Member facies were defined and described (Hovikoski et al., 2007; Hovikoski et al., 2008).

Core analysis of Alderson Member strata (Hatton Gas Pool area, southwest Saskatchewan) has determined that one of the most voluminous facies (approximately 20 – 25%) consists of a *Phycosiphon*-dominated sandy mudstone of offshore affinity. *Phycosiphon* is an irregularly meandering trace comprising a black fecal core surrounded by a pale halo of coarser silt. In drill-core, *Phycosiphon* typically appears as tiny, dark, pin-head sized spots (transverse section), or dark lines (longitudinal section) which may be discontinuous and surrounded by a pale silt halo (Figure 3.3) (Wetzel, 1984; Bromley, 1990; Goldring et al., 1991; Pemberton, 2001). The characteristic silty halo reflects the segregation of coarser grained sediment within the substrate by a worm-like organism. *Phycosiphon*-dominated sandy mudstones are dominated by a grazing behaviour trace-fossil suite and represent a distal expression of the *Cruziana* Ichnofacies—a common and widespread fabric in the rock record (MacEachern et al., 2007a; MacEachern et al., 2007b). Due to its extremely fine grained and pervasively bioturbated nature, a facies of this variety is generally not thought

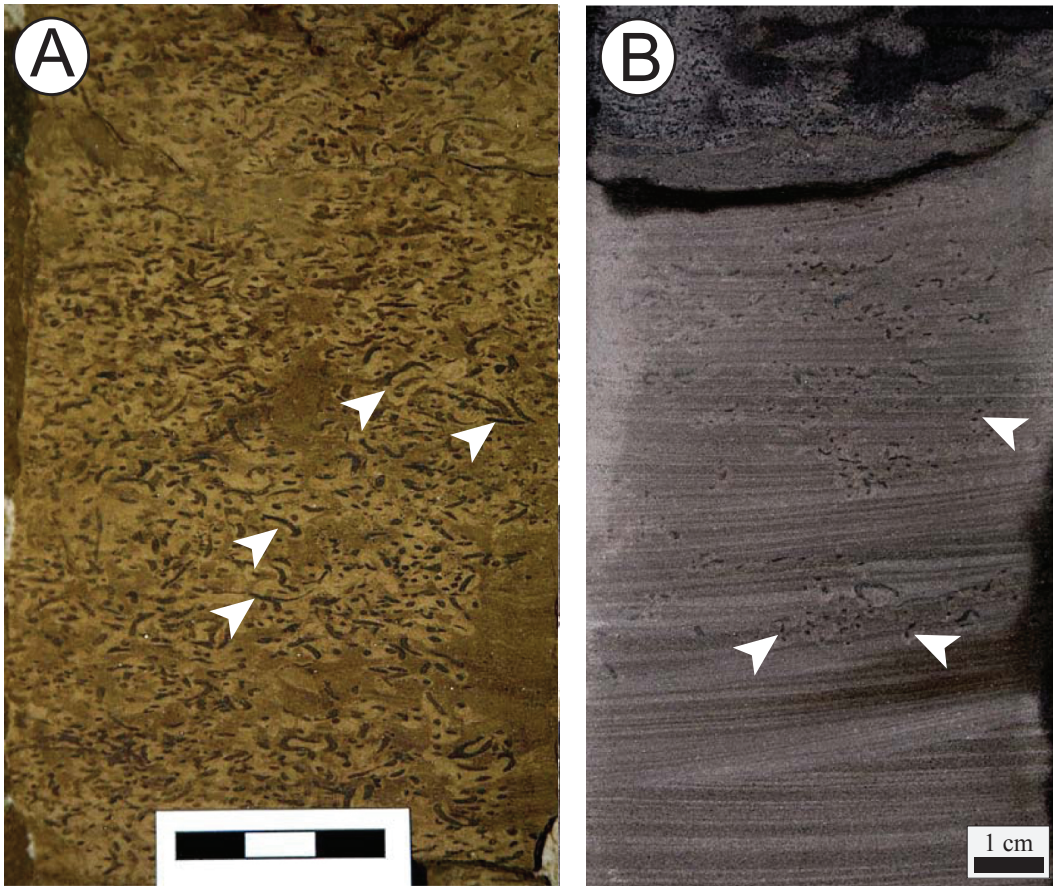


FIGURE 3.3: Core photos of samples comprising *Phycosiphon*-dominated sandy mudstones (Facies 1A). *Phycosiphon* is small and consists of a dark colored fecal core (mud) surrounded by a pale colored halo of silt. **A)** White arrows highlight longitudinal sections through *Phycosiphon* (3 cm scale card). **B)** Transverse sections through *Phycosiphon* (indicated by white arrows).

of as a potential gas reservoir; however, based on its volumetric abundance, and the highly productive nature of Alderson Member strata, it is believed this facies could provide a considerable contribution to resource potential of Hatton Gas Pool wells.

This paper consists of a comprehensive examination of Alderson Member strata using ten cores retrieved from the Hatton Gas Pool area of southwest Saskatchewan, Canada. The Hatton Gas Pool covers approximately 6434 km² (~4000 mi²), spanning Townships 11 to 22, and Ranges 22W3 to R30W3 (Figure

3.4). For the purposes of this study, numerous hydrocarbon leases in this area have been coalesced. Subsurface cores from Hatton are sparse; at the time of study, only 23 cores penetrated portions of the Alderson Member, the majority of which displayed extensive intervals of poorly recovered strata. The study area along with the locations of examined core is shown in Figure 3.4. The purpose of this paper is to investigate whether or not highly prevalent *Phycosiphon*-dominated sandy mudstones contribute to the resource potential of Alderson Member deposits. Spot-minipermeametry conducted on eleven one-third-slab samples, along with data collected from six samples run under high-pressure mercury injection porosimetry have allowed for a better understanding of the porosity and permeability characteristics of this facies. These results have been compared with tests conducted on other Alderson Member facies. These data have shed light on the potential implications *Phycosiphon*-dominated sandy mudstones have on the overall resource potential of the Hatton Gas Pool. There may be further implications of this work elsewhere as pervasively bioturbated intervals appear to be common within other highly prolific, low-permeability gas-producing provinces.

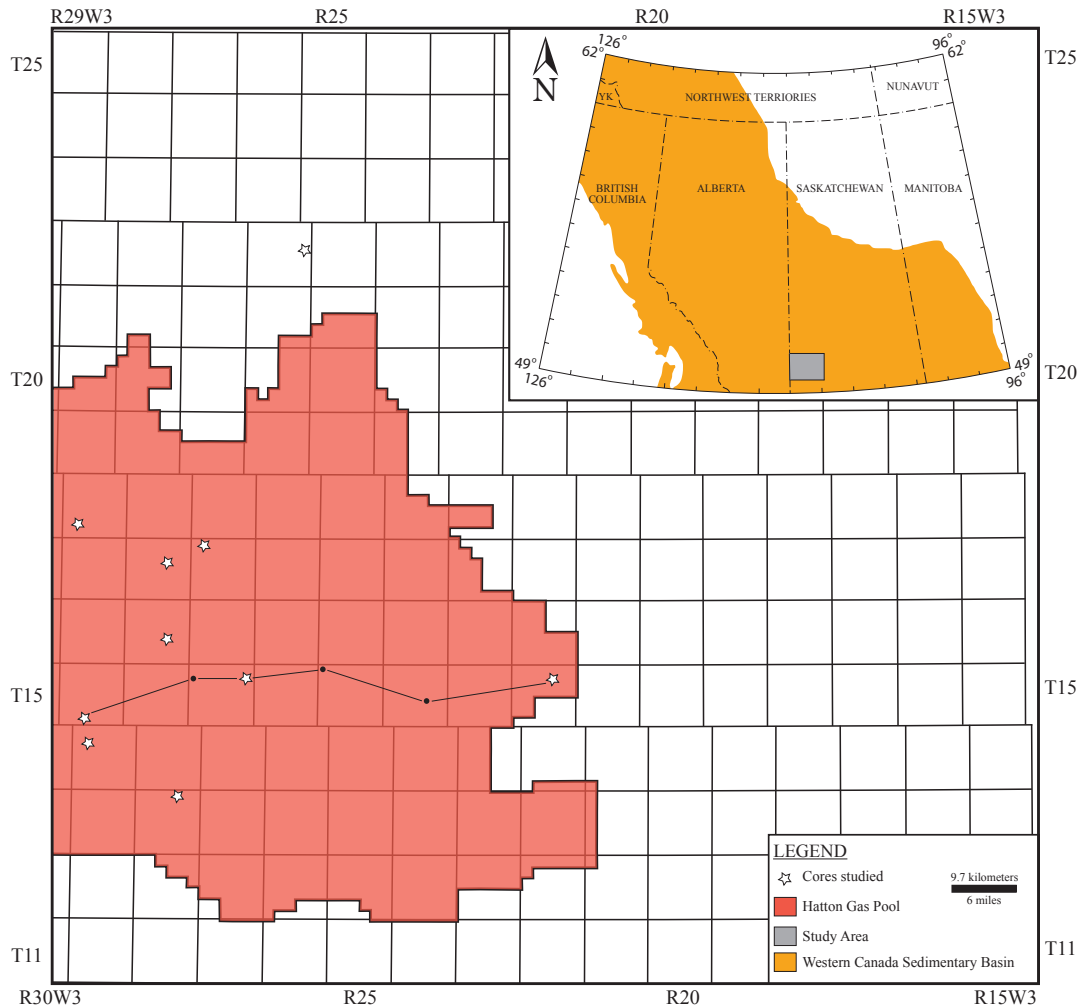


FIGURE 3.4: Study area. Large-scale map (top right corner) shows the areal extent of the Hatton Gas Pool area with respect to the Western Canada Sedimentary Basin. The more detailed map outlines the boundaries of the Hatton Gas Pool (pool boundaries are defined as of January 2003). In this study, Alderson Member strata were analyzed using 10 drill-cores derived from the Hatton Gas Pool and surrounding area. A line-of-section (LOS) highlights the wells used in the construction of a west – east subsurface cross-section. This transect is presented in Figure 3.8.

METHODS

Ten conventional drill cores along with accompanying petrophysical logs from the Hatton Gas Pool area were used to collect sedimentary, stratigraphic, and ichnological data from the Alderson Member (Figure 3.4). Core analysis focused on descriptions of lithology, grain size (visual estimation), texture, primary and

secondary sedimentary structures, bedding contacts and character of bedding, soft-sediment deformation structures, mineralogical accessories (*e.g.*, glauconite, pyrite, etc.), and the identification of important stratigraphic surfaces. Ichnological data comprises description of ichnogenera and/or ichnospecies, trace-fossil assemblage, and bioturbation index (BI of Reineck (1963). Later modified by Droser & Bottjer (1986), and again by Taylor & Goldring (1993)).

Alderson Member Facies

Hovikoski et al. (2008) conducted a regional subsurface study of the Alderson Member using cores from southwest Saskatchewan and southeast Alberta. Based on sedimentological and ichnological characteristics, seven facies, and seven subfacies were described. Core analysis conducted for the purposes of this study incorporated the facies classification developed by Hovikoski (2008) as similar lithologies were encountered in the Hatton Gas Pool area.

Within Hatton, five facies were identified from the suite of cores studied (F1 through F5; Table 3.1). These facies were further subdivided where distinct sedimentological or ichnological characteristics allowed. Facies descriptions are summarized in Table 3.1.

Descriptions	Occurrence / Contacts	Sedimentological Characteristics	Ichnological Characteristics	Interpretation
<p>Facies 1 (F1) F1A Phycosiphon-dominated sandy mudstone</p>	<ul style="list-style-type: none"> commonly occurs in the basal portion of upward-coarsening successions gradationally interbedded with F1B and F2 typically represents the zone of maximum flooding within a sequence 	<ul style="list-style-type: none"> light grey sandy mudstone sharp based, bioturbated sand lenses occur locally low organic matter content 	<ul style="list-style-type: none"> pervasively bioturbated (BI 4 – 6) low trace fossil diversity, including: Ph, a, Ch, m, Hm, r, Zo, r, 	<ul style="list-style-type: none"> trace fossil suite represents a distal expression of the <i>Cruziana</i> ichnofacies, consistent with deposition in offshore settings lack of organic matter points to a weak deltaic influence or non-deltaic origin
<p>F1B Sandy mudstone bearing a mixed-ethology assemblage</p>	<ul style="list-style-type: none"> moderately common within middle and upper portions of the Alderson Member gradationally overlies F1A occurs below F1C, F2B, or F3 (gradational contacts) 	<ul style="list-style-type: none"> light to dark grey sandy mudstone locally high sand contents 	<ul style="list-style-type: none"> moderately to intensively burrowed (BI 2 – 6) displays a mixed-ethology assemblage moderate trace fossil diversity, including: As, r, Sch, m; Sch(f), m; Sco, r; Ar, r; Th, m; Pl, c; Ch, c; Zo, r; Ph, a; Hm, a; fu, c typically, several size classes of each ichnogenus are present 	<ul style="list-style-type: none"> upper offshore – offshore transition environments
<p>F1C Burrow-mottled sandy mudstone</p>	<ul style="list-style-type: none"> common near the top of the Alderson Member gradationally overlies F1B, F2, or F3 grades upward into F4 or is erosionally overlain by F5 	<ul style="list-style-type: none"> light to dark grey sandy mudstone rhizoliths present crosscutting the ichnofossil assemblage 	<ul style="list-style-type: none"> pervasively bioturbated (BI 5 – 6) low diversity trace fossil suite consisting of indistinct burrow mottling recognized trace fossils include; small Pl, c; Pa, r; Te, r; Dp, r; Th, r 	<ul style="list-style-type: none"> stressed (low-salinity?) setting gradation from F1C to F4 represents a change from subaqueous deposition to a subaerially exposed setting low-energy or episodic sediment accumulation in a sheltered locale
<p>Facies 2 (F2) F2A Interlaminated fine-grained sands, silts, and muds</p>	<ul style="list-style-type: none"> common in the middle portion of upward-coarsening successions within the lower Alderson Member gradationally overlies F1 grades vertically into F1C, F2B, or F3 	<ul style="list-style-type: none"> mud-dominated heterolithic bedding characterized by interlaminated sands and shales, and lenticular bedding soft-sedimentary deformation forms metre-scale successions undulating, massive dark grey shale laminae commonly 1 to 10 mm thick sandstone intervals occur as muddy and planar-parallel laminations and as mud-draped ripples high amounts of terrestrially derived organic matter 	<ul style="list-style-type: none"> Mud rich examples: <ul style="list-style-type: none"> low-diversity suite of sand filled Pl, c bioturbation intensity variable, typically low (BI 2 – 3) locally, diminutive Ch, r; Te, r; Ph/Hm, r; are present Sandier examples: <ul style="list-style-type: none"> contain a moderate- to low-diversity ichnofossil assemblage, including: diminutive Ph, c; Sch(f), m; Zo, r; Th, r; Ar, r; Hm, c Th burrows sand-filled, occasionally display a muddy mantle 	<ul style="list-style-type: none"> periods of rapid episodic deposition, high sediment water contents, low and/or fluctuating salinities and high turbidity stresses, likely the result of deltaic sediment-gravity flows and wave-reworking tidal influence
<p>F2B Bioturbated heterolithic bedding</p>	<ul style="list-style-type: none"> common near the top of upward-coarsening successions gradationally overlies F2A in places, burrowed shale-on-shale erosional contacts occur 	<ul style="list-style-type: none"> bioturbated heterolithic bedding sand lithosome consists of 1 to 5 cm thick, normally graded lenses or beds sand intervals comprise scour-and-fill structures, symmetric ripples, and locally thin intervals of low-angle cross-stratification or heterolithic planar lamination interbedded mud lithosome typically consist of alternating micro-laminated, unburrowed, massive sandy shale and bioturbated shale (F1A) 	<ul style="list-style-type: none"> sand lithosome bioturbated with robust Hm, c; “lam-scrum” fabric bioturbated intervals consist of either F1A or F1B (BI 2 – 6) 	<ul style="list-style-type: none"> tempestivities active deposition under wave and/or current influence

TABLE 3.1

<p>Facies 3 (F3) Low-angle cross-stratified sandstone</p>	<ul style="list-style-type: none"> found in distinct levels near the tops of major upward-coarsening successions basal contact sharp or gradational with F2B grades vertically into F4 or F1 (rare) 	<ul style="list-style-type: none"> low-angle cross-stratified, fine- to medium-grained sandstone typically observed in 10 to 20 cm thick successions locally cemented by calcite or siderite 		<ul style="list-style-type: none"> records intervals of increased exposure to wave activity and shallower water depths siderite consistent with a paucity of ocean-derived sulphate which can be attributed to the presence of freshwater or groundwater influx inshore localities associated with LST
<p>Facies 4 (F4) Root-bearing fine-grained sandy shale</p>	<ul style="list-style-type: none"> present in the middle and upper portions of the Alderson Member gradationally overlies F1C or F2A gradationally overlain by F1 Locally, upper contact is erosional with F5 	<ul style="list-style-type: none"> grey, root bearing, massive appearing, bioturbated or heterolithically laminated to bedded, rubbly shale thin sandy interlaminae, shell-hash, and abundant terrestrial organic matter observed (coal) 10 cm to several metre thick successions pedogenic slickensides occur locally in thin intervals 	<ul style="list-style-type: none"> bioturbation typically consists of indistinct burrow mottling bioturbated, heterolithically bedded intervals display high bioturbation intensities (BI 5 – 6) lower bioturbation intensities are associated with heterolithically laminated to bedded, rubbly, fine-grained sandy shale intervals (BI 1 – 3) 	<ul style="list-style-type: none"> muddy coastal plain subaerial exposure and incipient pedogenic alteration
<p>Facies 5 (F5) Conglomerate / massive coarse- to medium-grained sandstone</p>	<ul style="list-style-type: none"> discrete, sharp-based surfaces in the lower and upper portions of the Alderson Member erosionally overlies F3, F4, and to a lesser extent, F1C upper contact gradational with F1 	<ul style="list-style-type: none"> cm-thick, clast- or matrix-supported conglomeratic beds framework clasts subrounded to sub-angular, and are up to 10 mm in diameter glauconite observed locally within sandy matrix locally cemented by siderite 		<ul style="list-style-type: none"> denotes a transgressive surface of erosion (flooding surface) co-planar surface of erosion

TABLE 3.1 (continued): Facies descriptions derived from the sedimentological and ichnological logging of Alderson Member strata (Hatton Gas Pool area, southwest Saskatchewan). Interpretations are expanded upon in the main body of the text. Terminology and abbreviations used in this table are summarized in a terminology and abbreviations section prior to Chapter 1.

Spot-Minipermeametry

Thirty-two core samples (10 centimetre diameter and one-third-slab) from Alderson Member cores were obtained from Saskatchewan Industry and Resources Core Facility in Regina, Saskatchewan. Samples we selected in order to assess the intra-facies heterogeneity present within each facies. This helped to ensure a wide-ranging data set for permeability testing. Of the samples collected, eleven comprised *Phycosiphon*-dominated sandy mudstone (F1A – Table 3.1).

Spot-permeability analysis required a flat surface for measurements.

To facilitate this, full diameter core samples were slabbed at the University of Alberta. After each cut, compressed air was blown across the sample's test surface in order to remove sediment build up. Spot-minipermeametry was then conducted using Core Laboratories PDPK – 400 Pressure-Decay Profile Permeameter (PDPK – 400; Figure 3.5). Measurements were performed in two manners: 1) using a 5 mm or 1 cm grid pattern; and, 2) on a fabric-selective basis, allowing the assessment of the permeability of individual trace fossils.

The PDPK – 400 is a pressure decay system that measures gas permeabilities from 0.001 millidarcy to greater than 30 Darcy (Core Laboratories Instruments, 1996). A schematic diagram of the PDPK – 400 is presented in Figure 3.5. Main components of this instrument include the probe assembly or travelling case (discussed below), an air tank (supplies nitrogen to the probe assembly), the core rack (holds sample), a monitor (displays measurement results), and a computer (data storage). The probe assembly comprises four

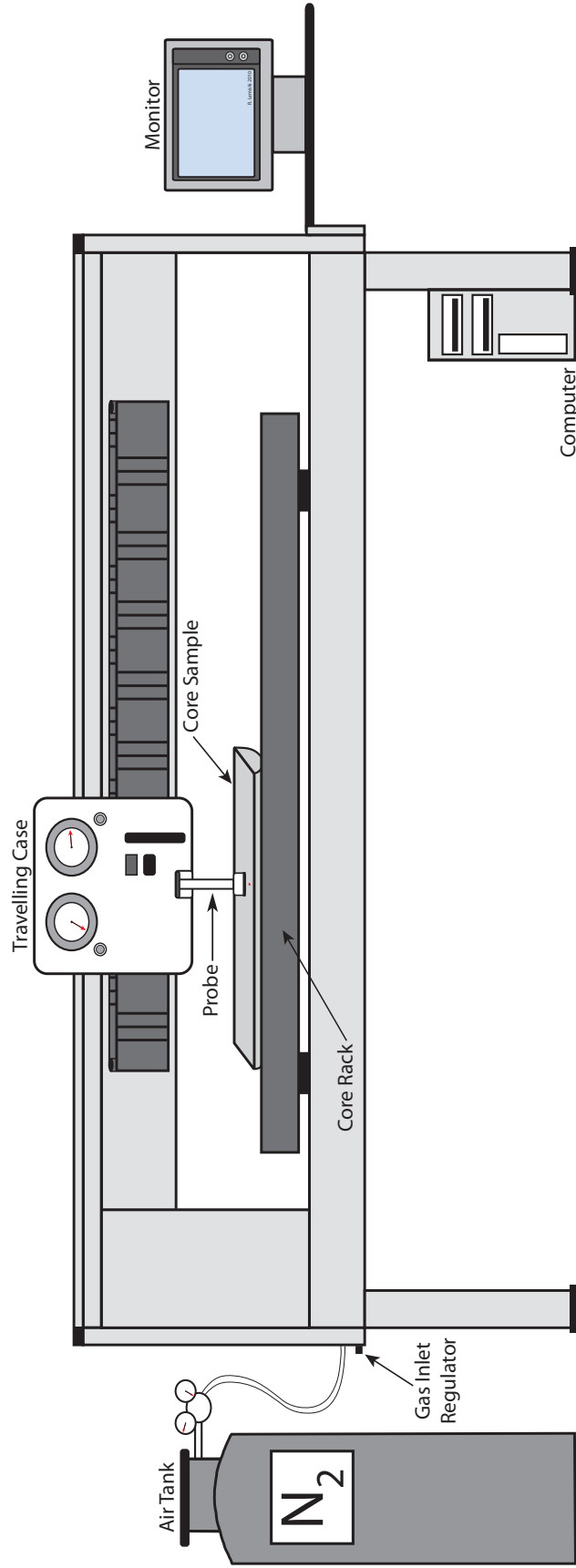


FIGURE 3.5: Core Laboratories PDPK – 400 Pressure Decay Profile Permeameter. Major components have been annotated. Modified from Core Laboratories Instruments, 1996.

accurately calibrated volumes that are initially charged with nitrogen. These volumes are referred to as the “tank supply”. Permeability measurement control devices are located on the front panel of the probe assembly. These controls consist of the tank supply and probe regulators, their respective gauges, and a firing button (initiates a permeability measurement).

Spot-minipermeametry testing was conducted by positioning the probe assembly and core rack at a desired location. To perform a permeability measurement, the probe’s rubber tip (0.46 cm diameter O-ring) was then sealed against the sample using a pneumatic cylinder. Subsequently, a computer-controlled probe valve was opened and the pressure in the tank and probe assembly was recorded as a function of time. The maximum run time of a permeability measurement is normally set at 24 seconds; however, extreme accuracy and repeatability is required for low-permeability samples (less than 0.01 md) (Core Laboratories Instruments, 1996). For that reason, a maximum run time of 30 seconds was used during spot-minipermeametry testing of Alderson Member strata.

This testing method was performed in order to determine average permeability to air values (K_a) for sedimentary fills associated with biogenically produced structures, and values for the surrounding matrix. Due to the highly sensitive nature of this method, samples must be prepared in a consistent fashion prior to analysis. Because of this, direct comparison of permeability values with those derived from other studies is not possible as it is impossible to establish

consistency of sample preparation outside this study. All samples were handled and prepared by the senior author. This ensured a consistent test surface for all samples subjected to spot-permeability analysis.

Five measurements were obtained from each test location. Permeability values were calculated as the average of the three closest measurements.

Anomalously high measurements acquired from locations where a poor probe tip seal (*e.g.*, unlevel testing surface, edge effects, etc.) or microfracturing was apparent were eliminated from the data set. Contour maps of permeability were then generated using the Surfer 9 gridding and contouring software package (Rockware ®, Inc., 2009). Minor contour editing was performed in order to highlight the lithologically constrained nature of the permeability domains.

Spot-minipermeametry proved to be excellent at providing precise permeability measurements, however, due to the relatively large area tested by the probe (~0.46 centimetre diameter), the permeability of diminutive trace fossils was extremely difficult to assess.

High-pressure Mercury Injection Porosimetry Testing

In order to characterize pore-throat size distribution, pore geometry, and to reconcile subtle porosity and permeability heterogeneities—such as those present within Alderson Member *Phycosiphon*-dominated sandy mudstones—high-pressure mercury injection porosimetry was performed on six samples. Samples were obtained from both the pervasively burrowed and the non-burrowed (muddy

matrix) fabrics of the *Phycosiphon*-dominated sandy mudstone facies. Each sample was cut into a cube approximately 1 cm to a side using a variable speed handheld rotary tool and subsequently blown with compressed air. Mercury injection testing was then conducted using a Micromeritics Autopore IV machine (Experimental Geophysics Group, University of Alberta).

Details of this testing method can be found in Jennings, 1987; Vavra et al., 1992; Webb, 2001; and the American Society for Testing and Materials (ASTM International). High-pressure mercury porosimetry tests involved placing a sample into a vacuum chamber and subsequently evacuating it in order to remove contaminant vapors (usually water). Upon the removal of contaminants, mercury is added to the chamber. Through this process, an environment comprising a solid (the sample), a non-wetting liquid (mercury), and mercury vapor was established. The pressure within the chamber was then increased toward ambient and the total volume of mercury entering the largest voids within the sample was monitored. When pressure has reached equilibrium, pores approaching approximately 12 mm in diameter will have been invaded (Webb, 2001). At this time, the chamber was placed inside a pressure vessel for the remainder of the test. A maximum pressure of approximately 414 MPa (60 000 psi) was possible using the Micromeritics Autopore IV. At maximum pressure, mercury penetrates apertures as small as 0.003 micrometres in diameter. This is necessary when attempting to obtain permeability and porosity data from extremely fine-grained sediments (Webb, 2001).

To obtain accurate, high resolution data, the intrusion process must be allowed to equilibrate before increasing pressure as any slight change to the pressure inside the vessel shall induce imbibition of the next smaller-sized pore class. In other words, high-resolution data, particularly in smaller pore-throat ranges, requires mercury porosimetry to be conducted by way of a series of pressure steps. Here, pressure is raised, and subsequently held until mercury flow into the sample ceases. Once mercury intrusion has stopped, pressure is increased for the next incremental reading (Webb, 2001).

The pressure required to inject additional mercury into the pore volume of a sample is a function of pore-throat size distribution. With increasing pressure, imbibition of mercury occurs through smaller and smaller pore apertures. Since mercury is a non-wetting fluid with a contact angle θ of approximately 141.3° , the penetration of mercury can be expressed as:

$$D = -\frac{l}{P} 4\gamma \cos\theta, \quad (3.1)$$

where D is the pore throat diameter, γ is the surface tension of mercury (480 mN/m²), θ is the contact angle (wetting angle), and P is the pressure. This relationship is commonly known as the Washburn equation (Washburn, 1921) and is based on the assumption that pore-throats are cylindrical in morphology. The Washburn equation was used to calculate pore-throat size distribution within Alderson Member rock fabrics; however, it should be noted that in almost any porous media cylindrically shaped pore-throats do not exist.

High-pressure mercury intrusion curves (HPMIC) were produced using the information gathered during porosimetry testing. HPMIC curves were created for the burrowed and non-burrowed fabrics of the Alderson Member *Phycosiphon*-dominated sandy mudstone facies. These plots were then compared with HPMIC curves produced for other Alderson Member facies. The HPMIC curves provided a basis for comparison of fluid-hosting properties between facies within the Alderson Member and the effects bioturbation has within a particular facies.

Spot-Minipermeametry Test Results

Figure 3.6 displays core photos annotated with spot-permeability test locations and corresponding permeability measurements (in millidarcy). On the right, permeability measurements are contoured to illustrate permeability distribution within the respective samples. The samples presented in Figure 3.6 exhibit permeability characteristics and distribution of permeability fields within pervasively bioturbated rock fabrics (Facies 1A) and heterolithic bedded strata (Facies 2B). These properties are used to compare and contrast the fluid hosting potential of these rock types (see discussion).

In general, spot-minipermeametry testing of Alderson Member facies has demonstrated that permeability in pervasively burrowed intervals appears to be slightly enhanced when compared to the accompanying muddy matrix. Tests conducted on *Phycosiphon* burrowed sandy mudstones typically display

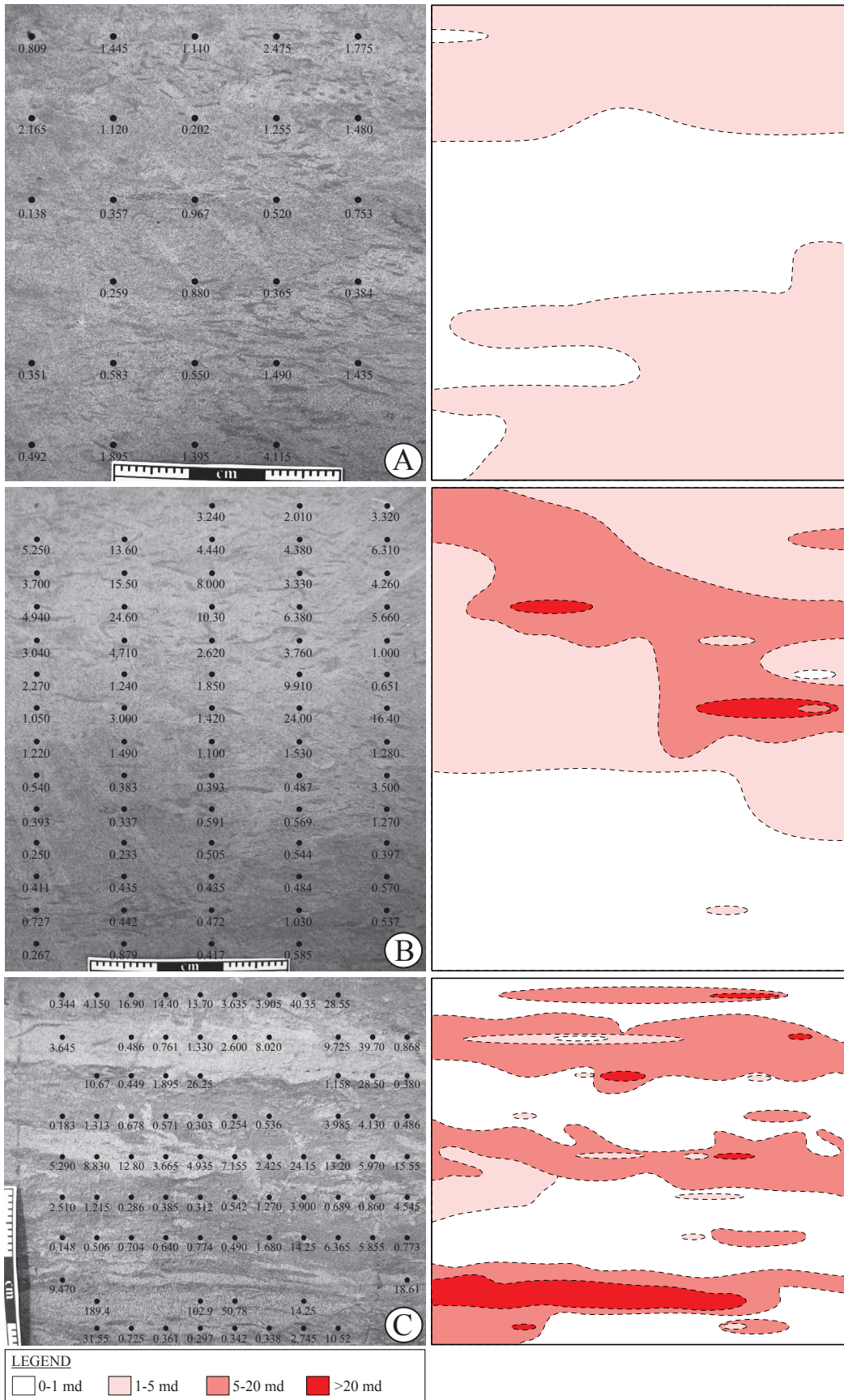


FIGURE 3.6 (previous page): Results of spot-minipermeametry tests conducted on Alderson Member facies. On the left hand side, core photos have been annotated with spot-minipermeametry test locations and the corresponding permeability to air (K_a) measurements in millidarcy. On the right, permeability measurements have been contoured using a combination of computer generated contours and manual contour editing. Higher permeability fields are indicated by dark pink to red coloured contours, while light pink to white colours indicates low permeability fields. **A)** *Phycosiphon*-dominated sandy mudstone facies (Facies 1A) tested using a 1 cm grid pattern. In general, burrow-associated permeability appears to be slightly enhanced relative to the background muddy matrix (right). 08-25-15-27W3 (~ 439.52 m). **B)** *Phycosiphon*-dominated sandy mudstone facies (Facies 1A) tested using 5 mm grid spacing in the x-direction, and 1 cm spacing in the y-direction. As with figure A, the bioturbated fabric of this sample displays elevated permeability measurements when compared to the muddy matrix (right). Anomalously high permeability measurements may be the result of a poor probe tip seal. 10-27-15-22W3 (~ 478.10 m). **C)** Bioturbated heterolithically bedded facies (Facies 2B) tested using a 5 mm grid pattern. Within this facies, the highest permeabilities are associated with discontinuous sand lenticles. The permeability characteristics of these sand lenses allow for the preferential migration of gas (“permeability streaks”). The highest permeability measurements recorded from Alderson Member strata are associated with Facies 2B. 10-27-15-22W3 (~ 475.70 m).

spot-permeabilities ranging from 3×10^{-1} to over 1 md, while fabrics comprising muddy matrix exhibit a permeability range of $1 \times 10^{-1} - 5 \times 10^{-1}$ md. Because matrix permeability is within two orders of magnitude relative to burrow-associated permeability, Alderson Member *Phycosiphon*-dominated sandy mudstones can be considered a dual-porosity flow network system.

Spot-minipermeability test results also demonstrate that the highest permeability values within the Alderson Member are associated with heterolithic bedded, sand lenticle bearing units (F2B – Table 3.1), with permeability measurements as high as 4×10^2 md. Interlaminated sand, silt, and mud intervals (F2A – Table 3.1) typically exhibit permeabilities on the order of $2 \times 10^{-1} - 1$ md.

High-pressure Mercury Injection Porosimetry Test Results

Mercury porosimetry test results from *Phycosiphon*-dominated sandy mudstone, interlaminated sand, silt, and mud, and muddy matrix samples are presented in Figure 3.7. The x-axis of the HPMIC curves provides information on the

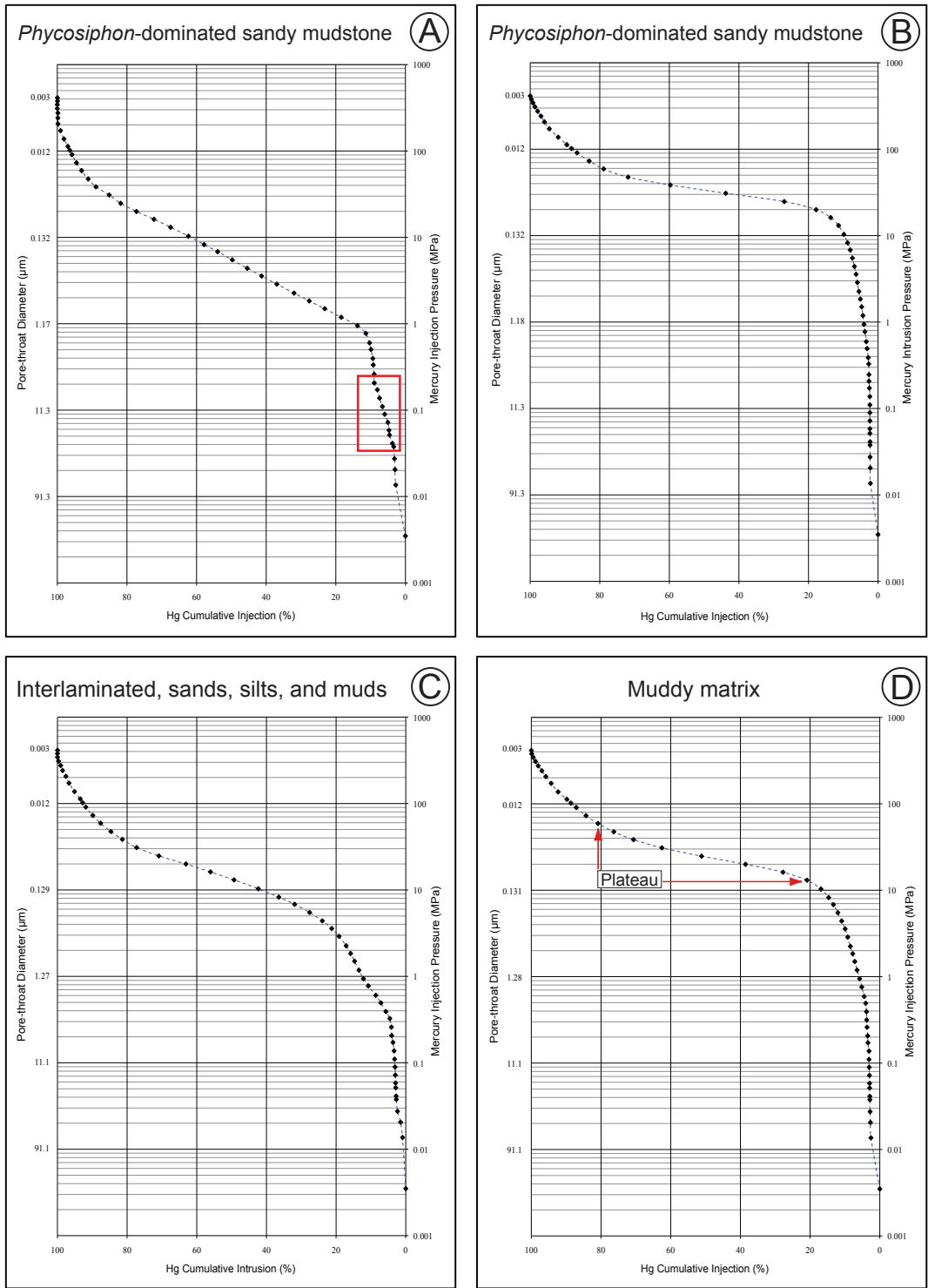


FIGURE 3.7: High-pressure mercury injection porosimetry test results from Alderson Member rock fabrics comprising *Phycosiphon*-dominated sandy mudstone (**A & B**), interlaminated sand, silt, and mud (**C**), and muddy matrix (**D**). Red box in **A** highlights the transition between pore-throat families I and II (*i.e.*, “step”).

cumulative amount of mercury intruded into each sample, while the y-axis exhibits the pressure applied (right side), and the approximate size of the pore-throats through which mercury has penetrated (left side; calculated using equation 3.1).

Parameters such as pore-throat sorting (PTS), reservoir grade, and oil columns for 50% and 75% oil saturations can be extracted from mercury injection porosimetry data (Jennings, 1987). PTS, as the name implies, is a measure of the sorting of pore-throat sizes contained within a rock sample (Jennings, 1987). This is done by applying a numerical value to the slope of the plateau found on a semi-log plot of mercury porosimetry data. For illustrative purposes, a plateau has been annotated in Figure 3.7D. PTS values can be obtained using an equation developed by Trask (1932); however, for the purposes of this analysis, PTS is described qualitatively as opposed to providing numerical values for plateau slope. For example, well-sorted samples tend to display characteristically horizontal plateau morphologies (slope approaching zero), with pore-throat sorting becoming poorer as the plateau steepens (Jennings, 1987).

In most cases, *Phycosiphon* burrowed sandy mudstone samples display a subtle step like that shown in Figure 3.7A (~ 0.04 – 0.2 MPa; see red box). *Phycosiphon* burrowed sandy mudstones appear to exhibit porosity and permeability characteristics similar to those contained within interlaminated sands, silts, and muds, as samples comprising this rock fabric also contain a step in their HPMIC curves (Figure 3.7C). Within these samples, HPMIC data reveals

the presence of two pore-throat families (pore-throat families I & II). Pore-throat family I occurs below the step contained within the intrusion plot of Figure 3.7A (~ 0.04 – 0.2 MPa). This data displays a narrow standard deviation, indicative of a small range in larger pore-throat diameters. Within *Phycosiphon* burrowed sandy mudstone samples, larger pore-throat diameters typically comprise 9 to 12 per cent of the total pore-throat volume. In samples consisting of interlaminated sand, silt, and mud, 11 to 15 per cent of the total pore-throat volume is dominated by larger pore-throat sizes. This suggests the presence of larger (sand sized; ~ 0.1667 – 0.0625 mm) pore spaces within these samples.

Pore-throat family II occurs above the steps contained within the HPMIC plots of Figure 3.7A and 3.7C. This pore-throat family dominates both the *Phycosiphon* burrowed sandy mudstone and interlaminated sand, silt, and mud samples. Pore-throat family two exhibits a large standard deviation and is indicative of a broad continuum of smaller pore throat diameters. This is likely the result of grain or particle sizes dominated by silts and clays. By in large, samples comprising *Phycosiphon*-dominated sandy mudstones and interlaminated sands, slits, and muds, are moderately sorted. This is indicated by inclined plateau shape morphology.

In rare instances, *Phycosiphon* burrowed sandy mudstone samples exhibit smooth HPMIC curves (Figure 3.7B) that are analogous to the HPMIC curves derived from muddy matrix samples (Figure 3.7D). The smooth nature of these curves indicates the presence of extremely small pore spaces and grain sizes

dominated by silt and clay. The plateau shape within these plots is relatively horizontal indicating nearly uniform pore-throat size distribution.

DISCUSSION

Until recently, the effect of bioturbation on the resource potential of highly prolific Alderson Member strata was poorly understood. Spot-minipermeametry and high-pressure mercury injection porosimetry of Alderson Member samples has shown that the most permeable fabrics are associated with sand dominated, heterolithically bedded intervals (F2B – Table 3.1). Results demonstrate that sand bodies of this nature can store large quantities of gas and also provide preferential migration pathways. The characteristics of these sand bodies allow much more effective fluid transmission than that of the interstratified muds. It is these properties that have allowed rock fabrics of this type to be classified as “permeability streaks,” or dual-permeability flow network systems. Data shown here support previous authors who have proposed sand dominated, heterolithically bedded intervals as the main gas reservoir within the Alderson Member (Shurr and Ridgley, 2002; O’Connell, 2003; Pedersen, 2003; Payenberg, 2003; Gatenby, 2004). Within the heterolithic units, interbedded mud lithosomes consist of unburrowed, micro-laminated mudstones, and *Phycosiphon*-dominated sandy mudstones (F1A – Table 3.1). In situations where heterolithic units are interbedded with burrowed sandy mudstones, biogenically enhanced permeability

appears to be important in providing fluid communication between discontinuous sand interbeds and lenticles (see Figure 3.8).

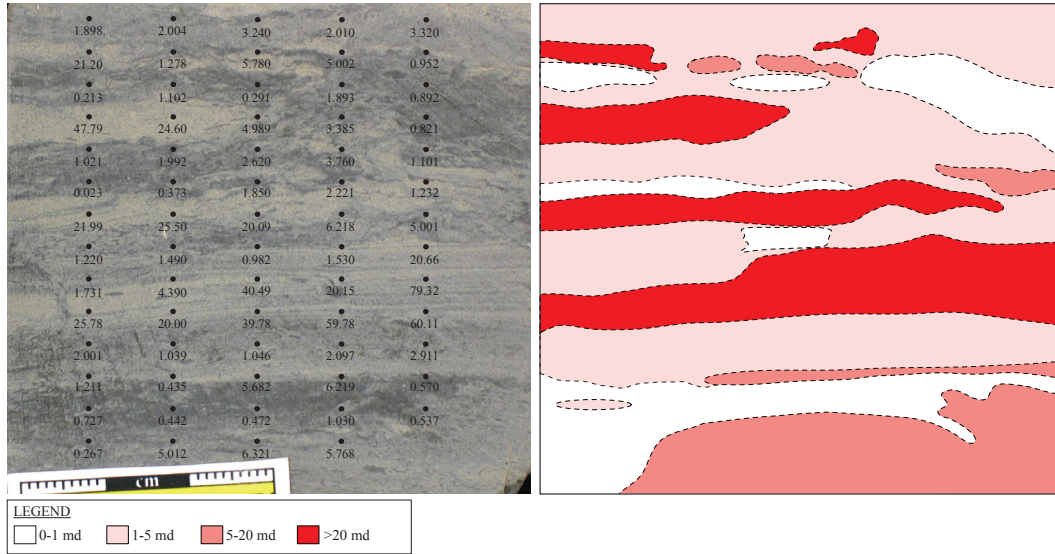


FIGURE 3.8: Core sample comprising interbedded *Phycosiphon*-dominated sandy mudstone (Facies 1A) and bioturbated heterolithic intervals (Facies 2B). Spot-minipermeametry testing was conducted using 5 mm grid spacing in the x-direction, and 1 cm spacing in the y-direction. Permeability test locations and the corresponding test results (in millidarcy) are annotated on the left hand side. On the right, permeability measurements are contoured using a combination of computer generated contours and manual contour editing. Higher permeability fields are indicated by dark pink to red colored contours, while light pink to white colors indicates low permeability fields. In this sample, elevated permeability characteristics (light pink permeability field, 1 – 5 md values) associated with interbedded *Phycosiphon*-dominated sandy mudstones (Facies 1A) appear to establish fluid communication between otherwise discontinuous sand lenticles (Facies 2B). 10-27-15-22W3 (~ 493.78 m).

Spot-minipermeametry experiments demonstrate that pervasively bioturbated intervals enhance the overall bulk permeability of the Alderson Member compared to muddy unburrowed beds. Results from high-pressure mercury injection porosimetry testing (Figure 3.7) have shown that pore-throat size distribution within bioturbated media is similar to the bulk distribution of pore-throat sizes contained in interlaminated sands, silts, and muds. The elevated permeability values of *Phycosiphon*-dominated sandy mudstones likely result

from: 1) the admixing of sand and silt sized clasts into an otherwise extremely fine-grained, low-permeability matrix; or, 2) textural segregation such that larger pore-throat sizes occur within more continuous domains (burrows) that are distinct from domains concentrated with small pore-throat sizes (matrix). In other words, biogenic processes appear to enhance the resource characteristics of otherwise extremely low-permeability Alderson Member strata.

The complex storage characteristics of pervasively bioturbated *Phycosiphon* flow networks provide tortuous pathways for fluid interaction and transmission; however, the nature of these tortuous networks suggests that higher permeability zones may be common. Tortuous, heterogeneous media present a notable complication for reservoir development. Unlike fractured rock, which can be viewed as a dual-permeability system with distinctly mobile and immobile zones, burrow-mottled media provide a heterogeneous dual-porosity system where zones exhibit a limited but significant range of mobility (Gingras et al., 1999; Gingras et al., 2004a). Tortuous pathways can have dramatically different effects on fluid migration. Depending on the type of fluids present, the production of hydrocarbons from reservoirs comprising complex migration pathways can be quite variable. In pervasively bioturbated reservoirs saturated by more than one phase, dead-end zones created by the biogenic churning of sediment tend to isolate higher viscosity fluids and inhibit their drainage. On the other hand, in pervasively bioturbated gas-bearing intervals, tortuous flow conduits tend to slow rather than inhibit the production of gas as it must migrate through a complex

pore network (Gingras et al., 2004a). *Phycosiphon* provide flow conduits that interact extensively with the surrounding matrix. These factors may account for the steady and long-lived production lives of wells targeting fine-grained, pervasively bioturbated intervals.

The permeability and porosity characteristics of pervasively burrowed Alderson Member media suggest that subtle dual-porosity is associated with *Phycosiphon*-dominated sandy mudstones. This dual-porosity nature suggests that *Phycosiphon*-dominated sandy mudstones likely make a significant contribution to the storativity and deliverability of gas from the Hatton Gas Pool. In fact, the reservoir character of the burrowed media may be surprisingly similar to the flow behavior predicted in interlaminated sand, silt, and mud intervals. Contrary to dual-permeability flow networks, where production is solely derived from the higher permeability textural component—where production by-passes the lower permeability component of the reservoir volume—dual-porosity flow network systems (e.g., Alderson Member *Phycosiphon*-dominated sandy mudstones) allow production of hydrocarbons from both pervasively bioturbated and background matrix fabrics albeit with complexity not seen in homogeneous reservoir materials.

Attempting to assess the distribution of permeable fabrics within the Hatton Gas Pool and their potential effects on production potential is challenging. Alderson Member successions consist of stacked metre-thick parasequences of extremely subtle, upward-coarsening units (Pedersen, 2003; Hovikoski et al.,

2008). A west – east transect through the Hatton Gas Pool reveals that in a lateral sense, facies distribution—and thus the distribution of permeable rock fabrics—within the Alderson appears to be highly variable. Subsurface observations have been tied to gamma-gamma-plots (*i.e.*, gamma-ray butterfly curves) and correlations from the Hatton Gas Pool based on these are presented in Figure 3.9. Gamma-gamma-plots consist of two components: 1) the original gamma-ray curve obtained from petrophysical measurement of a particular wellbore (left limit of gamma-gamma-plot; see Figure 3.9); and, 2) the mirrored image of the original gamma-ray curve (right limit of gamma-gamma-plot). The two curves, once joined, comprise the gamma-gamma-plot for a particular well. These plots allow for the estimation of the overall shaliness of a rock body based on the shape of the corresponding gamma-ray butterfly curve. For example, elevated proportions of uranium, thorium and potassium are usually associated with shaley lithologies. As a result, higher API values are measured using a conventional gamma-ray tool (gamma-ray [GR] responds with a kick to the right on a standard GR plot). Mirroring such a response shall produce a characteristic “narrowing” of a gamma-ray butterfly curve. On the other hand, sandier lithologies are much less radioactive (less amounts of uranium, thorium and potassium) when compared to their shaley counterpart. Consequently, a characteristic “widening” of a gamma-ray butterfly curve results. Unlike a conventional gamma-ray curve, gamma-gamma-plots provide observable variability when dealing with relatively homogeneous lithologies. Therefore, gamma-ray butterfly curves are extremely

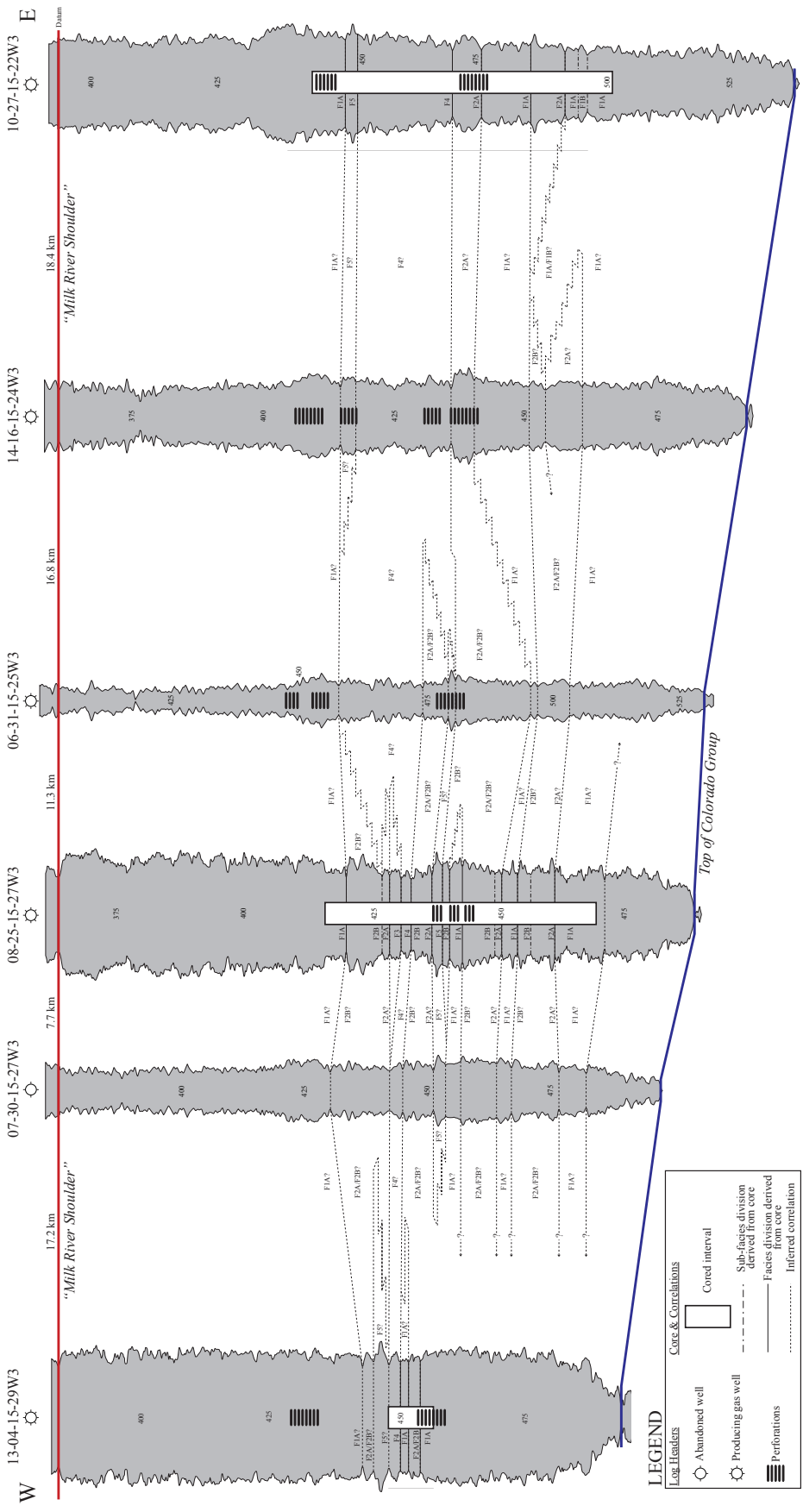


FIGURE 3.9 (previous page): West – east stratigraphic transect through the Hatton Gas Pool. Locations of the wells used in the construction of this cross-section are presented in Figure 3.4 (see line of section). Crude facies correlations were derived using subsurface observations and gamma-gamma-plots (gamma-ray butterfly curves). Facies distribution within the Alderson appears to be extremely variable in both lateral and vertical directions. In some instances, perforations coincide with Facies 1A. The Milk River Shoulder was chosen as the datum for this section. This surface corresponds to the transition from the overall regressive Milk River / Lea Park Formations to the transgressive Pakowki formation.

useful when attempting to interpret GR logs obtained from fine-grained, relatively homogeneous strata like that of the Alderson Member.

Detailed sedimentological, stratigraphical, and ichnological observations from cores used in the construction of Figure 3.9 are summarized in Figure 3.10. This data demonstrates that perforated intervals were likely selected based on clean gamma-ray responses and an increase in resistivity (resistivity log not displayed on cross section). In many cases, this led to the perforation of the *Phycosiphon*-dominated sandy mudstone facies, or portions thereof.

Like most low-permeability shallow-gas wells, production from the Alderson Member typically displays high initial gas flow rates followed by a steady decline in production. Over a short period of time, production levels tend to equilibrate and gas production remains fairly consistent—the typical life of unconventional, low-permeability gas wells is between 20 and 40 years, occasionally more (O’Connell, 2007). High initial flow rates likely result from delivery of gas hosted within rock fabrics exhibiting higher permeability. As production continues, interactions with lower permeability dual-porosity fabrics become more prevalent (*e.g.*, *Phycosiphon*-dominated sandy mudstones). However, high clay content within Alderson Member strata decreases resistivity,

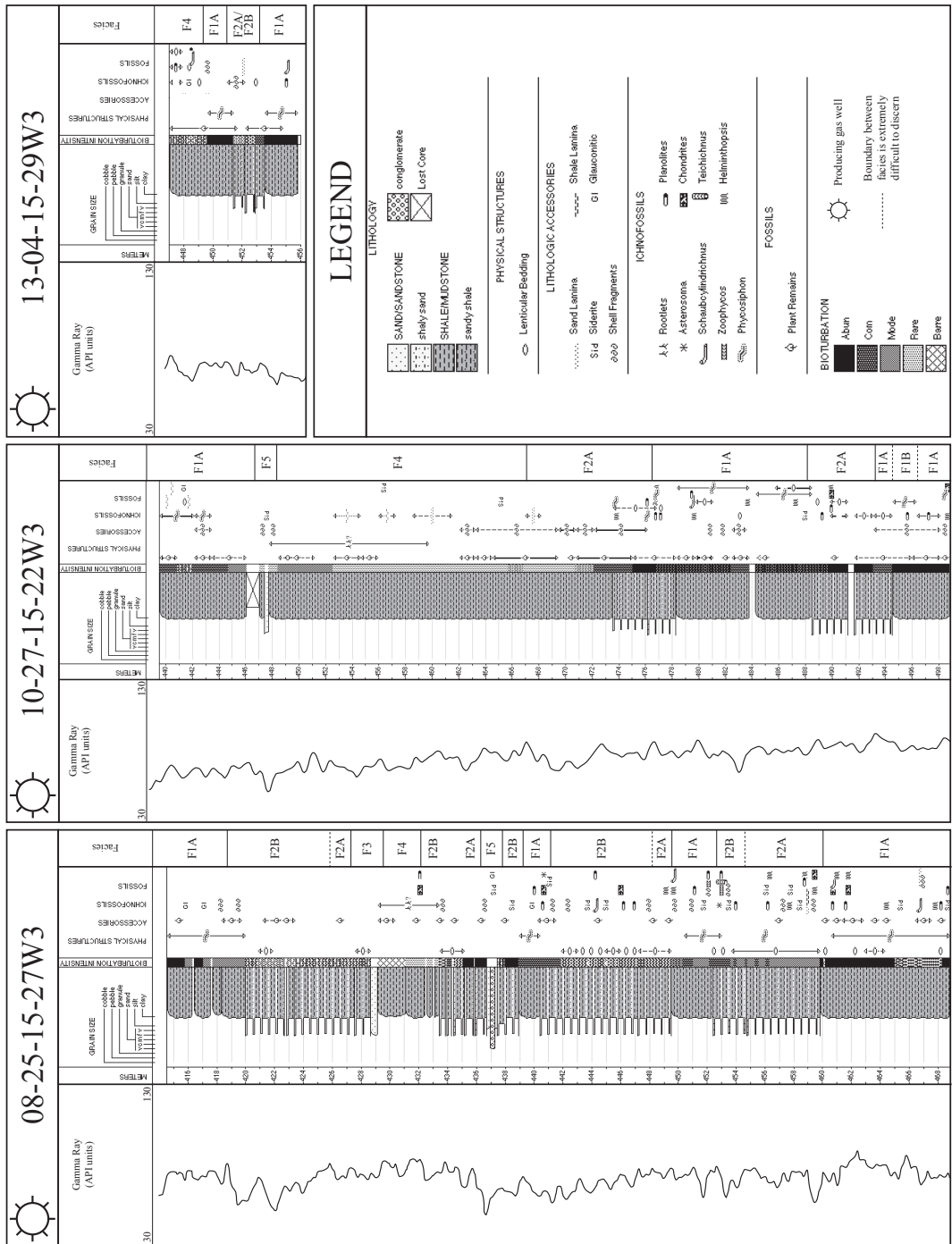


FIGURE 3.10: Details of sedimentological, ichnological, and stratigraphical observations from the cored intervals presented in Figure 3.9.

increases ineffective porosity, and retains large volumes of bound water (O'Connell, 2003). As a result, conventional log calculations (*i.e.*, Archie's equation) conducted on pay zone intervals demonstrate that the Alderson Member is 'water wet' (O'Connell, 2007). This presents a problem, as it is extremely difficult to predict gas and water production from target reservoirs. To avoid complications, reservoir development must be meticulous. Once flooded (*i.e.*, during secondary recovery), rock fabrics such as *Phycosiphon*-dominated sandy mudstones will isolate the gas-bearing matrix and cease the production of hydrocarbons (Gingras et al., 2004a). An understanding of the flow dynamics from the resulting anisotropic permeability allows for improved production techniques applied to the management of pervasively bioturbated low-permeability gas reservoirs, and thus, provides a potentially powerful developmental tool.

SUMMARY AND CONCLUSIONS

Low-permeability, gas-charged reservoirs have unique ichnological, lithological, petrophysical, porosity, and permeability properties. Previously, failure to fully understand these attributes has led to a misunderstanding of fluid distributions in the subsurface. Recent work has shown that certain bioturbated rock fabrics can enhance the vertical and lateral transmission of hydrocarbons within bioturbated intervals (*e.g.*, Meadows and Tait, 1989; Lavoie et al., 2000; Schmidt et al., 2002; Bastardie et al., 2003; Katrak and Bird, 2003; Pemberton and Gingras, 2005;

Gingras et al., 2007; Cunningham et al., 2009). A detailed understanding of the specific trace fossil genera and species, their diversity and morphology, and their relationship with other physical and biological fabrics can lead to a much improved evaluation of reservoir and fluid flow architecture.

This paper presents a comprehensive examination of Alderson Member strata (Lea Park Formation) conducted on ten cores from the Hatton Gas Pool area of southwest Saskatchewan, Canada. Shallow biogenic gas produced from this prolific play is derived from pervasively bioturbated marine shales, mudstones, siltstones, and fine-grained sandstones. Conservative gas-in-place estimates of Milk River Formation / Alderson Member reserves range from 10 to 21 TCF (28-60 Mm³) (O'Connell, 2003; Pemberton 2009, personal communication). Core analysis has determined that one of the most volumetrically abundant facies within the Alderson Member (approximately 20-25%) consists of a *Phycosiphon*-dominated sandy mudstone of offshore affinity (Facies 1A – Table 3.1). The regular occurrence of this facies combined with the highly productive nature of the Alderson Member has led to the suggestion that *Phycosiphon*-dominated sandy mudstones could contribute to the overall storage of gas within this unit.

The mechanisms responsible for the enormous gas reserves contained within the Alderson Member have, until recently, remained poorly understood. In order to better understand the reasons responsible for these substantial gas reserves, Hovikoski et al. (2008) conducted a regional subsurface study of Alderson Member cores. Based on sedimentological and ichnological criteria,

Alderson Member strata were subdivided into seven facies, and seven subfacies (Hovikoski et al., 2008). Five of the facies described by Hovikoski (2008) are present within the Hatton Gas Pool area.

Phycosiphon-dominated sandy mudstones contribute to the resource potential of Alderson Member deposits. Using spot-minipermeametry and high-pressure mercury injection porosimetry, the complex porosity and permeability characteristics of pervasively bioturbated rock fabrics contained within the Alderson were assessed. Spot-minipermeametry was conducted on eleven one-third-slab samples, while mercury porosimetry data was obtained using six cube samples measuring approximately 1 cm to a side. Test results demonstrate that sand dominated, heterolithically bedded intervals (Facies 2B – Table 3.1) are likely the main gas storage mechanism within the Alderson Member. However, permeability experiments conducted on *Phycosiphon*-dominated sandy mudstones have shown that bioturbated fabrics can locally act to enhance reservoir properties. The data demonstrates that *Phycosiphon*-dominated sandy mudstones tend to exhibit slightly enhanced permeability characteristics relative to an otherwise extremely low-permeability matrix, thus representing a dual-porosity flow network system. This facies also seems to be important in linking discontinuous or improving communication between sand interbeds and lenticles present within the sand dominated, heterolithically bedded intervals of Facies 2B.

The production of gas from Alderson Member reservoirs is complicated by many factors. The complex storage characteristics of pervasively bioturbated *Phycosiphon*-dominated sandy mudstone units create tortuous fluid migration pathways. Furthermore, high clay contents within Alderson Member strata result in the presence of large volumes of bound water (O'Connell, 2007). Water saturation calculations conducted on Alderson Member strata suggest that the reservoir exists in a water-wet state (O'Connell, 2007). This presents a significant problem, as it is extremely difficult to predict gas and water behavior within its complex pore system. If development is mismanaged, flooding of the reservoir during secondary recovery could isolate the gas-bearing matrix resulting in the cessation of hydrocarbon production (Gingras et al., 2004a). These factors should be taken into consideration if successful production from pervasively bioturbated, low-permeability, gas-charged reservoirs like those present within the Alderson Member is to occur.

REFERENCES CITED

- BASTARDIE, F., CAPOWIEZ, Y., DE DEREUY, R., AND D. CLUZEAU, 2003, X-ray tomographic and hydraulic characterization of burrowing by three earthworm species in repacked soil cores: *Applied Soil Ecology*, v. 24, p. 3 – 16.
- BROMLEY, R.G., 1990, *Trace fossils; biology and taphonomy*: Unwin Hyman, London, 280 p.
- CORE LABORATORIES INSTRUMENTS, 1996, *Profile Permeameter PDPK – 400 Operations Manual*, 40p.

- CUNNINGHAM, K.J., SUKOP, M.C., HUANG, H., ALVAREZ, P.F., CURRAN, H.A., RENKEN, R.A., AND J.F. DIXON, 2009, Prominence of ichnologically influenced macroporosity in the karst Biscayne aquifer: Stratiform “super-K” zones: Geological Society of America, Bulletin, v. 121, p. 164 – 180.
- DAWSON, W.C., 1978, Improvement of sandstone porosity during bioturbation: American Association of Petroleum Geologists, Bulletin, v. 62, p. 508 – 509.
- DROSER, M.L., AND D.J., BOTTJER, 1986, A semiquantitative field classification of Ichnofabrics: Journal of Sedimentary Petrology, v. 56, p. 558 – 559.
- FUEX, A.N., 1977, The use of stable carbon isotopes in hydrocarbon exploration: Journal of Geochemical Exploration, v. 7, p. 155 – 188.
- FURNIVAL, G.M., 1946, Cypress Lake map-area, Saskatchewan: Geological Survey of Canada, Memoir 242, 161p.
- GATENBY, W., AND M. STANILAND, 2004, Preliminary sedimentology of Milk River equivalent in the New Abby/Lacadena gas fields, Saskatchewan (abstract): Canadian Society of Petroleum Geologists, Core Conference Abstract Book, p. 55 – 68.
- GINGRAS, M.K., PEMBERTON, S.G., MENDOZA, C.A., AND F. HENK, 1999, Assessing the anisotropic permeability of *Glossifungites* surfaces: Petroleum Geoscience, v. 5, p. 349 – 357.
- GINGRAS, M.K., MACMILLAN, B., BALCOM, B.J., SAUNDERS, T., AND S.G. PEMBERTON, 2002, Using magnetic resonance imaging and petrographic techniques to understand the textural attributes and porosity distribution in *Macaronichnus*-burrowed sandstone: Journal of Sedimentary Research, vol. 72, no. 4, p. 552 – 558.
- GINGRAS, M.K., MENDOZA, C.A., AND S.G. PEMBERTON, 2004a, Fossilized worm burrows influence the resource quality of porous media: American Association of Petroleum Geologists, Bulletin, v. 88, p. 875 – 883.
- GINGRAS, M.K., PEMBERTON, S.G., MUEHLENBACHS, K., AND H. MACHEL, 2004b, Conceptual models for burrow-related, selective dolomitization with textural and isotopic evidence from the Tyndall Limestone: Geobiology, v. 2, p. 21 – 30.

- GINGRAS, M.K., PEMBERTON, S.G., HENK, F., MACEachern, J.A., MENDOZA, C., ROSTRON, B., O'HARE, R., SPILA, M., AND K. KONHAUSER, 2007, Applications of ichnology to fluid and gas production in hydrocarbon reservoirs, *in* MacEachern, J.A., Bann, K.L., Gingras, M.K., and Pemberton, S.G., eds., *Applied Ichnology: SEPM, Short Course Notes 52*, p. 129 – 143.
- GILL, J.R., AND W.A. COBBAN, 1973, Stratigraphy and geologic history of the Montana Group and equivalent rocks, Montana, Wyoming and North and South Dakota: United States Geological Survey, Professional Paper 776, 37p.
- GOLDRING, R., AND P. BRIDGES, 1973, Sublittoral sheet sandstones: *Journal of Sedimentary Petrology*, v. 43, p. 736 – 747.
- GOLDRING, R., POLLARD, J.E., AND A.M. TAYLOR, 1991, Ichnofabric-forming trace fossil in post-paleozoic offshore siliciclastic facies: *Palaios*, v. 6, p. 250 – 263.
- GUNATILAKA, A., AL-ZAMEL, A., SHERMAN, A.J., AND A. REDA, 1987, A spherulitic fabric in selectively dolomitized siliclastic crustacean burrows, northern Kuwait: *Journal of Sedimentary Petrology*, v. 57, p. 927 – 992.
- HOVIKOSKI, J., LEMISKI, R., GINGRAS, M., PEMBERTON, S.G., AND J. MACEachern, 2007, Preliminary notes on the depositional setting of the Late Cretaceous Alderson Member (Lea Park Formation), *in* Summary of Investigations 2007, Volume 1, Saskatchewan Geological Survey, Sask. Industry Resources, Misc. Rep. 2007-4.1, CD – ROM, Paper A-10, 11p.
- HOVIKOSKI, J., LEMISKI, R., GINGRAS, M., PEMBERTON, S.G., AND J. MACEachern, 2008, Ichnology and sedimentology of a mud-dominated deltaic coast: Upper Cretaceous Alderson Member (Lea Park Fm.), Western Canada: *Journal of Sedimentary Research*, v. 78, p. 803 – 824.
- JENNINGS, J.B., 1987, Capillary Pressure Techniques: Application to Exploration and Developmental Geology, American Association of Petroleum Geologists: *Bulletin*, v. 71, p. 1196 – 1209.
- KATRAK, G., AND F.L. BIRD, 2003, Comparative effects of the large bioturbators, *Trypaea australiensis* and *Heloecius cordiformis*, on intertidal sediments of Western Port, Victoria, Australia: *Marine and Freshwater Research*, v. 54, p. 701 – 708.

- LAW, B.E., AND J.B. CURTIS, 2002, Introduction to unconventional petroleum systems: American Association of Petroleum Geologists, Bulletin, v. 86, no. 11, p. 1851 – 1852.
- LAVOIE, D.L., VAUGHAN, W.C., AND D.H. EASLEY, 2000, Quantitative effects of bioturbation on permeability determined using a whole-tank permeameter: Eos, Transactions, 2000 Fall Meeting, v. 81, p. F650.
- MACEachern, J.A., PEMBERTON, S.G., BANN, K.L., AND M.K. GINGRAS, 2007a, Departures from the archetypal ichnofaices: effective recognition of environmental stress in the rock record, *in* MacEachern, J.A., Bann, K.L., Gingras, M.K., and Pemberton, S.G., eds., Applied Ichnology: SEPM, Short Course Notes 52, p. 65 – 94.
- MACEachern, J.A., PEMBERTON, S.G., GINGRAS, M.K., AND K.L. BANN, 2007b, The Ichnofacies concept: a fifty-year retrospective, *in* Miller, W., III, ed., Trace Fossils: Concepts, Problems, Prospects: Amsterdam, Elsevier, p. 50 – 75.
- McKINLEY, J.M., LLOYD, C.D., AND A.H. RUFFELL, 2004, Use of variography in permeability characterization of visually homogeneous sandstone reservoirs with examples from outcrop studies: Mathematical Geology, v. 36, p. 761 – 779.
- MEADOWS, P.S., AND J. TAIT, 1989, Modification of sediment permeability and shear strength by two burrowing invertebrates: Marine Biology, v. 101, p. 75 – 82.
- MEHRTHENS, C., AND B. SELLECK, 2002, Middle Ordovician section at Crown Point Peninsula, *in* J. McLelland and P. Karabinos, eds., Guidebook for fieldtrips in New York and Vermont. University of Vermont, p. B5.1 – B5.16.
- MEIJER DREES, N.C., AND D.W. MYHR, 1981, The Upper Cretaceous Milk River and Lea Park Formations in southeastern Alberta: Bulletin of Canadian Petroleum Geology, v. 29, p. 42 – 74.
- O'CONNELL, S.C., 2001, The Second White Specks, Medicine Hat and Milk River formations – A shallow gas workshop, consult. rep.
- O'CONNELL, S., 2003, The unknown giants – low permeability shallow gas reservoirs of southern Alberta and Saskatchewan, Canada: Canadian Society of Exploration Geophysicists, Conference Abstracts.

- O'CONNELL, S., 2007, The Second White Specks, Medicie Hat and Milk River formations – A shallow gas workshop, consult. rep.
- O'CONNELL, S.C., CAMPBELL, R., AND J. BHATTACHARYA, 1999, The stratigraphy, sedimentology and reservoir geology of the giant Milk River gas field in southeastern Alberta and Saskatchewan: Canadian Society of Petroleum Geologists, Annual Meeting, Abstract 99 – 83 O.
- PAYENBERG, T.H.D., 2002a, Integration of the Alderson Member in southwestern Saskatchewan into a litho- and chronostratigraphic framework for the Milk River/Eagle shoreline in southern Alberta and north-central Montana, *in* Summary of Investigations 2002, Volume 1, Saskatchewan Geological Survey, Sask. Industry Resources, Misc. Rep. 2002-4.1, CD – ROM, p. 134 – 142.
- PAYENBERG, T.H.D., 2002b, Litho-, chrono- and allostratigraphy of the Santonian to Campanian Milk River and Eagle formations in southern Alberta and north-central Montana: Implications for differential subsidence in the Western Interior Foreland Basin. University of Toronto, PhD Thesis, 221p.
- PAYENBERG, T.H.D., BRAMAN, D., DAVIS, D., AND A. MIALI, 2002, Litho- and chronostratigraphic relationships of the Santonian-Campanian Milk River Formation in southern Alberta and Eagle Formation in Montana utilizing stratigraphy, U-Pb geochronology, and palynology: Canadian Journal of Earth Sciences, v. 39, p. 1553 – 1577.
- PEDERSEN, P., 2003, Stratigraphic relationships of Alderson (Milk River) strata between the Hatton and Abbey-Lacadena Pools, southwestern Saskatchewan—preliminary observations, *in* Saskatchewan Geological Survey, Summary of Investigations 2003, Volume 1, p. 1 – 11.
- PEMBERTON, S.G., SPILA, M., PULHAM, A.J., SAUNDERS, T., MACEachern, J.A., ROBBINS, D., AND I.K. SINCLAIR, 2001, Ichnology and sedimentology of shallow to marginal marine systems: Ben Nevis and Avalon reservoirs, Jeanne d'Arc Basin: Geological Association of Canada, Short Course Notes Volume 15
- PEMBERTON, S.G., AND M.K. GINGRAS, 2005, Classification and characterizations of biogenically enhanced permeability: American Association of Petroleum Geologists, Bulletin, v. 89, p. 1493 – 1517.
- REINECK, H.E., 1963, Sedimentgefüge im Bereich der südlichen Nordsee. *Abhandlungen der senckenbergische naturforschende Gesellschaft*, v. 505, p. 1 – 138.

- RIDGLEY, J.L., 2000, Lithofacies architecture of the Milk River Formation (Alderson Member of the Lea Park Formation), southwestern Saskatchewan and southeastern Alberta – its relation to gas accumulation, *in* Summary of Investigations 2000, Volume 1, Saskatchewan Geological Survey, Sask. Energy Mines, Misc. Rep. 2000-4.1, p. 106 – 120.
- ROCKWARE ®, INC., 2009, Surfer 9.0 Gridding and Contouring Software.
- SCHMIDT, G., GINGRAS, M.K., SAUNDERS, T., AND S.G. PEMBERTON, 2002, Biogenic sorting in wave dominated shorelines in the western Canadian sedimentary basin: Canadian Society of Petroleum Geologists Annual Meeting 2002, Calgary, p. 306
- SHURR, G., AND J. RIDGLEY, 2002, Unconventional shallow biogenic gas systems: American Association of Petroleum Geologists, Bulletin, v. 86, p. 1939 – 1969.
- SUTTON, S.J., ETHERIDGE, F.G., ALMON, W.R., DAWSON, W.C., AND K.K. EDWARDS, 2004, Textural and sequence-stratigraphic controls on sealing capacity of Lower and Upper Cretaceous shales, Denver basin, Colorado: American Association of Petroleum Geologists, Bulletin, v. 88, p. 1185 – 1206.
- TAYLOR, A.M., AND R. GOLDRING, 1993, Description and analysis of bioturbation and ichnofabric: Journal of the Geological Survey, London, vol. 150, p. 141 – 148.
- TRASK, P.D., 1932, Origin and environment of source sediments of petroleum: Houston Gulf Publishing Company, 323p.
- TOVELL, W.M., 1956, Some aspects of the geology of the Milk River and Pakowki Formations (southern Alberta). University of Toronto, Thesis, v. 2, 114p.
- VAVRA, C.L., KALDI, J.G., AND R.M., SNEIDER, 1992, Geological Applications of Capillary Pressure: A review: American Association of Petroleum Geologists, Bulletin, v. 76, p. 840 – 850.
- WASHBURN, E.W., 1921, Note on a method of determining the distribution of pore sizes in a porous material: Proceedings of the National Academy of Sciences, vol. 7, p. 115 – 116.
- WEBB, P.A., 2001, An introduction to the physical characterization of materials by mercury intrusion porosimetry with emphasis on reduction and presentation of experimental data, Micromeritics Instrument Corp., p. 3 – 11.

WETZEL, A., 1984, Bioturbation in deep-sea fine-grained sediments: Influence of sediment texture, turbidite frequency and rates of environmental change: *in* Stow, D.A.V., and Piper, D.J.W., eds., *Fine-grained Sediments: Deep Water Processes and Facies*: Geological Society of London Special Publication, no. 15, p. 595 – 608.

ZENGER, D.H., 1992, Burrowing and dolomitization patterns in the Steamboat Point Member, Bighorn Dolomite (Upper Ordovician), northeast Wyoming: *Contributions to Geology*, v. 29, p. 133 – 142.

CHAPTER IV – CONCLUSIONS

In the Hatton Gas Pool area, core analysis of Alderson Member strata was conducted using ten-drill cores. Based on sedimentological and ichnological criteria, a facies classification scheme consisting of five facies, and five subfacies, was developed.

Alderson Member strata have been interpreted to represent deposition from hyperpycnal and hypopycnal fluid mud accumulation. Low substrate consistencies and high depositional rates are commonly associated with hyperpycnal fluid muds. In Alderson Member facies, these conditions are reflected through the preservation of unburrowed massive or micro-stratified mud intervals (laminae or bed scale), fluid escape structures, and sediment loading structures (Bhattacharya and MacEachern, 2009). Characteristic ichnological features of these depositional affinities include reduced and/or fluctuating bioturbation intensities, reductions in trace-fossil size, deformed mantled burrows, and the presence of locally monospecific, *Planolites*-dominated trace-fossil suites (MacEachern et al., 2005; MacEachern et al., 2007a). Moreover, the interpretation of buoyant hypopycnal fluid mud accumulation (sediment plumes) within Alderson Member strata is reflected by the presence of a characteristic ichnofaunal assemblage comprising predominantly deposit-feeding and grazing structures (*e.g.*, *Phycosiphon*, *Helminthopsis*, and *Chondrites*). The lack of more specialized structures (*e.g.*, vertical filter-feeding burrows) suggests high turbidity

levels within hypopycnal intervals. Additionally, complex feeding structures such as *Zoophycos* are locally observed in facies characteristic of shallower water depths, likely owing to the bountiful food resources available in these settings. As a result, ichnofossil assemblages attributable to distal expressions of the *Cruziana* Ichnofacies occur in shallower water than normally expected.

Abundant wave and onshore tidal indicators suggest a coastal affinity for Alderson Member strata in the Hatton Gas Pool area. Tidal influence is reflected by the presence of mud-draped ripple foresets and paired mud-drapes, while wave activity is commonly demonstrated by the presence of parallel-laminated scour-and fill structures, combined flow ripples, and thin intervals of low-angle cross-stratified sandstone. Furthermore, mud-dominated intervals are typically micro-laminated and contain shale-on-shale erosional contacts, further suggesting active deposition under wave and current influence. By in large, the distribution of wave-generated structures suggests: 1) a limited supply of sand sized clasts within the depositional system; and, 2) deposition above storm-weather wave base along a low-gradient, dissipative shoreline.

Based on the stratigraphic arrangement of Alderson Member facies, two types of successions have been interpreted in the Hatton Gas Pool area, these include: 1) “subaqueous deltas”; and, 2) shore margin settings consisting of offshore, muddy shorface (or tidal flat), and muddy coastal plain environments. Subaqueous deltaic successions are reflected by stacked parasequences of subtle, upward-coarsening units in which a fluvial point source cannot be traced. These

successions are laterally extensive (traceable for tens of kilometres), contain ample evidence of wave and tide reworking, and locally pass upwards into root-bearing muds (Facies 4). These characteristics suggests the alongshore redistribution of mud wedges rather than direct seaward prograding river deltas. On the other hand, shore margin successions comprise (in ascending order) bioturbated mud intervals (Facies 1A – muddy offshore to offshore transition), heterolithic bedding (Facies 2 – muddy shoreface), and root-bearing sandy shales (Facies 4 – muddy coastal plain). Shore margin successions demonstrate considerable variability in ichnofossil content, intensity of bioturbation, degree of wave influence, and sand to mud ratios. Furthermore, mud dominated shore margin successions exhibit decreasing wave energy in a landward direction, suggesting a low-gradient, dissipative shoreline.

Using spot-minipermeametry and high-pressure mercury injection porosimetry, the complex porosity and permeability characteristics of Alderson Member strata were assessed. Test results demonstrate that sand dominated heterolithic bedded intervals (Facies 2B – Table 2.1) are the main gas storage mechanism within the Alderson Member. Bioturbated heterolithically bedded intervals exhibit well defined, highly contrasting permeability fields, where matrix- and burrow-associated permeabilities differ by more than two orders of magnitude (Table 2.2). Permeability characteristics of this type are defined as dual-permeability flow networks (Gingras et al., 2007). Within flow networks such as these, the higher permeability portions of the rock provide the only

transmissive fluid conduits. However, permeability experiments conducted on *Phycosiphon*-dominated sandy mudstones (Facies 1A – Table 2.1) have shown that bioturbated fabrics can locally act to enhance reservoir properties within the Alderson Member. Permeability data demonstrates that *Phycosiphon*-dominated sandy mudstones tend to exhibit slightly enhanced permeability relative to an otherwise extremely low-permeability matrix. Biogenic flow networks, wherein matrix permeability is within two orders of magnitude relative to burrow-associated permeability represent dual-porosity flow network systems (Gingras et al., 2007). In dual-porosity flow media, much of the rock volume is used to conduct fluids. Flow is focused through the higher permeability zones, but flow interactions between burrows and the matrix are extensive (Gingras et al., 2007). In situations where heterolithic units are interbedded with heavily burrowed sandy mudstones, biogenically enhanced permeability appears to be important in providing fluid communication between discontinuous sand interbeds and lenticles within the Alderson Member.

High clay content within Alderson Member strata decreases resistivity, increases ineffective porosity, and retains large volumes of bound water (O'Connell, 2003). As a result, conventional log calculations (*i.e.*, Archie's equation) conducted on pay zone intervals demonstrate that the Alderson Member is 'water wet' (O'Connell, 2007). This presents a problem, as it is extremely difficult to predict gas and water production. To avoid complications, reservoir development must be meticulous. Once flooded (during secondary

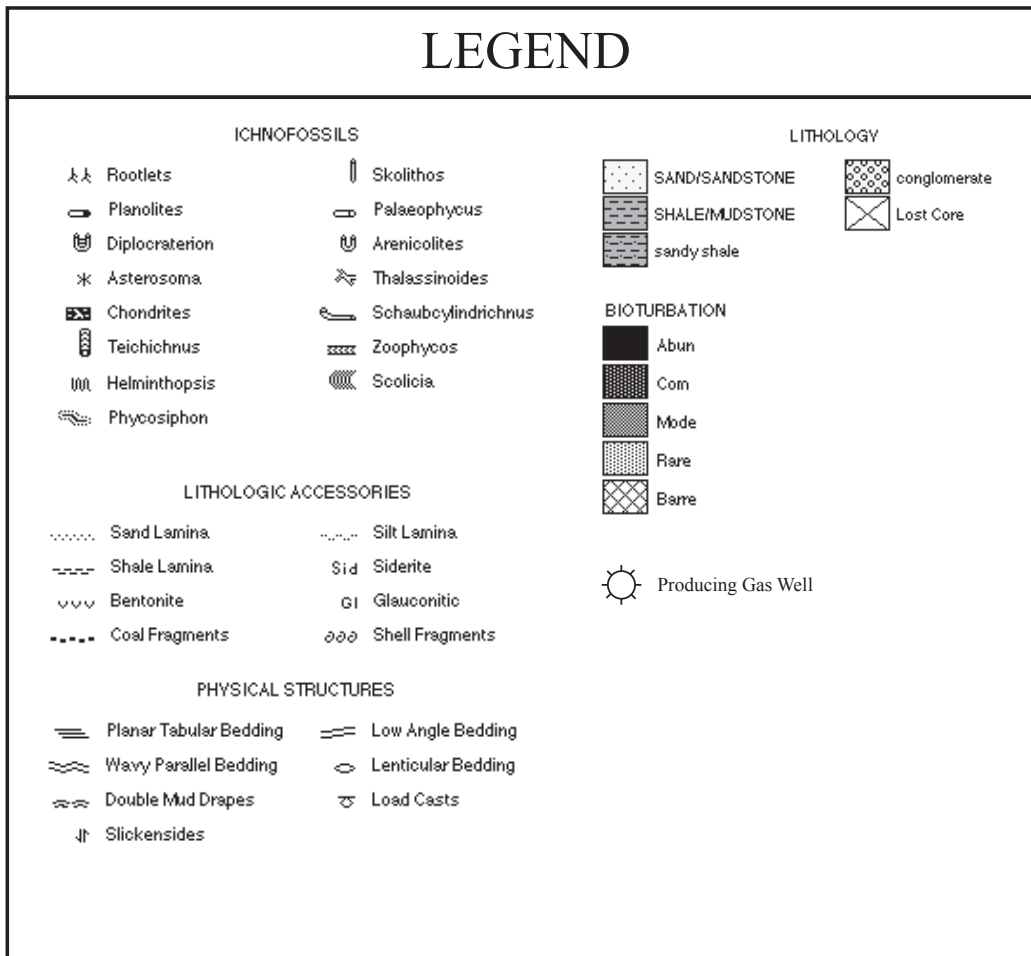
recovery processes), rock fabrics such as *Phycosiphon*-dominated sandy mudstones will isolate the gas-bearing matrix and cease the production of hydrocarbons (Gingras et al., 2004a). An understanding of the flow dynamics from the resulting anisotropic permeability allows for improved production techniques applied to the management of pervasively bioturbated, low-permeability gas reservoirs.

REFERENCES CITED

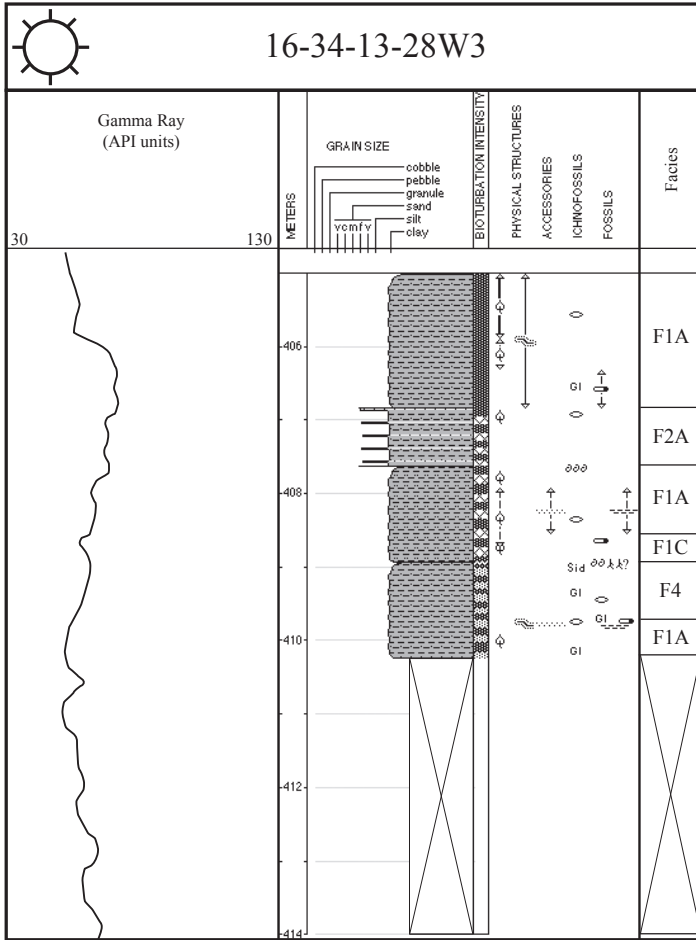
- BHATTACHARYA, J.P., AND J.A. MACEachern, 2009, Hyperpycnal rivers and prodeltaic shelves in the Cretaceous seaway of North America: *Journal of Sedimentary Research*, v. 79, p. 184 – 209.
- GINGRAS, M.K., MENDOZA, C.A., AND S.G. PEMBERTON, 2004a, Fossilized worm burrows influence the resource quality of porous media: *American Association of Petroleum Geologists, Bulletin*, v. 88, p. 875 – 883.
- GINGRAS, M.K., PEMBERTON, S.G., HENK, F., MACEachern, J.A., MENDOZA, C., ROSTRON, B., O'HARE, R., SPILA, M., AND K. KONHAUSER, 2007, Applications of ichnology to fluid and gas production in hydrocarbon reservoirs, *in* MacEachern, J.A., Bann, K.L., Gingras, M.K., and Pemberton, S.G., eds., *Applied Ichnology: SEPM, Short Course Notes 52*, p. 129 – 143.
- MACEachern, J.A., BANN, K.L., BHATTACHARYA, J.P., AND C.D. HOWELL, 2005, Ichnology of deltas: organism responses to the dynamic interplay of rivers, waves, storms and tides, *in* Bhattacharya, B.P., and Giosan, L., eds., *River Deltas: Concepts, Models and Examples: SEPM, Special Publication 83*, p. 49 – 85.
- MACEachern, J.A., PEMBERTON, S.G., BANN, K.L., AND M.K. GINGRAS, 2007a, Departures from the archetypal ichnofacies: effective recognition of environmental stress in the rock record, *in* MacEachern, J.A., Bann, K.L., Gingras, M.K., and Pemberton, S.G., eds., *Applied Ichnology: SEPM, Short Course Notes 52*, p. 65 – 94.
- O'CONNELL, S., 2007, The Second White Specks, Medicine Hat and Milk River formations – A shallow gas workshop, consult. rep.

APPENDIX

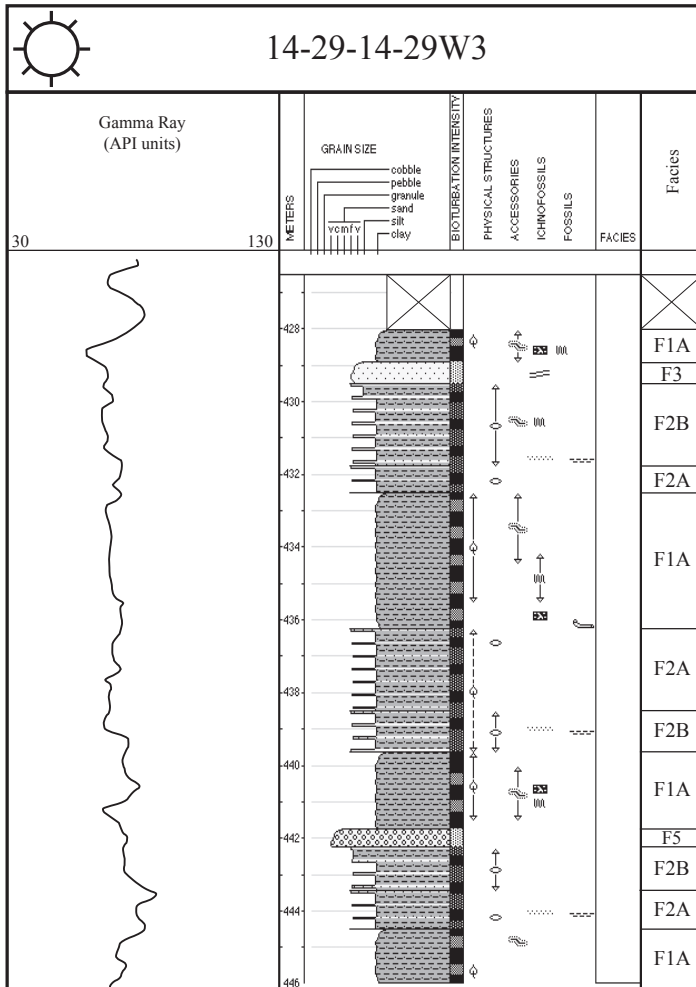
LEGEND



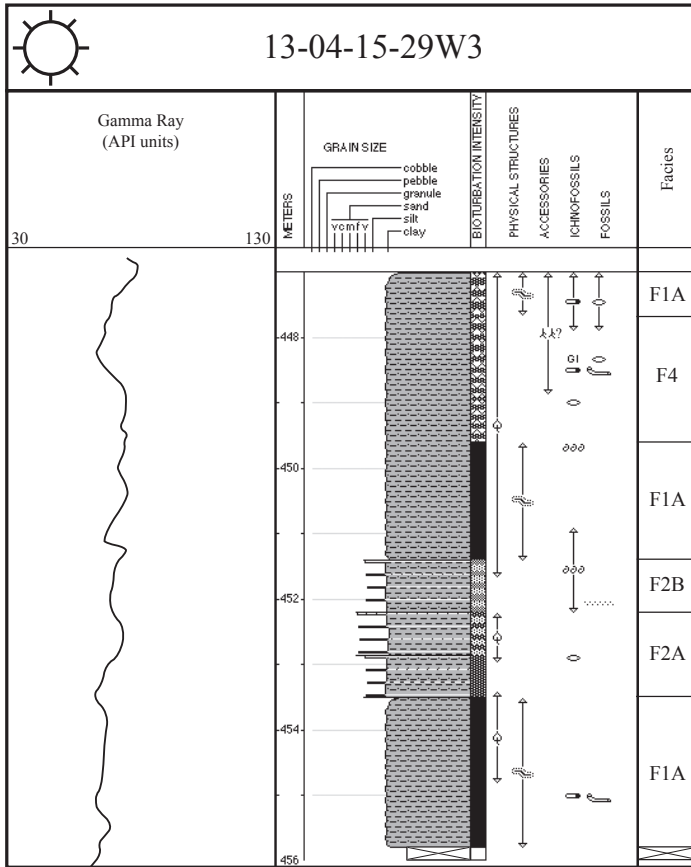
Core 1
16-34-13-28W3



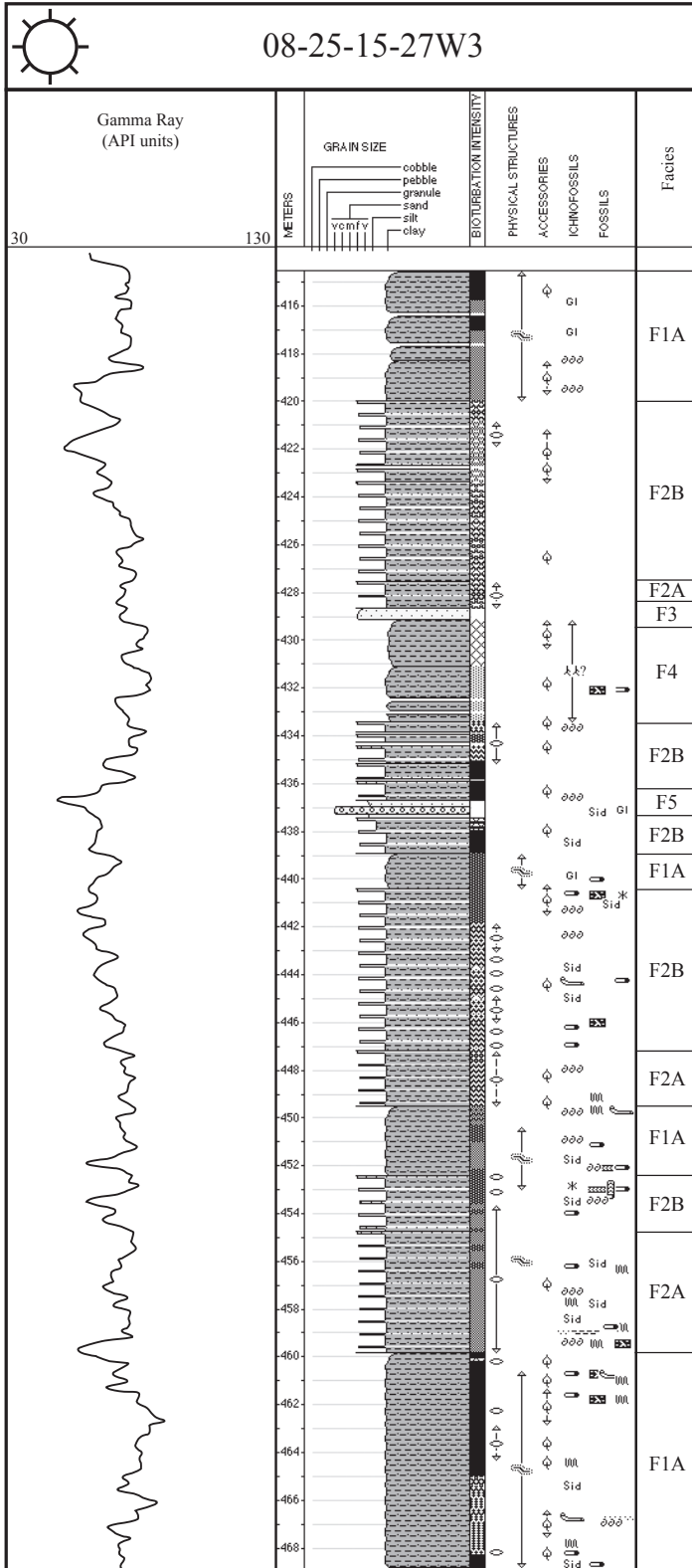
Core 2
14-29-14-29W3



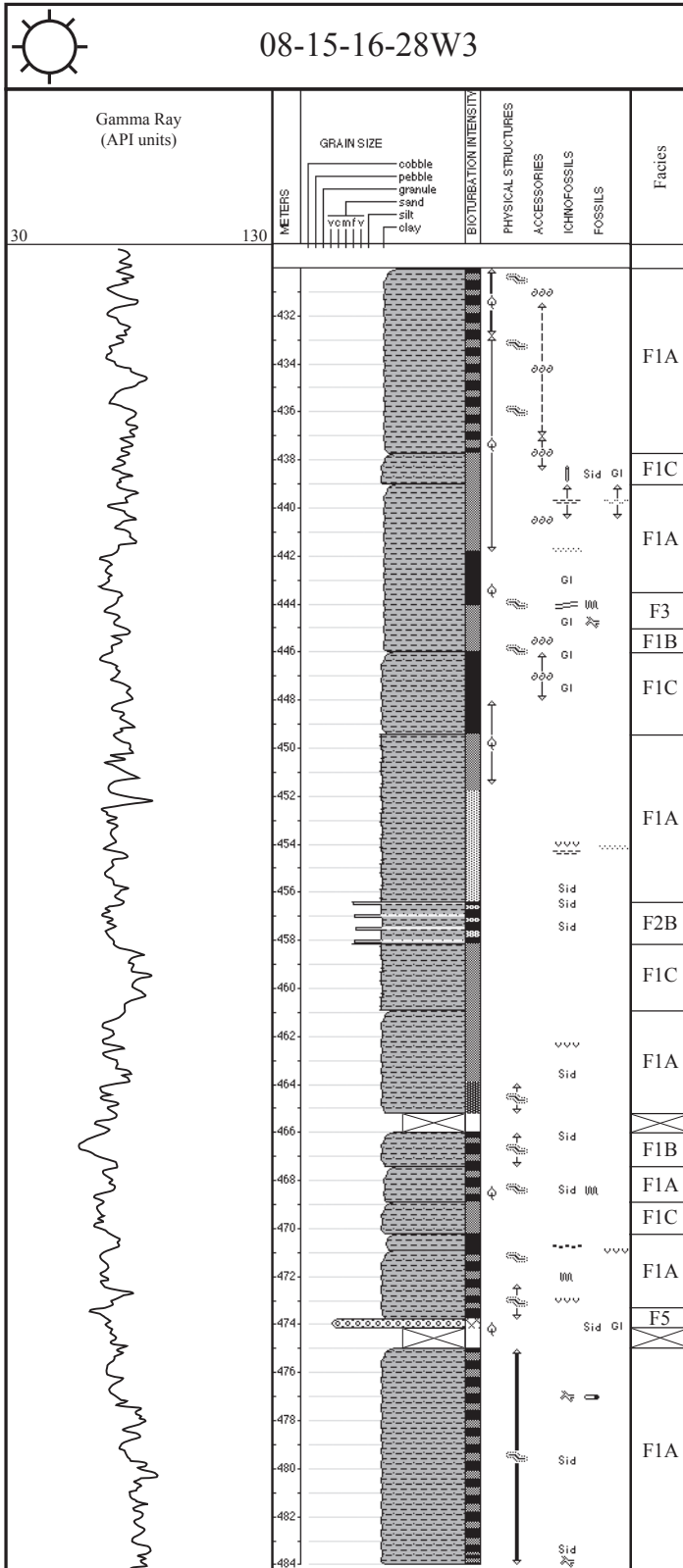
Core 3
13-04-15-29W3



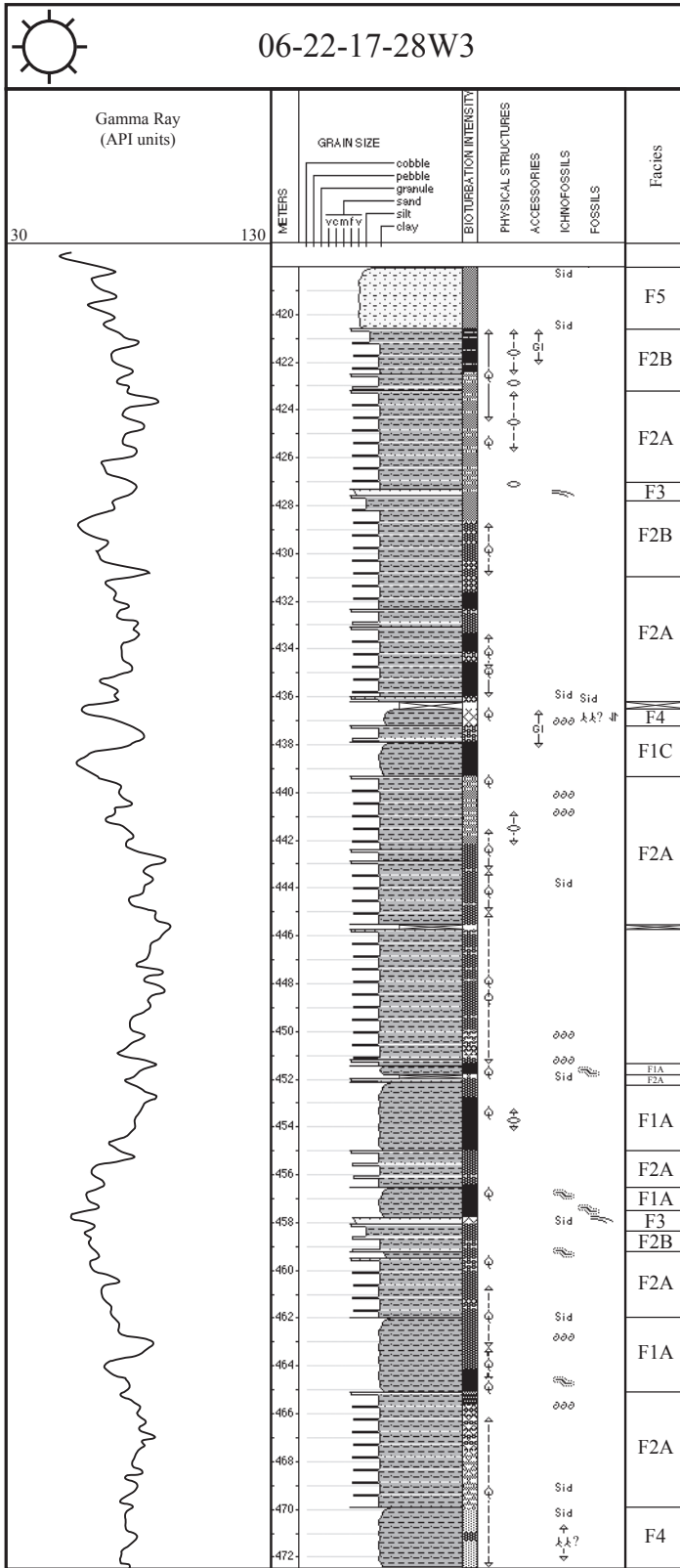
Core 4
08-25-15-27W3



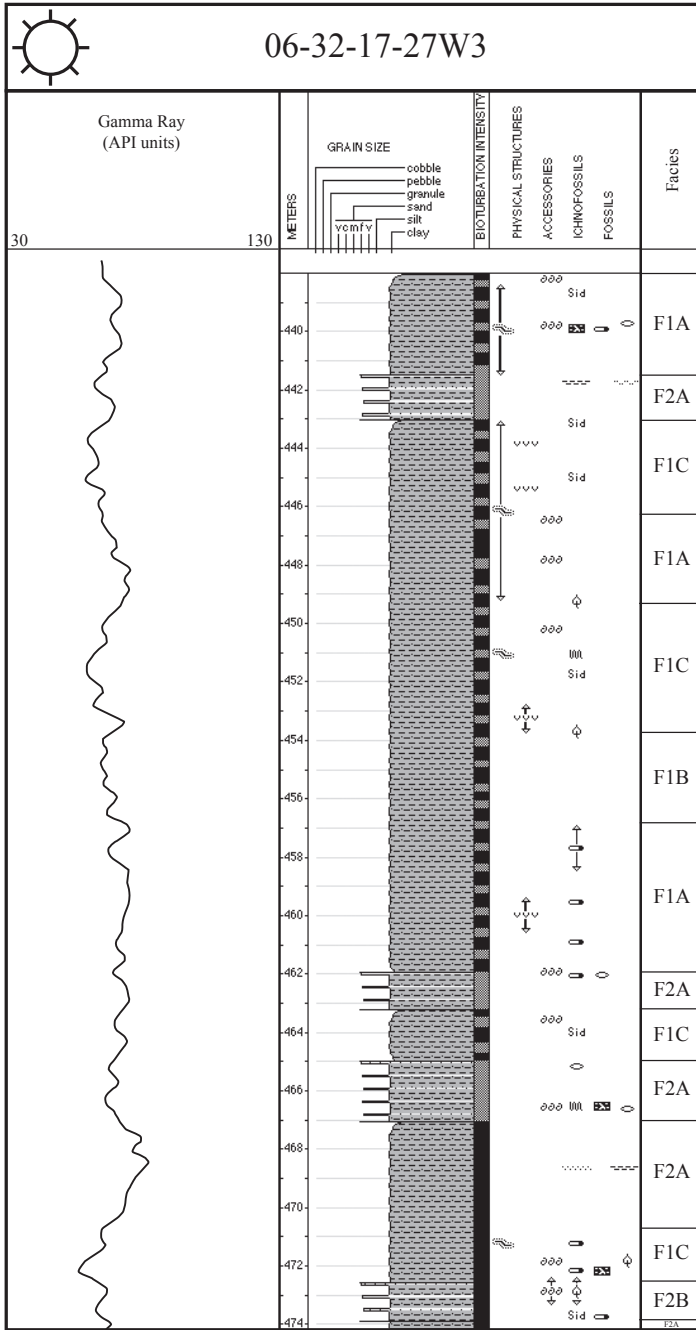
Core 6
08-15-16-28W3



Core 7
06-22-17-28W3



Core 8
06-32-17-27W3



Core 9
11-08-18-29W3

